

**ANALYZING VITAMIN D<sub>3</sub> SUPPLEMENTATION AND DEFICIENCY IN THE  
SPINAL CORD OF TRANSGENIC G93A MOUSE MODEL OF AMYOTROPHIC  
LATERAL SCLEROSIS**

Elnaz Moghimi

A THESIS SUBMITTED TO THE FACULTY OF GRADUATE STUDIES IN  
PARTIAL FULFILLMENT OF THE REQUIREMENTS FOR THE DEGREE OF  
MASTER OF SCIENCE

GRADUATE PROGRAM IN KINESIOLOGY AND HEALTH SCIENCE

YORK UNIVERSITY

TORONTO, ONTARIO

March 2015

© Elnaz Moghimi, 2015

## ABSTRACT

Vitamin D3 (D3) may impact ALS, a motoneurodegenerative disease. The study analyzed D3 supplementation at 50x the adequate intake (AI) and restriction at 2.5% the AI in the spinal cord of transgenic G93A, a mouse model of ALS. At 25 d, mice were provided food ad libitum with adequate (AI; 1 IU D3/g feed), high (HiD; 50 IU D3/g feed) or deficient (DEF; 0.025 IU D3/g feed) D3. At 113 d, the spinal cords underwent protein analysis. HiD females exhibited D3 toxicity, evidenced by increased oxidative damage and apoptosis and lower antioxidant capacity vs. AI. HiD males exhibited lower oxidative damage, inflammation, apoptosis and neuron damage vs. AI. DEF females exhibited higher inflammation and a compensatory increase in GPx1 vs. AI. DEF males exhibited higher lipid peroxidation and lower antioxidant capacity vs. AI. In G93A mice, non-toxic doses of D3 attenuate disease pathophysiology, whereas deficiency worsens it in a sex-specific manner.

## ACKNOWLEDGEMENT AND DEDICATION

I start by thanking my supervisor Dr. Mazen J Hamadeh. Thank you for all the hours you spent training, mentoring and supporting me. You have taught me to not only be a more meticulous researcher, but to also appreciate and respect research as a whole. You made me rediscover the passion I have towards science and scientific discovery and for that, I will always be grateful to you. These two years were the best years of my life and I leave this lab as a better and stronger person thanks to you and the opportunity you gave me. Thank you Dr. Ola Adegoke and Dr. Mina Singh for being on my thesis defense committee, providing constructive feedback and making my thesis defense a pleasant experience.

I would also like to thank Shayan Shahsavari and Siavash Taheri for the time they took to train and prepare me for my research project. I wish you the best of luck in your future endeavours. Thank you Sanjeev Thampinathan, Mahshad Kolahehdouzan and Safoura Sadeghimehr for all the hours you spent volunteering in the lab. This research project became what it is today because of all the help and effort you put into it. I am so blessed to have worked with such remarkable people and leave the lab with three wonderful friends with whom I share so many great memories. I know that whatever path you choose in life, you will be met with the outmost success because of the kindness, perseverance and positive work ethic you possess.

Lastly, but certainly not least, I would like to thank my family, friends and FE. Thank you for your endless love and support. Mom, thank you for teaching me the value of being an honest, strong and independent woman in society. Love you all.

## TABLE OF CONTENTS

<b>ABSTRACT .....</b>	<b>ii</b>
<b>ACKNOWLEDGEMENT AND DEDICATION .....</b>	<b>iii</b>
<b>TABLE OF CONTENTS .....</b>	<b>iv</b>
<b>LIST OF TABLES .....</b>	<b>vii</b>
<b>LIST OF FIGURES .....</b>	<b>viii</b>
<b>LIST OF ABBREVIATIONS .....</b>	<b>ix</b>
<b>AUTHOR CONTRIBUTIONS .....</b>	<b>xii</b>
<b>THESIS OVERVIEW .....</b>	<b>xiii</b>
<b>INTRODUCTION.....</b>	<b>1</b>
<b>RATIONALE, OBJECTIVES, HYPOTHESIS AND PILOT STUDIES .....</b>	<b>41</b>
Rationale.....	41
Objectives.....	41
Hypotheses .....	41
Pilot Studies.....	43
<b>MANUSCRIPT #1: .....</b>	<b>46</b>
<b>Vitamin D<sub>3</sub> supplementation at 50x the adequate intake attenuates disease pathophysiology in the spinal cord of male, but is toxic in female, G93A mouse model of amyotrophic lateral sclerosis .....</b>	<b>46</b>
<b>Abstract.....</b>	<b>48</b>
<b>Introduction .....</b>	<b>49</b>
<b>Methods .....</b>	<b>52</b>
Ethical Statement.....	52
Animals.....	52
Study Design.....	52
Tissue Collection .....	54
Spinal Cord Homogenization .....	54
Western Blot .....	55
Calculations .....	57
Statistical analysis .....	57
<b>Results.....</b>	<b>58</b>
Oxidative Damage .....	58
Antioxidant Enzymes .....	58
Inflammation .....	59
Apoptosis.....	59

Caspase 3 .....	60
Neurotrophic Factor .....	60
Neuron Damage .....	60
Spinal cord weights .....	61
<b>Discussion .....</b>	<b>72</b>
<b>Acknowledgements .....</b>	<b>82</b>
<b>Author Contributions .....</b>	<b>82</b>
<b>MANUSCRIPT #2: .....</b>	<b>92</b>
<b>Dietary D<sub>3</sub> restriction exacerbates disease pathophysiology in the spinal cord of the G93A mouse model of amyotrophic lateral sclerosis .....</b>	<b>92</b>
<b>Abstract .....</b>	<b>94</b>
<b>Introduction .....</b>	<b>95</b>
<b>Methods .....</b>	<b>97</b>
Ethical Statement .....	97
Animals .....	97
Study Design .....	98
Tissue Collection .....	100
Spinal Cord Homogenization .....	100
Western Blot .....	101
Calculations .....	103
Statistical analysis .....	103
<b>Results .....</b>	<b>104</b>
Oxidative Damage .....	104
Antioxidant Enzymes .....	104
Inflammation .....	104
Apoptosis .....	105
Caspase 3 .....	105
Neurotrophic Factor .....	106
Neuron Damage .....	106
<b>Discussion .....</b>	<b>118</b>
<b>Acknowledgements .....</b>	<b>128</b>
<b>Author Contributions .....</b>	<b>128</b>
<b>References .....</b>	<b>129</b>
<b>Summary and future research .....</b>	<b>139</b>
<b>Summary .....</b>	<b>139</b>
Oxidative damage .....	139
Antioxidant Capacity .....	140
Inflammation .....	141
Apoptosis .....	142

Neurotrophic Factor .....	143
Neuron Damage .....	143
Future Research .....	144
<b>APPENDIX A.....</b>	<b>168</b>
<b>A priori hypotheses and representative western blot bands FOR MANUSCRIPT</b>	
<b># 1:.....</b>	<b>168</b>
<b>APPENDIX B.....</b>	<b>174</b>
<b>A priori hypotheses and western blot representative bands FOR MANUSCRIPT</b>	
<b># 2:.....</b>	<b>174</b>
<b>APPENDIX C .....</b>	<b>180</b>
<b>Extended Western blot methodology for manuscript #1 and #2.....</b>	<b>180</b>
Western Blot .....	181

## LIST OF TABLES

### **MANUSCRIPT #1:**

<b>Table 1.1</b> Nutrient content of the adequate intake (AI) and high (HiD) vitamin D <sub>3</sub> diets .....	53
<b>Table 1.2</b> Food intake, vitamin D <sub>3</sub> intake and body weight of G93A mice.....	54
<b>Table 1.3.</b> Spinal cord weight between the diets and sexes at 113 d. ....	71

### **MANUSCRIPT #2:**

<b>Table 2.1</b> Nutrient content of the adequate intake (AI) and deficient (DEF) vitamin D <sub>3</sub> diets.....	99
<b>Table 2.2</b> Food intake, vitamin D <sub>3</sub> intake and body weight of G93A mice.....	100
<b>Table 2.3.</b> Spinal cord weight between the diets and sexes at 113 d. ....	117

### **APPENDIX A:**

<b>Table S1.1</b> Rationale for establishing a priori hypotheses .....	169
<b>Table S1.2</b> Summary of a priori hypotheses and corresponding supporting studies.....	170

### **APPENDIX B:**

<b>Table S2.1</b> Rationale for establishing a priori hypotheses .....	175
<b>Table S2.2</b> Summary of a priori hypotheses and corresponding supporting studies.....	176

## LIST OF FIGURES

### **MANUSCRIPT #1:**

<b><u>Figure 1.1</u></b> Oxidative damage in HiD vs. AI G93A mice.....	62
<b><u>Figure 1.2</u></b> Antioxidant enzymes in HiD vs. AI G93A mice.....	63
<b><u>Figure 1.3</u></b> Inflammation in HiD vs. AI G93A mice.....	64
<b><u>Figure 1.4</u></b> Apoptosis in HiD vs. AI G93A mice.....	65
<b><u>Figure 1.5</u></b> Caspase 3 in HiD vs. AI G93A mice.....	66
<b><u>Figure 1.6</u></b> Neurotrophic factor in HiD vs. AI G93A mice.....	67
<b><u>Figure 1.7</u></b> Neuron count in HiD vs. AI G93A mice.....	69
<b><u>Figure 1.8</u></b> Body weight-adjusted spinal cord weights at 113 d.....	70

### **MANUSCRIPT #2:**

<b><u>Figure 2.1</u></b> Oxidative damage in DEF vs. AI G93A mice.....	108
<b><u>Figure 2.2</u></b> Antioxidant enzymes in DEF vs. AI G93A mice.....	109
<b><u>Figure 2.3</u></b> Inflammation in DEF vs. AI G93A mice.....	110
<b><u>Figure 2.4</u></b> Apoptosis in DEF vs. AI G93A mice.....	111
<b><u>Figure 2.5</u></b> Caspase 3 in DEF vs. AI G93A mice.....	112
<b><u>Figure 2.6</u></b> Neurotrophic factor in DEF vs. AI G93A mice.....	113
<b><u>Figure 2.7</u></b> Neuron count in DEF vs. AI G93A mice.....	115
<b><u>Figure 2.8</u></b> Body weight-adjusted spinal cord weights at 113 d.....	116

### **Appendix A:**

<b><u>Figure 1.1</u></b> Western blot representative bands for markers of oxidative damage, antioxidant enzymes, inflammation, apoptosis, neurotrophic factor and neuron damage.....	173
--	-----

### **Appendix B:**

<b><u>Figure 2.1</u></b> Western blot representative bands for markers of oxidative damage, antioxidant enzymes, inflammation, apoptosis, neurotrophic factor and neuron damage.....	179
--	-----

## LIST OF ABBREVIATIONS

1 $\alpha$ (OH)ase	25(OH)D <sub>3</sub> -1 $\alpha$ -hydroxylase
1,25(OH) <sub>2</sub> D <sub>3</sub>	calcitriol
25(OH)D <sub>3</sub>	calcidiol
3 NY	3-nitrotyrosine
4-HNE	4-hydroxynonenal
AD	Alzheimer's disease
AI	adequate intake
ALS	amyotrophic lateral sclerosis
ALSFRS	amyotrophic lateral sclerosis functional rating scale
AMPA	$\alpha$ -amino-3 hydroxyl-5-methyl-4-isoxazole-propionate receptor
ATP	adenosine triphosphate
AUC	area under the curve
BAX	bcl-2-associated x protein
BBB	blood-brain barrier
BC	body condition
BCL-2	b cell lymphoma 2
BSCB	blood-spinal cord barrier
B.Wt.	body weight
C9ORF72	chromosome 9 open reading fram 72
CASP3	caspase 3
CAT	catalase
CHAT	choline acetyltransferase
CS	clinical score
CS2	clinical score of 2
CS4	clinical score of 4
CS5	clinical score of 5
CNS	central nervous system
COX-2	cyclooxygenase-2
CRP	C-reactive protein
CSF	cerebrospinal fluid
Cu	copper
D <sub>3</sub>	vitamin D <sub>3</sub>
D76Y	aspartic acid to tyrosine switch at the 76 <sup>th</sup> codon
D90A	aspartic acid to alanine switch at the 90 <sup>th</sup> codon
DEF	vitamin D <sub>3</sub> deficient group
DISPRO	disease progression from CS2 to CS5
EAAT2	excitatory amino acid transporters-2
EAE	experimental allergic encephalomyelitis
EMG	electromyography
ETC	electron transport chain
fALS	familial amyotrophic lateral sclerosis
FDA	Food and Drug Administration
FNB	Food and Nutrition Board

FUS/TLS	fused in sarcoma/translocated in sarcoma
G37R	glycine to arginine switch at the 37 <sup>th</sup> codon
G41S	glycine to serine switch at the 41 <sup>st</sup> codon
G72S	glycine to serine switch at the 72 <sup>nd</sup> codon
G85R	glycine to arginine switch at the 85 <sup>th</sup> codon
G86R	glycine to arginine switch at the 86 <sup>th</sup> codon
G93A	glycine to alanine switch at the 93 <sup>rd</sup> codon
GDNF	glial-derived neurotrophic factor
GpX1	glutathione peroxidase 1
H <sub>2</sub> O <sub>2</sub>	hydrogen peroxide
H46R	histidine to arginine switch at the 46 <sup>th</sup> codon
HED	human equivalent dosage
HiD	high vitamin D <sub>3</sub> group
HR	hazard ratio
IgG	immunoglobulin G
IL-1	interleukin-1
IL-6	interleukin-6
IL-10	interleukin-10
IL-12	interleukin-12
IOM	Institute of Medicine
LPS	lipopolysaccharide
IU	international unit
LMN	lower motor neuron
MDA	malondialdehyde
MMP	matrix metalloproteinase
MP	motor performance
MPTP	mitochondrial permeability transition pore
MS	multiple sclerosis
NAHNES	national health and nutrition examination survey
NF-L	light neurofilament
NO	nitric oxide
NOS	nitric oxide synthase
O <sub>2</sub> <sup>-</sup>	superoxide
ONOO <sup>-</sup>	peroxynitrite
•OH	hydroxyl radicals
PaGE	paw grip endurance
PCR	polymerase chain reaction
PD	Parkinson's disease
PGE <sub>2</sub>	prostaglandin-E <sub>2</sub>
RA	rheumatoid arthritis
RCT	randomized controlled trial
RDA	recommended daily allowance
sALS	sporadic amyotrophic lateral sclerosis
SEM	standard error of the mean
SD	standard deviation
SMI-32	neurofilament h non-phosphorylated

SMI-36	neurofilament h phosphorylated
SOD1	Cu/Zn superoxide dismutase
SOD2	Mn superoxide dismutase
TARDBP	tar dna-binding protein
TNF- $\alpha$	tumour necrosis factor
UCP3	uncoupling protein 3
UMN	upper motor neuron
UVR	ultraviolet ray
VDR	vitamin D receptor
Zn	zinc

## AUTHOR CONTRIBUTIONS

MANUSCRIPT #1, *Vitamin D<sub>3</sub> supplementation at 50x the adequate intake attenuates disease pathophysiology in the spinal cord of male, but is toxic in female, G93A mouse model of amyotrophic lateral sclerosis (ALS)*

I was responsible for extraction, homogenization and protein content measurement of practice mouse spinal cord for antibody optimization, antibody optimization, G93A mouse spinal cord homogenization and measuring their protein content, western blot analysis, data input, data processing, statistical analysis, literature search and writing of the manuscript.

MANUSCRIPT #2, *Dietary vitamin D<sub>3</sub> restriction exacerbates disease pathophysiology in the spinal cord of the G93A mouse model of amyotrophic lateral sclerosis (ALS)*

I was responsible for extraction, homogenization and protein content measurement of practice mouse spinal cord for antibody optimization, antibody optimization, G93A mouse spinal cord homogenization and measuring their protein content, western blot analysis, data input, data processing, statistical analysis, literature search and writing of the manuscript.

## THESIS OVERVIEW

The thesis that you are about to read is comprised of 2 manuscripts that will be submitted to peer-reviewed scientific journals and completed as part of my MSc degree.

### Manuscript #1:

The first manuscript is a pilot study investigating the effects of vitamin D<sub>3</sub> supplementation (50 fold the adequate intake vs. the adequate intake) in the spinal cord of the G93A mouse model of ALS on disease pathophysiology. In addition, we investigated the effect of high vitamin D<sub>3</sub> supplementation on the established sexual dichotomy in this animal model of ALS.

### Manuscript #2:

The second manuscript is a pilot study investigating the effects of vitamin D restriction (1/40<sup>th</sup> the adequate intake vs. the adequate intake) in the spinal cord of the G93A mouse model of ALS on disease pathophysiology. In addition, we investigated the effect of vitamin D restriction on the established sexual dichotomy in this animal model of ALS.

## INTRODUCTION

Amyotrophic lateral sclerosis (ALS), also known as Lou Gehrig's and motor neuron disease (UK), is a chronic, progressive and fatal neurodegenerative disease, first described by Charcot in 1874 (1). Though age of diagnosis can vary, ALS is typically a late-onset disease with diagnosis usually occurring between the ages of 45 and 60 years (2, 3). It is the most commonly occurring adult-onset motor neuron disease of unknown cause (4, 5). It is characterized by "amyotrophy" and "lateral sclerosis". "Amyotrophy" or muscle wasting is due to denervation of muscle fibers as a result of motor neuron degeneration (6). "Lateral sclerosis" refers to the hardening of ventral and lateral corticospinal tracts, areas progressively replaced by gliosis (the reaction to damage in the central nervous system, involving proliferation and hypertrophy of neuroglia at sites of damage) (6). The corticomotoneuronal system, which includes the corticomotoneurons in the motor cortex and motor neurons in the brain stem and spinal cord, is the central target of the disease (7). The lifetime risk of developing the disease is 1 in 2000 (1). ALS has an average incidence and prevalence rate of 1-2 cases per 100 000/year and 6 cases per 100 000/year respectively (5, 8). These rates are for the most part uniform throughout North America but can vary depending on geographic location, exclusion and inclusion criteria, statistical methodology and epidemiological studies (5). In recent decades, studies have noted an increase in prevalence rates, most likely a result of improved quality of care (9). Incidence rates are higher in the western pacific, including Guam Island and Japan (10). The occurrence of the disease is higher in males vs. females with a ratio of 1.6:1 (8). This is especially observed in Europe and the United States (11). The

exact time of biological onset is unknown but it is hypothesized that the disease may manifest itself early in life and then become clinically apparent in later stages (2).

Currently, the only available therapy for ALS is riluzole, an antiglutamatergic drug. 100 mg oral consumption of the drug may extend life for approximately 2-3 months and may increase the likelihood of survival in the first year by 9% (12). However, riluzole is a very expensive drug and costs approximately \$10,000/year in the US and £4056/year in the UK.

### **Etiology**

Progressive degeneration of upper motor neurons (UMN: run from motor cortex in the brain to the spinal cord) and lower motor neurons (LMN: run from spinal cord and brainstem and extend out to muscles) eventually lead to muscular weakness and atrophy, fasciculation, spasticity and paralysis (2, 13). The most commonly described pathological feature of ALS has been the degeneration and atrophy of the large motor neurons in the anterior horn of the spinal cord (14). There is selective atrophy of motor neurons where those that control eye movement and the bladder (i.e. Onuf's nucleus located in the sacral cord) are, for the most part, not affected (1). It is not well understood exactly why motor neurons are the most vulnerable targets of the disease. They are the largest cells in the central nervous system and possess extremely long axons ( $>10^4$  times larger than its cell body) (14) where 99.9% of the radial growth of its cell volume resides (15). These cells require a robust cytoskeleton, high amounts of neurofilament protein and a high metabolic rate, which can make them susceptible to a plethora of insults (16).

How motor neuron degeneration occurs is currently unknown, but it is believed to result from a multitude of factors, including oxidative stress, glutamate excitotoxicity, protein misfolding and aggregation, abnormal protein secretion, mitochondrial dysfunction, reduced neurotrophic factor secretion, ruptures in axonal passage and dysregulated calcium metabolism (3, 17). In its primary stage, axon connections start to break down and retract, no longer innervating LMN and muscle which initiates the start of symptoms and disease progression (2). Initially, more resistant neurons can compensate for this degenerative effect via axonal sprouting and collateral re-innervation (18). As the disease progresses, this compensational mechanism fails and neuronal cell bodies become abnormal, resulting in neuronal atrophy, as observed in animal models (2, 18-20). Such abnormalities include reactive gliosis, intracytoplasmic neurofilament abnormalities and axonal spheroids (1). Axonal spheroids are comprised of large eosinophilic and argentophilic masses that form at the initial segment of lower motor neuron axons, representative of the early stages of ALS disease progression (14). Exactly when this cascade of events occurs in human ALS patients is unknown, but it is observed in rare post-mortem studies on patients who have died very early on in the disease(20).

With the lack of neural guidance and a breakdown of neuromuscular junctions, skeletal muscle becomes denervated and is unable to acquire the signals needed to initiate movement. This results in a reduction in muscle mass, fibres (including fibre diameter) and force (9, 21), and spontaneous uncoordinated muscle activity (22). Muscle atrophy is first observed in proximal limbs or body region, and, over time with progression of the disease, spreads to distal muscles (23). A gradient loss of motor neurons is observed from the area of disease onset (24).

Ultimately, denervation of the diaphragm results in alveolar hypoventilation leading to death by respiratory failure within 3-5 years of initial symptoms (25-27). 50% of patients die within 30 months post-symptom onset and another 20% survive 5-10 years post-symptom onset (28). Usually, the patient will slip into a coma due to increased hypercapnia prior to death (8). There is a large variability in disease duration amongst patients which ranges from months to approximately two decades (2). ALS patients who are members of the same family and have the same genetic mutation can experience large differences in disease duration and age of onset, suggesting there are external factors modulating phenotypic outcomes (29).

### **Environmental risk factors**

There are multiple environmental risk factors proposed for ALS, most having to do with physical and toxic risk factors (8).

Many epidemiological studies have shown a multitude of risk factors attributed to ALS. Education attainment has been associated with lower odds of ALS (30). This may likely be due to an increased awareness to work and live in environments with lower toxic exposure. Though studies have been mixed, cigarette smoking may be considered an established risk factor of sALS (31), a prospective study in the US reported elevated ALS risk with formaldehyde (a component of cigarettes) exposure among current female smokers compared to never smokers (RR = 1.67, 95% CI = 1.24-2.24, P = 0.002) (32).

There is an elevated risk of ALS diagnosis in specific cohorts of people. Lifetime of intensive sport or physical exertion has been observed as a potential risk factor possibly due to an increased exposure and transport of the toxins, and heightened

susceptibility of target cells to toxic damage (33, 34). Many studies have shown no association between ALS and physical activity (32) but the results remain inconclusive. Military personnel who have active participation in the US armed forces have also been observed as a risk group (35). As well, a retrospective study of soccer players from the Italian professional leagues showed an increase in standardized morbidity ratios for the development of ALS, in particular younger-onset disease (36). Soccer players, particularly those in the active midfield position for more than five years were at the highest risk of developing ALS (36). As well, ALS has been diagnosed in a cluster of amateur English soccer players (37).

Human and murine viruses and prion diseases are also being investigated as possible initiators of the disease (11, 13). It is believed that constant viral infections might cause sALS (13). In the 1983 study by Salazar et al., of the 33 ALS patients with dementia tested, 3 patients with “atypical” features compatible with ALS characteristics were able to transmit the disease to monkeys via brain tissue injection (38). The atypical features coincided with features of amyotrophy found in patients with Creutzfeldt-Jakob disease (38). As well, 50 cases of proven prion disease have shown LMN signs (38).

Toxins may also play a role in the genesis of the disease. It has been suggested that the reason for elevated levels in the western pacific, particularly Guam, has to do with the presence of the neurotoxin  $\beta$ -methyl-amino-L-alanine (BMAA) in cycad tissue (39). Of cyanobacterial origin, this toxin bioaccumulates as it travels higher in the food chain (39). BMAA has the ability to pass the blood-brain barrier and many hypotheses have been proposed to explain its toxic action. Chronic ingestion of BMAA may cause it to become integrated in nerve cells and protein structure, altering it and causing it to

malfunction and aggregate, ultimately leading to death (40). BMAA may also be wrongfully integrated into proteins, particularly in place of serine (41). This is important, as serine plays an important role in phosphorylating protein sites and altering this process is a known mechanism in the pathogenesis of neurodegenerative diseases. Inhabitants of Guam Island, the Chamorro population, have a traditional diet that includes the fruit bat, which feeds on cycad seeds and thus bioaccumulates BMAA. Guamanian ALS patients have been shown to have a significant concentration of this neurotoxic amino acid in their brains (39).

Free-radical-mediated mechanisms are also a possible cause of neurodegeneration. The ALS spinal cord has increased levels of selenium and manganese (42, 43). Manganese can inhibit neurotransmission (44), and high levels have been observed in Guam's soil (45).

Many chemicals have been associated with higher ALS risk with the strongest evidence coming from agricultural pesticides, fertilizers, herbicides and insecticides. There is an association between fertilizer exposure and ALS (32, 46). After adjusting for education, smoking and other occupational exposures such as metals, solvents and electromagnetic fields, a significant association was found between occupational exposure to pesticides and ALS (OR = 6.50, 95% CI = 1.78-23.77) (47). A systematic review confirmed a significant association between pesticide exposure and ALS (48). The harsh effects of these chemicals in ALS patients may be due to a group of proteins known as paraoxonases. Paraoxonase 1 in particular allows the body to eliminate toxins such as organophosphates. Compared to the general population, ALS patients are often carriers of certain variants of the genes, possibly reducing the detoxification effects of the protein.

In contrast to previous smaller studies showing an association,, a genetic meta-analysis of the literature has shown insignificant evidence (49). The challenge with meta-analyses is the pooling of different publications, thus disregarding differences between populations.

### **Classification of ALS**

There are multiple classification systems for ALS (50). The simplest and most widely used classification is based on the localization of disease onset, which is a known predictor of disease progression (5). They are, bulbar-onset (25% of cases) and spinal onset (75% of cases), categorized according to the primary region of upper or lower motor neuron degeneration (5, 50). Bulbar onset, having a shorter survival time, initially affects the tongue, throat and lip muscles and progresses into dysarthria (slurred speech) and dysphagia (difficulty swallowing) (8, 51, 52). Spinal onset initially affects limb and trunk muscles resulting in muscle weakness, paralysis and atrophy, fasciculations and cramps (51, 52).

### **Diagnosis**

In the late 1980s, the EI Escorial diagnostic criteria for ALS was developed (and subsequently revised) which provides a structured way to objectively assess patients who may have ALS (53, 54). It utilizes a combination of UMN and LMN signs in order to administer a score of diagnostic certainty (55). Scores are divided into 5 main categories: definite (LMN and UMN signs in three regions), probable (LMN and UMN signs in two regions), probable with laboratory support (LMN and UMN signs in one region or UMN signs in one or more regions with electromyography indicating acute muscle denervation in two or more limbs), possible (LMN and UMN signs in one region) and suspected

(LMN signs only in one or more regions or UMN signs only in one or more regions) (53). All categories must show that the sensory signs are not comorbid with other diseases and disease progression should be visible (54). Currently, the most widely used rating scale in clinical trials is the amyotrophic lateral sclerosis functional rating scale (ALSFRS), which records disease progression in patients and evaluates functional status and change (56).

### **Subtypes of ALS**

ALS patients can be classified into two clinically indistinguishable subtypes: familial and sporadic. Familial ALS (fALS) undergoes Mendelian inheritance patterns, high penetrance and in almost all cases is autosomal dominant (X-linked or recessive types are extremely rare) (2, 17). It occurs in approximately 5%-10% of cases with ~12% of these cases being a result of a mutation in the  $\text{Cu}^{2+}/\text{Zn}^{2+}$  super-oxide dismutase 1 (SOD1) gene (1, 57-59). Currently, there are variants of approximately 30 gene mutations that are known to cause ALS in humans (60, 61) with the most notable ones being TARDBP, C9ORF72 and FUS/TLS (17). Sporadic ALS (sALS) is a more common form occurring in approximately 90% of patients, and is diagnosed in patients who do not have family members with the disease and thus do not fall under fALS (2, 62). This is not to say that a genetic component is not present in sALS, however there has been limited success in finding sALS-associated gene mutations (17). 1% of SALS cases can be explained by a mutation in the SOD1 gene (59). Epidemiological and pathophysiological mechanisms in sALS can be understood by investigating familial forms because of the clinical and pathological similarity between the two (17).

## Superoxide dismutase 1 (SOD1) and its mutation

Copper/zinc superoxide dismutase (SOD1) was discovered in 1993 as the first ALS gene (57). It is one of three isoforms of superoxide dismutases in mammalian cells that are responsible for the conversion of superoxide ( $O_2^{\bullet-}$ ) to hydrogen peroxide ( $H_2O_2$ ) (63). Mutation in SOD1 is recognized as the major genetic cause of ALS (17). The SOD1 protein is a ubiquitous homodimer (64-66), and its gene consists of 153 codons on chromosome 21q22.1 and possibly 21q22.2 (67). The majority of the protein has an eight-strand beta-barrel conformation and is one of the most stable proteins known due to its extensive hydrogen bonding along the peptide backbone. Its cofactors are zinc and copper. SOD1 is mostly found in the motor neurons and glial cells of the spinal cord (64-66), specifically the cytosol (in peroxisomes) as well as the intermitochondrial membrane space (68).

The most important function of SOD1 is that it converts superoxide ( $O_2^{\bullet-}$ : a toxic one-electron reduced by-product of mitochondrial oxidative phosphorylation) to water and hydrogen peroxide ( $H_2O_2$ ) (69). As an oxidizing agent,  $H_2O_2$  has a very low reactivity and can impair cellular structures directly or combine with iron or copper ions to generate  $\bullet OH$ , a potent free radical. Spinal motor neurons, which are the primary targets of ALS, are very sensitive to  $H_2O_2$  and go through apoptosis when exposed to it in primary culture (70).

SOD1 clears superoxide rapidly from the cell, even if the antioxidant enzyme's levels are reduced by 50% (71). Superoxide is produced *in vivo* via the catalyzed one electron reduction of molecular oxygen through different biological systems including

mitochondrial electron transport chain, NADPH oxidases, and xanthine oxidase (72). Mediation of the catalysis of superoxide by SOD1 is in two asymmetric steps that require a copper atom in order to occur which becomes alternately reduced and oxidized by superoxide (69). Superoxide is found to be made largely in the mitochondrial matrix (73, 74), and has also been found in the intermembrane space(68), areas in which the superoxide dismutase family has also been found.

SOD1 is a very stable protein, and when bound to its cofactors (holo state) it can retain its activity in 6 M urea and survive heating to 80°C (75). However, in the apo state when both metals are missing, the protein denatures at a faster rate. Thus, it is mutations affecting the protein's binding to its cofactors that make it more susceptible to denaturation and aggregation. The main consequence mutations have on these proteins is that they destabilize their overall structure. This was confirmed by Bosco et al who showed that an important underlying factor of both fALS and sALS may be a misfolding both in wild-type as well as mutant SOD1 giving it a disease-specific and toxic profile (76). Assays of SOD1 activity in extracts from red blood cells, brain tissues and lymphoblastoid cells revealed ~50% reduction in fALS patients when compared to normal controls (77), indicating that lower SOD1 activity can induce pathways leading to oxidative damage and thus fALS symptoms.

There are currently 160 recorded mutations in the SOD1 gene that can result in ALS with a majority being missense, where one residue is substituted with another (nonsense and deletion are rare) (50). Some amino acid sites can have as many as six different substitutions. More than 90 of the 160 mutations have 40 out of the 153 amino acid residues involved (13). These mutations are found within the primary and three-

dimensional protein structure (69). The majority is found scattered throughout the protein in key areas of the dimer interface, active site and beta barrel (78). Despite the fact that the overall distribution of mutation sites is random, the majority of the mutations affect side chains facing inside the hydrophobic interior of the protein or within the dimer interface.

All SOD1 mutations are dominant except for D90A (an aspartate is exchanged for an alanine at position 90), which can be recessive (79) or dominant (80). The most common SOD1 mutation is A4V (alanine is exchanged for valine at position 4) (13). It has one of the fastest progressing forms of ALS, with survival under 1 year post diagnosis (81). The type of SOD1 mutation can dictate many characteristics of the disease such as age of onset, survival and clinical classification (i.e. bulbar or spinal) (13).

Mutations in the gene cause the antioxidant to gain a toxic function independent of the levels of SOD1 activity (69) that leads to MND (50). SOD1 not only has a dismutation function but it also has a peroxidative function whereby  $\text{H}_2\text{O}_2$  and anionic radical scavengers such as glutamate are used as substrates to produce free radicals such as  $\bullet\text{OH}$  (82). In G93A mice, both WT and mSOD1 have dismutation activities (though mSOD1 has 93% of WT dismutation activity). What differs between the two is that the free-radical generating function is enhanced in mSOD1 relative to WT (82). This is due to  $\text{H}_2\text{O}_2$  in mSOD1 having lower  $K_m$  (i.e. higher affinity) compared to WT. The lower  $K_m$  value may be a result of mutations that destabilize the  $\beta$  barrel backbone of the enzyme which opens the active channel causing a higher accessibility of  $\text{H}_2\text{O}_2$  to the active site, resulting in lower  $K_m$  and thus elevated production of  $\bullet\text{OH}$ . In both ALS

patients and G93A mice, the presence of elevated glutamate levels raises the concentration of glutamate-derived free radicals which damage glutamate transport machinery and receptors (77)

Although SOD1 is found in the cytosol of the cell, its mutant form becomes colocalized with the mitochondria in the CNS and generates free radicals, yet it still maintains the dismutation function found in normal human SOD1 (83). In mice that develop MND, removal of normal SOD1 genes in order to inhibit the expression of a dismutase inactive mutant (SOD1<sup>G85R</sup>) has no effect on onset or survival (84). Pathology in SOD1 mice is non-cell autonomous. This means motor neuron death and degeneration and the associated neurological symptoms require mSOD1 expression in other cells in addition to neurons, such as glia to initiate neuron toxicity, degeneration and death (85-87).

In ALS profiles, mutated SOD1 becomes involved in oxidative stress, excitotoxicity, mitochondrial dysfunction, neuroinflammation, endosomal trafficking, axonopathy and apoptosis (50, 88). The exact mechanism of toxicity that SOD1 utilizes to cause neurodegeneration is currently unknown (17, 69). There is a general consensus that mutations in SOD1 structurally weaken the antioxidant enzyme to form a partially unfolded intermediate (89). According to a multitude of studies, the first step in unfolding of SOD1 is due to the loss of the structural zinc atom as SOD1 has a naturally modestly reduced affinity for the metal (89). A loss in zinc causes SOD1 to become more accessible, more redox reactive and a better catalyst for tyrosine nitration (89). As well, aggregation of the protein occurs after loss of its metals, with zinc most likely to be

lost first as it is bound 7000 times more weakly than copper (90). As is the case in mSOD1, loss of zinc is equally toxic in WT SOD1 to motor neurons (91).

A loss of zinc from SOD1 causes a partial disorganization in portions of the SOD1 protein which protect the attached copper causing it to become extremely toxic to motor neurons via a mechanism requiring nitric oxide (89). Zinc itself is not involved in the catalytic dismutation of superoxide, but instead provides the structural support for the active site. The redox properties of SOD1 are significantly altered with the loss of zinc. It has been postulated that the loss of zinc can cause the remaining copper to be more accessible to intracellular reductants by disordering the two largest loops that normally restrict access of copper to only superoxide (78). The reduced copper can be reoxidized by molecular oxygen to produce superoxide and could continue to be in a reduced state in the CNS as a result of the high concentrations of ascorbate, a reducing agent (millimolar in concentration and highest in the body). It is important to note that mutant SOD1 that was carefully purified to contain both the zinc and copper cofactors was just as protective as WT SOD1 to motor neurons deprived of neurotrophic factors (91).

### **Mouse models of ALS**

Though ALS is not a naturally occurring disease in mice (*Mus musculus*), manipulation of their genome can give rise to this disease and thus allow it to be studied. Transgenic mice that ubiquitously overexpress different mSOD1 genes at levels equal to or several folds higher than endogenous SOD1 levels (1) adopt a neurodegenerative profile that follows the same pathology and outcome as the human disease (17). However, in transgenic mice that overexpress WT human SOD1 or mutant SOD1 only in

neurons and glial cells, the disease does not develop (84, 86, 92). Currently it is unknown exactly why the SOD1 gene has to be expressed ubiquitously in order to induce targeted damage to the motor neurons. Virtually all studies that have used mouse models use endogenous murine SOD1 promoter that causes overexpression of the mutant SOD1 gene to be present in all tissues (17).

In mouse models, overexpression of either G37R, G85R, G86R, D90A, G93A, H46R/H48Q or H45R/H48Q/H63G/H120G, L126Z and G127X mutant SOD1 protein leads to motor neuron degeneration in the spinal cord and myelinated axons in the ventral motor roots (17).

Of the different mutations, G93A is the most widely used model in research where an alanine substitutes a glycine at codon 93 (93). In 1994, Gurney et al were successful in producing the first SOD1<sup>G93A</sup> mouse line [Tg(SOD1\*G93A)1GUR] in which the cDNA of a human mutant SOD1 (hSOD1) was randomly inserted into the genome of fertilized eggs from C57BL6XSJL F1 hybrid mice (93). Modeling the neurodegenerative pattern of ALS, motor neuron atrophy and progressive paralysis occurred, ultimately resulting in death. With progression of the disease, the mice exhibited hind limb paralysis, deteriorating paw grip strength and endurance, muscle and tissue atrophy resulting in palpable bony structures, inability to groom or scavenge for food and water and limited mobility (94, 95). Unique to the highly toxic SOD1 mutant in mice is that they also possess prominent ubiquitin-positive intracellular aggregates of SOD1 in their motor neurons and astrocytes (1). These aggregates can stop normal proteasomic function, causing a disruption in vital cellular functions and axonal transport systems (55)

Their disease pathology closely resembles that which is found in humans. Transgenic mice routinely develop paralysis in the hind limb within 3 and 12 months of age (69). Weakness in the hind limbs corresponds with increased progressive spinal motor neuron ascending and descending fibre track degeneration (69). Fragmented Golgi apparatus and neuroinflammation caused by astro- and microgliosis in damaged motor neurons also occur in these models (17, 96-99). As well, mutations result in abnormal gait and movement (95), altered axonal transport (100, 101) and elevated levels of mSOD1, particularly in the brain and spinal cord (99, 100, 102).

#### *Timeline of disease progression and death in mutant mice*

Age of onset, disease progression and duration can vary amongst the different models and can depend on genetic background (103) and gene dosage (17). The life span and disease progression of ALS mouse models are inversely proportional to the amount of mutant genes inserted into the genome (gene dosage), which can affect the amount of mutant SOD1 protein present in the CNS (17). In high-copy mouse models, ~25 copies of the human transgene is randomly inserted into chromosome 12 (93). An indication of motor degeneration is observed via a change in gait of the high-copy G93A mice, which occurs between 85-110 d (94, 95). Paralysis occurs at  $124 \pm 10$  days and death occurs by ~135 days (94, 95). The main criticism that arises from using high copy mice is the fact that they have overexpression of the SOD1 protein up to 24-folds higher than what is found in humans which can result in phenotypic features that are not due to the SOD1<sup>G93A</sup> mutation itself (104). However, extraneous effects on motor neurons have not been observed (105). Conversely, low-copy mouse models (Tg(SOD1\*G93A<sup>dl</sup>))<sup>1</sup>Gur (SOD1<sup>G93A<sup>dl</sup></sup> or G1del) have also been developed by Jackson Laboratories via a deletion

in the transgene array of a SOD1<sup>G93A</sup> mouse (Jackson Laboratory Stock #002299). These low-copy mice carry ~eight to ten copies of the human SOD1<sup>G93A</sup> transgene (105). Paralysis in these mice occurs between 24 and 34 weeks of age (106). Death usually occurs at ~34 weeks (105). Due to ethical reasons, endpoint must be established in order to prevent the animals from experiencing pain, distress and/or suffering (107). Currently, there is no universal endpoint for rodent models of ALS accepted by all researchers (95). There is an array of criteria that different labs utilize in order to establish endpoints. The most notable ones include a combination of two or more of the following criteria: righting reflex where mice are placed on their sides and must right themselves to sternum within 3-30 s otherwise they are euthanized, significant decrease in grip strength or motor performance, complete hindlimb paralysis and as a result inability to splay them, cannot obtain food or water, reduction in body weight from peak weight, eye infection, lack of self-grooming, lack of response to pain and/or a predetermined time where no spontaneous breathing or movement occurs (95).

As of now, a righting reflex of at least 3 seconds is most commonly used to establish endpoint (95).

## **Pathophysiology**

### *Oxidative Stress*

Oxidative stress occurs early in ALS and is present when damage in proteins, lipids and DNA generate reactive oxidative (ROS) and/or nitrogen (RNS) species. ROS/RNS are very reactive and present in the primary stages of neural dysfunction

where they interact with different components of the cell to initiate cell death and neurodegeneration.

To generate ROS, activation of molecular oxygen must take place. Physiologically, univalent and divalent reduction of oxygen is an important attribute of aerobic cellular respiration and an intrinsic part of normal metabolism. Under normal conditions, ROS are used for cell functions such as alcohol oxidation or phagocytosis (108). Due to the toxicity of ROS, cells have developed powerful metabolic activities to deal with these harmful intermediates and to keep their concentrations in a harmless range. Problems arise when these regulatory systems that physiologically protect the cell break down and become destructive (109).

Despite the mitochondria playing a central role in energy metabolism and cell survival, it can generate superoxide during energy production. In the mitochondrial electron transport chain, reducing equivalents in the form of NADH (insert in complex I) and FADH<sub>2</sub> (insert in ubiquinone then goes to complex II) in the form of electrons flow through complex III and IV (110). During this process, an electrochemical gradient (also known as membrane potential) is established as protons are pumped into the intermembrane space. High membrane potential or inhibition at the complexes can restrict electron flow and increases the chance of electron leakage from complex I and III. The electrons are then transferred to O<sub>2</sub> for O<sub>2</sub><sup>•-</sup> generation.

Nitric oxide (NO) is a free radical in which the unpaired electron is delocalized between two different atoms (111). In the CNS, it is produced as a major signaling molecule that can aid in regulating blood flow, neurotransmission, memory and synaptic

plasticity. NO can exert neuroprotective effects via two mechanisms: stimulation of sGC/cGMP system and induced expression of antioxidant and pro-survival pathways (78).

Paradoxically, the same concentrations of NO that are purposeful for neurological function can also mediate cytotoxicity and neurodegeneration (78). Under stressful conditions where superoxide is being generated, NO can trigger and amplify neurotoxicity. It can participate as a cytotoxic effector molecular and/or a pathogenic mediator when produced at high rates by either inflammatory stimuli-induced nitric oxide synthase (iNOS) or overstimulation of the constitutive forms (eNOS and nNOS) (112). NO has the ability to form peroxynitrite ( $\text{ONOO}^-$ ), a dangerous and specific oxidant through a diffusion-limited reaction with superoxide (113).

Peroxynitrite, despite being a nonradical, is more damaging to human tissues than superoxide or nitric oxide. It is a strong oxidizing agent, oxidizing biological molecules including lipids, DNA and proteins. It is formed during the near instantaneous reaction of nitric oxide with superoxide anion (114). Low levels of peroxynitrite can be detoxified by enzymatic and nonenzymatic systems which allow the direct toxic effects of nitric oxide and superoxide to be neutralized (115). The conversion of superoxide to peroxynitrite by NO is 3x faster than the rate at which normal SOD can catalyze superoxide to hydrogen peroxide (116). Peroxynitrite levels are kept low because of the antioxidant capabilities of SOD, but small changes in NO and superoxide levels can greatly increase peroxynitrite formation (114). Peroxynitrite cannot be directly measured because it is a transient molecule with a biological half-life of 10-20 ms (extramitochondrial peroxynitrite) (117). Intramitochondrially produced peroxynitrite

has an even shorter half-life of 3-5 ms due to the large abundance of metalloproteins, fast-reacting thiols and CO<sub>2</sub> (118). These half-lives are both shorter than that of nitric oxide (1-30 s) (112).

### *Glutamate Excitotoxicity*

Glutamate is part of the family of excitatory amino acids (EAAs) and is the most prominent excitatory neurotransmitter found in the central nervous system (CNS) with levels ranging from 5-10 mmol/kg tissue (119). It is processed through several metabolic steps in the body. Initially,  $\alpha$ -ketoglutarate is converted to glutamate (a nonessential amino acid) via deamination by the enzyme glutamate dehydrogenase or by transamination by transaminase enzymes which get metabolized through the Krebs (tricarboxylic acid) cycle in order to obtain succinate, fumarate and then malate, successively (120). Cerebral glutamate is mainly produced in this manner. Another way that the body can obtain glutamate is by deamination of glutamine by the mitochondrial and possibly neuron-specific, phosphate activated enzyme, glutaminase (121).

A key characteristic of ALS is excessive stimulation of glutamate receptors which leads to excitotoxicity (120). Glutamate is released by the presynaptic neuron into the synaptic cleft where it binds and activates ionotropic receptors (ligand-gated ion channels) and metabotropic receptors (G protein-coupled receptors). Both ionotropic and metabotropic receptors can each be divided into three classes and can be localized in presynaptic terminal, postsynaptic element and the surrounding astrocytes (122, 123). Metabotropic receptors are divided into class I, II and III and serve as long-lasting modulators of glutamatergic transmission via G protein-regulated enzymes to produce

different second messengers such as cyclic adenosine monophosphate or  $\text{Ca}^{2+}$  (124). The ionotropic receptors are N-methyl-D-aspartic acid (NMDA),  $\alpha$ -amino-3-hydroxy-5-methyl-4-isoxazolepropionic acid (AMPA) and kainate (KA). These receptors are classified based on how responsive they are and their affinity to exogenous agonists (120). Contrary to the NMDA receptor, AMPA/KA receptors are impermeable to  $\text{Ca}^{2+}$ . The NMDA receptors are known to be responsible for time-consuming and long lasting excitatory transmission and are permeable to  $\text{Ca}^{2+}$ ,  $\text{Na}^+$ , and  $\text{K}^+$  (125). AMPA and KA have fast excitatory transmission led by the entrance of  $\text{Na}^+$  and  $\text{K}^+$  ions causing the depolarization of the neuron and the removal of the  $\text{Mg}^{2+}$  that blocks the NMDA receptors. The function of KA receptors is currently unknown. AMPA receptors lacking the subunit protein GluR2 (which makes them permeable to  $\text{Ca}^{2+}$ ), and NMDA receptors are the primary sources of intracellular  $\text{Ca}^{2+}$  in neurons due to their heightened permeability (125). These receptors are expressed in motor neurons (126, 127) and contribute greatly to glutamate excitotoxicity and the neurodegeneration that results from it.

In a normally functioning synapse, the presynaptic terminal releases glutamate where it then binds and activates NMDA and AMPA receptors resulting in an influx of  $\text{Na}^+$  and  $\text{Ca}^{2+}$  /  $\text{Na}^+$  ions respectively, causing the post synaptic cell to become depolarized and ultimately lead to an action potential (120). Under physiological conditions, intracellular calcium levels are maintained at a very low (micromolar) concentration relative to extracellular levels. Cytosolic free calcium concentration is regulated by plasma membrane calcium transporters such as the plasma membrane calcium pump (PMCA) and  $\text{Na}^+/\text{Ca}^{2+}$  exchanger. Within the cell, the endoplasmic reticulum (ER) and

mitochondria are significant sources of calcium stores. Free calcium from the cytosol is moved to the mitochondria while calcium is sequestered by the ER.

Once glutamate is no longer needed, its action is terminated when it is removed by systems mainly located in astrocytes that surround the synapse (120). Astrocytes convert glutamate into the inactive glutamine, which is then moved to the presynaptic neuron via a glutamine-reuptake system and converted back to glutamate. Normal extracellular glutamate concentrations are in the low micromolar range which can span between 0.02-20  $\mu\text{M}$  depending on the type of technology used to make the measurement (128, 129). These levels are too low to activate high-affinity glutamate receptors (120). During an action potential, glutamate release exceeds 1 mM for <10 ms and then quickly returns to <20 nM once glutamate is taken up by astroglia and presynaptic neurons (128).

Compared to controls, plasma glutamate levels are elevated by ~70% in ALS patients (130). Interestingly, glutamate levels are significantly decreased in all CNS regions studied in ALS patients (by 21-40%), with the greatest decrease observed in the spinal cord. However, there are mixed results as other studies have shown that glutamate levels are elevated in the CSF of sALS patients (131). This was first observed by Rothstein et al., who found a decrease in maximal velocity of transport for high-affinity glutamate uptake in synaptosomes from the spinal cord (-59%  $P < 0.001$ ), motor cortex (-70%,  $P < 0.001$ ) and somatosensory cortex (-39%,  $P < 0.05$ ) (132). The affinity of the transporter for glutamate was unchanged.

Excitotoxicity occurs when the activation of glutamate receptors is excessive and dysregulated as a result of increased glutamate concentrations surrounding the vicinity of

the neuron. This is speculated to be an evolutionary adaptation as a means of protecting the integrity of the CNS with a cellular apoptotic back-up plan to eliminate diseased cells (125).

This can also be induced by impaired glutamate uptake by astrocytes (120). Excitatory amino acid transporters (EAATs) are a family of 5 proteins (EAAT 1-5) that use the  $\text{Na}^+/\text{K}^+$  transmembrane gradient to transport glutamate back into the cells following its release (133). EAAT1-2 is mainly located in astrocytes, whereas EAAT3-5 is expressed mainly by cortical neurons. Astrocytes of SOD1 mice show an absence in glutamate transporter 1 (GLT-1) expression. EAAT2 (glutamate transporter 1 (GLT1) in rodents) is the predominant CNS glutamate transporter and accounts for over 90% of the total CNS glutamate uptake (134, 135). This is consistent with findings of decreased GLT-1 expression around the time of spinal motor neuron degeneration in SOD1 mice (1, 136).

The resulting excessive stimulation of the glutamate receptors causes a large influx of calcium ion into the post synaptic neuron by directly opening ions channels and affecting mechanisms necessary for calcium homeostasis. The influx of  $\text{Ca}^{2+}$  and  $\text{Na}^+$  as a result of stimulated glutamate receptors causes membrane depolarization which can activate voltage-dependent calcium channels, further increasing intracellular  $\text{Ca}^{2+}$  levels. A decrease in the sodium gradient across the cell membrane disallows the  $\text{Na}^+/\text{Ca}^{2+}$  exchanger to remove the excess intracellular calcium. Because ALS has also dysregulated ATP production, ATP-dependent calcium transporters and the energy-dependent  $\text{Na}^+/\text{Ca}^{2+}$  exchanger are adversely affected further increasing intracellular calcium levels.

Heightened accumulation of glutamate-induced intracellular calcium leads to a destructive cascade of membrane, cytoplasmic and nuclear events which lead to neurotoxicity and degeneration (137). This includes the activation of proteases, phospholipases, endonucleases and pro-oxidant enzymes (138). Over-activation of many enzymes such as protein kinase C, calcium/calmodulin-dependent protein kinase II, phospholipases, proteases and NO synthase also occurs (137). Some of these enzymes produce positive feedback loops which can increase the rate of neurodegeneration. For example, an increase in NO synthase activity can increase NO and superoxide levels, subsequently increasing peroxynitrite levels thus further inducing oxidative stress. Atrophy of neuronal cells can feed into a vicious cycle causing further elevation in extracellular glutamate levels and thus excitotoxic damage (120).

Inconsistent evidence in extracellular glutamate levels has been observed in chronic neurodegenerative diseases (139). Thus, the concept of “secondary” or “slow-onset excitotoxicity” has been developed. The hypothesis states that despite normal extracellular levels, glutamate can cause the death of specific neurons that may have been hypersensitized by a genetic, endogenous or exogenous metabolic factor (140). Potential factors that make the neuron susceptible to this condition include impairment of energy metabolism, trophic support, oxidative stress and altered GluR ionic permeability.

Glutamate levels are significantly high in ALS patients. Assessment of plasma (141) and cerebrospinal fluid (142) of 18-22 ALS patients showed their glutamate levels were double those in healthy controls and other neurological disorder patients. However, these results are inconsistent amongst other studies (125).

### *Protein Nitration*

Peroxynitrite selectively nitrates protein tyrosine residues (114), thereby damaging protein structure and function (143). It does this via a multitude of mechanisms involving direct reactions with target molecules (e.g thiols, transition metal centers) or by secondary decomposition to yield nitrogen dioxide ( $\text{NO}_2\bullet$ ), carbonate radical ( $\text{CO}_3\bullet^-$ ) and to a minor extent hydroxyl radicals ( $\bullet\text{OH}$ ), highly reactive free radicals. Protein nitration (addition of nitro group  $-\text{NO}_2$ ) is a very selective process that is limited to specific tyrosine residues on a small number of proteins. Under physiological conditions, both Cu/Zn SOD1 and zinc-deficient SOD1 can use peroxynitrite to catalyze tyrosine nitration (143). Tyrosine nitration has been found in both sporadic and familial ALS patients as well as animal models via antibody identification and mass spectrophotometry (89).

Protein nitration results in the formation of 3-nitrotyrosine (3-NY). Free radicals (i.e.  $\text{NO}_2\bullet$  and  $\text{CO}_3\bullet^-$ ) oxidize tyrosine residues (one electron abstraction) to form tyrosyl radicals which combine with  $\text{NO}_2\bullet$  via diffusion-controlled termination reaction to form 3-nitrotyrosine (3-NY). This peroxynitrite-mediated protein nitration has been observed in Tyr-108 of bovine SOD1 (113) and Tyr-34 of human SOD2 (144). 3-NY is an indicator of peroxynitrite-mediated damage that occurs in tissues and has been identified in the early stages of many neurodegenerative diseases in human and animal models (89).

The mitochondria are particularly important organelles, since they are the main sites of ROS production in the cell. They are an important source and target of nitrating

species (145). Although nitric oxide formation usually occurs outside the mitochondria, its ability to diffuse into the mitochondria and combine with superoxide to form peroxynitrite accounts for much of the disruption in mitochondrial metabolism and the nitration of mitochondrial proteins (115). Peroxynitrite promotes mitochondrial oxidative damage by primarily causing oxidation, secondly nitration and to a lesser extent nitrosation of mitochondrial components (145). It is noted that peroxynitrite can either diffuse from extramitochondrial compartments into the mitochondria (which can diffuse into the organelle) or be formed intramitochondrially (118).

### *Lipid Peroxidation*

Exogenous or endogenous peroxynitrite formation partially promotes mitochondrial lipid peroxidation due to its ability to produce free radicals (118). Polyunsaturated fats, the main target, is essential to membrane fluidity and is the most susceptible to free radical attack and lipid peroxidation (111). Free radicals such as  $\bullet\text{OH}$  and  $\text{NO}_2\bullet$  attack double bonds of unsaturated fatty acids (including fatty acid side chains of membrane lipids), such as linoleic acid and arachidonic acid to abstract  $\text{H}\bullet$  and generate very carbon-centered radicals which react with oxygen to produce peroxy radicals. These go on to further attack other unsaturated fatty acid (specifically adjacent fatty-acid side chains) (109). This chain reaction forms breakdown products which include 4-hydroxy-2,3-nonenal (4-HNE). Increased 4-HNE levels have been observed in the cerebrospinal fluid (CSF) of ALS patients (146). 4-HNE induce toxicity by crosslinking to cysteine, lysine and histidine residues via a Michael addition. This leads to protein modification and dysfunction resulting in inhibition of the neuronal glucose

transporter type-3, the glutamate transporter GLT-1 and Na<sup>+</sup>+K<sup>+</sup>-ATPases (147). 4-HNE can also induce apoptosis at pathophysiologically relevant concentrations (148).

### *Antioxidant Enzymes*

Increase in oxidative stress is accompanied by an upregulation of antioxidant enzymes which work to detoxify oxidative molecules such as hydrogen peroxide in the cell (149). As an oxidizing agent, hydrogen peroxide can impair cellular structures directly or react with iron or copper ions to generate •OH, a potent free radical. Aside from SOD1, there are other antioxidants the body utilizes in order to negate the effects of reactive oxidative species on neurons. Antioxidants such as SOD2, extracellular SOD3, glutathione peroxidase (GPx1) and catalase, have similar function as SOD1 and in some cases work with the enzyme to control superoxide and hydrogen peroxide levels.

Glutathione peroxidase (GPx1) and catalase degrade hydrogen peroxide produced by SOD into water (GPx1 and catalase) and O<sub>2</sub> (catalase) (150). In 95-day-old *ad libitum* high copy G93A mice, the normal adaptive response is to upregulate SOD1 (7-10 fold), SOD2 (5-fold) and catalase (2-fold) (83). Moreover, in similar animal models of ALS, 90- and 105-day-old G86R mice exhibit an increase in the mRNA expression of GPx1, a response that is attributed to denervation (151).

SOD2 (or MnSOD), an endogenous protein and an isoform of the SOD family, is responsible for scavenging superoxide in the mitochondrial matrix. It also plays a critical role in inhibiting the intramitochondrial formation of peroxynitrite. SOD2 is necessary for survival, and most knockout mice die at birth as a result of severe neurological deficits and oxidative injury (152). In transgenic mSOD1 mice, partial knockdown of

SOD2 accelerates motor neuron loss and disease progression (153). The cofactor for SOD2 is manganese (Mn) which assists in catalyzing superoxide dismutation in the active site and has a tyrosine at position 34 at the entrance to the active site. SOD2 converts  $O_2^{\bullet-}$  into  $H_2O_2$  and protects ROS-sensitive proteins in the ETC such as aconitase,  $\alpha$ -ketoglutarate dehydrogenase and succinate dehydrogenase from oxidative damage (110). SOD2 is a specific target of nitration (154). The agent responsible for SOD2 nitration and subsequent inactivation *in vivo* is peroxynitrite, which rapidly reacts with the Mn in the centre of the enzyme (155), nitrating and subsequently inactivating Tyr-34 residue on the enzyme (156). Tyr-34's high susceptibility to peroxynitrite is probably due to the fact that the Mn atom can catalyze its site-specific nitration (155) due to Mn's close proximity to the active site. Inactivation of SOD2 results in impaired function and thus an inability to scavenge superoxide which results in oxidative damage in the mitochondria. SOD2 can also be damaged by ROS. NO can reversibly inhibit cytochrome c oxidase (complex IV) of the respiratory chain (157) which inhibits electron flow, thereby increasing electron leakage at upstream complexes to form superoxide in the matrix and subsequently increase peroxynitrite production. When peroxynitrite nitrates and inactivate SOD2, it prevents the enzyme from scavenging superoxide and thus accelerates peroxynitrite formation (78). Eventually, this can trigger apoptotic signaling of cell death, in part by thiol oxidation-dependent assembly of the permeability transition pore (145).

Catalase is a ubiquitous enzyme that degrades hydrogen peroxide to water and oxygen with high efficiency (158). It is a porphyrin (ring structure) enzyme that contains iron. Catalysis of hydrogen peroxide by catalase occurs in two steps. The enzyme is

initially oxidized to a high-iron intermediate known as Compound I (Cpd I) which is subsequently reduced back to resting state by further reacting with hydrogen peroxide. Specifically, the oxidized iron binds to one of the oxygen atoms in hydrogen peroxide and splits it in order to attain water and oxygen ( $2\text{H}_2\text{O}_2 = 2\text{H}_2\text{O} + \text{O}_2$ ) and to regain its reduced iron form (158). Catalase is present in virtually all mammalian cell types (108). Specifically, it is found in peroxisomes, highly dynamic cell organelles that play important roles in many metabolic pathways (159). In order to function, peroxisomes interact with other cell organelles, including the mitochondria and the endoplasmic reticulum (ER) (159). In mammalian cells, peroxisomes and the mitochondria are metabolically linked (160), cooperate in antiviral signaling (161), and in defense share key components of their division machinery (162). Disturbances in peroxisomal metabolism triggers signaling/communication events that ultimately result in increased mitochondrial stress (163). For reasons unclear, increased ROS production inside peroxisomes rapidly disturbs the mitochondrial redox balance and leads to extreme amounts of mitochondrial fragmentation (164). Thus, it is important for the cell to have well-functioning peroxisome and antioxidant activity. Astrocytes surrounding motoneurons possess high levels of antioxidant systems to protect neurons against oxidative stress (165, 166). Despite the glutathione redox system being the most pronounced antioxidant system in astrocytes, neuroprotection of striatal neurons *in vitro* against hydrogen peroxide is mainly due to catalase activity in astrocytes (167).

GPx1 is a hydrogen peroxide removing enzyme that requires selenium for proper function. It is found in the cytosol and mitochondrial matrix and removes  $\text{H}_2\text{O}_2$  by using it to oxidize reduced glutathione (GSH) and converting it to oxidized glutathione

(GSSG). GSH is then regenerated from GSSG by glutathione reductase (GR), a flavoprotein enzyme that uses NADPH as a source of reducing power. GSH protects mitochondria against peroxynitrite-induced damage through different mechanisms (168, 169). GSH reacts with  $\text{NO}_2\bullet$ ,  $\text{CO}_3\bullet^-$  and  $\bullet\text{OH}$  formed during peroxynitrite/ $\text{CO}_2$  reactions (144) and can reduce protein radicals (thiyl, tyrosyl, tryptofanyl) through one-electron oxidations. This yields glutathionyl radical ( $\text{GS}\bullet$ ), which is converted to GSSG. Glutathione is a tripeptide of glutamate, cysteine and glycine bound via a gamma peptide linkage. Glutathione synthesis is governed by the enzymes of the  $\gamma$ -glutamyl cycle where glutamate is added and removed at discrete steps (170).  $\gamma$ -glutamyl cysteine ligase is the enzyme that utilizes glutamate to synthesize glutathione.

Postmortem studies on the precentral gyrus of 9 sALS patients showed that GPx1 activity (measured via spectrophotometric assay) was reduced significantly in sALS patients vs. controls ([mean  $\pm$  SEM]:  $13.8 \pm 2.6$  nmol/min/mg protein vs.  $22.7 \pm 0.5$  nmol/min/mg protein respectively) (171).

### *Neuroinflammation*

Inflammation is an important aspect of ALS pathology (87, 172). The cerebrospinal fluid (CSF) of ALS patients has shown abnormalities in the pro- and anti-inflammatory cytokines and growth factors which include IL-10, IL-6, GM-CSF, VEGF and IFN- $\gamma$  (173).

Sources of pro- and anti-inflammatory cytokines within the CNS are astrocytes that protect and promote survival of motor neuron cells. They are the most prevalent cell type found in the CNS. As well as their important structural role, they also regulate

homeostasis of the external environment, influence neuronal excitability by modulating the release of neurotransmitters and ions and promote neuron health by releasing growth factors (174, 175).

In comparison to ALS patients, astrocytosis and neuroinflammation is more dramatic in rats and mice possessing the SOD1 mutation (78, 84). This can possibly explain why degeneration occurs at a much faster rate in animals vs. humans. Upon activation by lipopolysaccharides (LPS) or cytokines, astrocytes adopt a toxic profile via mechanisms involving inflammatory-inducible NOS (iNOS) expression (176). Brief exposure to peroxynitrite, but not hydrogen peroxide, is sufficient to induce an inflammatory response in isolated spinal cord astrocytes which would initiate apoptosis of subsequently co-cultured motor neurons (177). Inflammation in mSOD1 is associated with apoptosis via activation of caspase 1 and caspase 3 (178).

### *Neurotrophic factors*

Survival of motor neurons relies heavily on appropriate support of neurotrophic factors (179, 180). Brain derived neurotrophic factor (BDNF), glial cell derived neurotrophic factor (GDNF) and vascular endothelial growth factor (VEGF) can rescue motor neurons from different insults to the cell (87). In disease, activated astrocytes affect motor neurons by reducing their release of neurotrophic factors. Evidence from cell cultures show that both exogenous and endogenous mSOD1 can increase the production of pro-inflammatory cytokines such as IL-6 and TNF- $\alpha$  and free radicals (181). The presence of mSOD1 can also reduce the expression of BDNF and IGF-1 which can amplify the effects of pro-inflammatory cytokines on vulnerable motor neurons (87).

Motor neurons cultured from embryonic rat spinal cord tissue exposed to BDNF constitutively express endothelial NOS (eNOS), which supports motor neuron survival by stimulating cyclic GMP (cGMP) synthesis through NO binding to the heme group of soluble guanylate cyclase (182).

Removal of neurotrophic factors increases NO production by upregulating neuronal NOS (nNOS) in cultured motor neurons. Deprivation of trophic factors also stimulates co-generation of superoxide, which promotes the endogenous production of peroxynitrite (78).

### *Apoptosis*

Endogenous production of peroxynitrite by cultured motor neurons can activate apoptotic cascades (183). In the presence of several different neurotrophic factors, motor neurons isolated from spinal cords or embryonic rats develop the phenotype of a mature motor neuron over a period of ~1 week (183). If at any point the trophic factors are withdrawn, ~50% of the motor neurons undergo apoptosis (184). As well, neurotrophic factor deprivation leads to increased 3-NY immunoreactivity and activates apoptosis within 24 h in more than 60% of cultured neurons (183). NO-dependent activation of cGMP can prevent apoptosis in motor neurons by blocking the expression of nNOS through sequestration of free intracellular calcium via cGMP and inhibition of calcium influx through NMDA receptor (185). Motor neuron death requires the simultaneous production of both nitric oxide and superoxide, suggesting that peroxynitrite serves as an early intermediate for activating apoptosis after trophic-factor deprivation (183).

Excessive ROS generation leads to dysregulation of intracellular calcium signaling. Calcium is an important mineral for signal transduction, and because of this calcium is sensitive to different stimuli and can elicit a multitude of responses in the cell. Evidence suggests that a disruption in calcium homeostasis is an important property of neurodegenerative diseases as it leads to the breakdown of a large amount of cellular processes. Abnormal influxes of calcium levels stimulate multiple pathways that lead to the activation of apoptotic cascades (109). ROS-induced calcium influxes lead to excitotoxic responses such as activation of the glutamate receptor that trigger a cascade (i.e. caspase 3 cascade) of events that lead to cell death. During apoptosis, cytochrome c is released by the mitochondria to the cytosol possibly via channels that make up the pro-apoptotic Bax (186). Bcl-2 block the release of cytochrome c, possibly by interfering with membrane insertion and pore formation by the Bax protein or through disruption of the mitochondria's membrane potential and membrane homeostasis (186). High expression of bcl-2 protein in SOD1<sup>G93A</sup> mice is able to slow disease onset and increase survival by 3 to 4 weeks (187)

A major outcome of SOD1 mediated cell death is the activation of caspase-3, an important cysteine-aspartate protease that is responsible for degrading cell components important for apoptosis (1). In SOD1<sup>G93A</sup> models, release of cytochrome c from the mitochondria is followed by activation of caspase-9, which subsequently activates caspase-3 by cleaving it. Caspase-3 goes on to cleave specific cell protein and DNA, which ultimately leads to cell death.

## Vitamin D

Vitamin D is a fat-soluble vitamin which functions like a steroid hormone to regulate immune function. It is important for different biological processes in the human body and is essential for health, growth and development (188). It has great importance for the metabolism of phosphorous and calcium and has anti-inflammatory, anti-proliferative and modulatory effects on CNS components such as neurotrophins, growth factors and neurotransmitters (189). On a cellular level, vitamin D regulates more than 200 genes and aids in cell angiogenesis, apoptosis and differentiation (190). 90-100% of human vitamin D intake is acquired from the contact of the sun's ultraviolet B (UVB) rays on skin (188, 191). 7-dehydrocholesterol, which lies under the skin, becomes converted into a pre-form of vitamin D once it is in contact with UVB rays at wavelengths of 290-315 nm. As a result of the body's temperature, the pre-form is then converted into cholecalciferol, better known as vitamin D<sub>3</sub>, after which it goes into the blood stream and enters the circulation. Cholecalciferol can also be acquired from the diet (10% of vitamin D intake) via animal products (191). Another form of the vitamin, ergocalciferol or vitamin D<sub>2</sub>, is acquired from plant products (191). Though a definitive difference has not been found between the body's efficiency towards the absorption of ergocalciferol vs. cholecalciferol, many studies have found that vitamin D<sub>2</sub> is less effective in humans compared to D<sub>3</sub> (192). Once the vitamin enters circulation, it is transported to the liver where it is hydroxylated to become calcidiol or 25-hydroxyvitamin D (25(OH)D<sub>3</sub>) via the enzyme 25-hydroxylase (CYP2R1 and CYP27A1). 25(OH)D<sub>3</sub> is the most predominant metabolite in circulation and is utilized as a means of evaluating overall vitamin D status in individuals (191). Calcidiol's use in

research as an indicator is also due to its long half life of 20-90 days, in comparison to calcitriol which has a half life of only 12-16 hours (193). In order to activate the vitamin, calcidiol must undergo hydroxylation in the kidneys via 25(OH)D<sub>3</sub> 1- $\alpha$ -hydroxylase (CYP27B1) to synthesize calcitriol or 1 $\alpha$ , 25-dihydroxyvitamin D<sub>3</sub> (1 $\alpha$ , 25(OH)<sub>2</sub>D<sub>3</sub>) (188, 191). Though 1- $\alpha$ -hydroxylase is found mainly in the kidneys, extrarenal 1- $\alpha$ -hydroxylase is expressed in many vitamin D target cells such as skin, lymph nodes, colon, pancreas, adrenal medulla, brain and placenta (194). For calcitriol to exert its effects, it can directly interact with the cell membrane or can act as a gene transcription modulator by binding to vitamin D receptors (VDR) either at a nuclear level or embedded within the cell membrane (191). Many cells within the body contain VDR allowing vitamin D to exert its effect on them. Such interactions can also allow calcitriol to exert its immunomodulatory effects (195). 1- $\alpha$ -hydroxylase is essential in allowing high-affinity binding to VDR. Though both can bind to the receptor, calcidiol affinity to VDR is 100-200 times lower than calcitriol (196)

According to Health Canada, children and adults aged 9-70 years have a recommended dietary intake (RDA) of 600 IU (15 mcg) of vitamin D per day (197). Food sources high in vitamin D content are fish such as salmon, cod and halibut, cheese and other dairy, or foods fortified with the vitamin such as orange juice and cereals (188). Both vitamin D<sub>2</sub> and D<sub>3</sub> can also be supplemented in 400, 800, 1000 and 2000 IU per one dose (188). Vitamin levels as high as 10 000-15 000 IU can be obtained via 10-15 minutes of sun exposure (188). There are multiple influencing factors that can affect the amount of vitamin D production, including time of day, season, skin colour, clothing, use of sunscreen and latitude. For adequate vitamin D levels, it is recommended to

expose large body parts such as arms and legs to sunlight for 5-30 minutes, twice a week (188). The most advantageous serum levels are between 90-100 nmol/L which is necessary in order to optimize the metabolism of calcium and phosphorous (to prevent osteoporosis and pathological fractures), and aid in preventing autoimmune diseases such as MS, infections, and three major cancers (colon, breast and prostate) (189).

#### *Calcidiol and Calcitriol Serum Levels*

Currently, there is much controversy surrounding adequate 25(OH)D<sub>3</sub> serum levels for good health. The variable normal ranges in different populations can be possibly a result of adaptation (198). The Institute of Medicine recommends 50 nmol/L (197). However, different studies have suggested different cut-off points for serum levels. Holick et al suggest <50 nmol/L to be deficient, 52.5-72.5 nmol/L to be sufficient and >72.5 nmol/L to be optimal (199). Hanley et al suggest <25 nmol/L to be deficient, 25-75 nmol/L to be sufficient and >75 nmol/L to be optimal (200). In adolescents 12-19 y, Saint-Onge et al suggest <27.5 nmol/L to be deficient, 27.5-50 nmol/L to be sufficient and >50 nmol/L to be optimal (201). Other studies have suggested minimum serum levels of 75 nmol/L (202), upper limit of 250 nmol/L (189) and toxic levels at 750 nmol/L (189). Serum calcidiol concentration of 75 nmol/L is considered to be optimal, since lower levels cause a stimulation of parathyroid hormone (PTH), and the occurrence of osteoporosis and pathological fractures increases (189). Conversely, the normal serum concentration of 1  $\alpha$ , 25(OH)<sub>2</sub>D<sub>3</sub> is clearly defined as being 0.03-0.14 nmol/L (203).

### *Vitamin D toxicity*

Vitamin D toxicity (hypervitaminosis D) results from excessive vitamin D intake. This results in an elevation of plasma concentrations of vitamin D<sub>3</sub>; 25(OH)D<sub>3</sub>; 24,25(OH)<sub>2</sub>D<sub>3</sub>; 25,26(OH)<sub>2</sub>D<sub>3</sub>; and 25(OH)D<sub>3</sub>-26,23-lactone, although toxicity rarely leads to a rise in plasma 1 $\alpha$ ,25(OH)<sub>2</sub>D<sub>3</sub> (204). 25-hydroxyvitamin D-24-hydroxylase (CYP24A1) plays an important role *in vivo*, regulating concentrations of both the precursor 25(OH)D<sub>3</sub> and the hormone 1 $\alpha$ ,25-dihydroxyvitamin D<sub>3</sub>. CYP24A1 degrades both 25(OH)D<sub>3</sub> and 1 $\alpha$ ,25(OH)<sub>2</sub>D<sub>3</sub> through a side-chain hydroxylation and cleavage pathway known as C-24 oxidation. Studies in the CYP24A1-null mouse has shown that CYP24A1 absence leads to an inability to degrade vitamin D metabolites resulting in hypercalcemia (high intracellular calcium levels), nephrocalcinosis, and death in 50% of animals (205). A study by Shephard and DeLuca investigated hypervitaminosis D in acutely intoxicated rats fed graded oral doses of vitamin D<sub>3</sub> (0.65 to 6500 ng/d for 14 d) or calcidiol (0.46 to 4600 ng/d for 14 d) (206) Plasma vitamin D<sub>3</sub> and calcidiol concentrations rose to micromolar levels in rats with the highest intakes of vitamin D<sub>3</sub>, resulting in marked hypercalcemia. The study showed that toxicity is not reached with calcidiol concentrations of 100-250 nmol/L, and that it is only when concentrations exceed 375 nmol/L that hypercalcemia occurs.

## **ALS and Vitamin D**

### *Vitamin D and ALS pathophysiology*

Vitamin D deficiency has been associated with the development of inflammatory and immune diseases such as type II diabetes (207), multiple sclerosis (195), dementia and Alzheimer's disease (208).

In rat mesencephalic culture, pretreatment with calcitriol protected dopaminergic neurons against the neurotoxic effects of glutamate and dopaminergic toxins (209). As well, 24-hour pretreatment with calcitriol inhibited the increase in intracellular ROS, after exposure to H<sub>2</sub>O<sub>2</sub>. In the rat model of perinatal asphyxia, calcitriol was neuroprotective when it was co-applied with glutamate or even after a delay of up to 6 hours during a 24-hour excitotoxic exposure to hippocampal and neocortical cells. As well, calcitriol reduces glutamate-induced caspase-3 activity in cerebellar granule cells dependent on cell maturity (210).

When investigating the effects of vitamin D on biomarkers of oxidative stress in obese children aged 7-14 y, obese children with calcidiol insufficiency (<50 nmol/L) had significantly elevated IL-6, malondialdehyde (MDA; a marker of lipid peroxidation) and 3-NY levels vs. non-deficient obese children (>50 nmol/L) (211). A partial correlation analysis showed an inverse relationship between calcidiol and 3-NY ( $r = -0.424$ ,  $P = 0.001$ ).

It has been shown that SOD is induced by activated vitamin D (212). In rats, supplementation with calcitriol can increase SOD activity levels and prevent DNA damage (213). In the arterial walls of rabbits, injection with high doses of calcitriol (10

000 IU/kg) was able to increase antioxidant activity (SOD, GPx and catalase) and lower lipid peroxidation (214).

Vitamin D increases neurotrophic factors which may assist in prolonging the lifespan of ALS patients. Insulin-like growth factor (IGF-1) and glial cell line-derived neurotrophic factor (GDNF) are examples of neurotrophic factors that are essential for the survival of motor neurons *in vivo* and *in vitro* (180). Vitamin D can induce the action of IGF-1 by increasing the number of IGF-1 receptors (215). GDNF has neurotrophic effects on several different types of neurons *in vivo*, including dopaminergic neurons of the substantia nigra (216, 217) and noradrenergic neurons of the locus coeruleus (218). Vitamin D<sub>3</sub> has the ability to enhance GDNF mRNA expression *in vitro* and *in vivo* (219)

Experimental evidence suggests that the metabolism of vitamin D in the CNS is responsive to inflammation (220). Experiments conducted in female experimental autoimmune encephalomyelitis (EAE) mice, a model of multiple sclerosis (MS), have shown that consumption of vitamin D<sub>3</sub> reduced the inflammation before EAE development (221). A study assessing circulating inflammatory cytokines in young adults (25-42 y) as well as serum calcidiol found that serum levels of subjects in the insufficient group (calcidiol  $\leq 80$  nmol/L, n = 14) had significantly higher pro-inflammatory cytokines (IL-1 $\beta$ , IL-2, interferon- $\gamma$ , TNF- $\alpha$ ) (P < 0.05) vs vitamin D-sufficient adults (222). The study suggested that vitamin D insufficiency, in part, could result in pro-inflammatory stress. Vitamin D also has positive effects on anti-inflammatory cytokines such as interleukin 10 (IL-10). In a study of 93 patients with congestive heart failure (CHF) where vitamin D<sub>3</sub> was supplemented at 2000 IU/d for 9

mo (which increased serum calcidiol levels from 35 nmol/L to approximately 67 nmol/L), IL-10 levels were 43% higher than baseline (2 pmol/L vs. 1.4 pmol/L, respectively) (223). The study suggested that vitamin D<sub>3</sub> reduces the inflammatory milieu in CHF patients and has the potential to serve as an anti-inflammatory agent for future disease treatment.

#### *Clinical trials of vitamin D supplementation in ALS patients*

In a retroactive study by Karam et al, of 37 consecutive ALS patients with an initial mean serum calcidiol of 55 nmol/L (81% had calcidiol < 75 nmol/L, and 43% had calcidiol < 50 nmol/L) (224) 20 of these patients with calcidiol < 75 nmol/L were supplemented with 2000 IU of vitamin D<sub>3</sub> for 12 months. ALS severity was recorded (ALSFRS-R) at the beginning and in 3-month increments afterwards. At the 6-month follow-up, median serum calcidiol rose in the supplemented group from 45 nmol/L to 77.5 nmol/L, and ALSFRS-R scores of all patients declined. However, at the 9-month follow up these scores had declined significantly less in the vitamin D group (P = 0.02). Supplementation with vitamin D showed trends towards higher ALSFRS-R scores at 3 and 6 months after age and baseline vitamin D levels were adjusted (P = 0.07 and P = 0.09 respectively). These results are supported by a retrospective study that found that ALS patients with serum calcidiol levels <25 nmol/L increased their death rate by 6 fold, their rate of decline by 4 times and were associated with a marked shorter life expectancy compared to patients with calcidiol levels >75 nmol/L (225).

*Effects of vitamin D in the G93A mouse model of ALS*

Vitamin D-deficient G93A mice had lower paw grip endurance and motor performance and higher clinical score when compared to AI vitamin D<sub>3</sub> mice (226). Alternatively, G93A mice supplemented with 10x AI had greater paw grip endurance and motor performance score compared to AI mice (227). In addition, 50x AI G93A mice had a greater paw grip endurance during disease progression compared to AI mice (228).

## **RATIONALE, OBJECTIVES, HYPOTHESES AND PILOT STUDIES**

### **Rationale**

Given that vitamin D modulates several pathophysiologies common to ALS, it can serve as a potential therapeutic.

### **Objectives**

To investigate the effects of dietary vitamin D<sub>3</sub> restriction, adequacy and supplementation on markers of oxidative damage, antioxidant enzymes, inflammation, apoptosis, neurotrophic factors and neuron count in the spinal cord of the G93A mouse model of ALS.

### **Hypotheses**

Based on our planned comparisons, we expect the following results:

1. For 4-HNE and 3-NY:
  - a. 50x vitamin D (HiD) lower vs. adequate intake (AI) in males but not females.
  - b. D<sub>3</sub> Deficiency (DEF) higher vs. AI in both males and females.
2. Antioxidant enzymes SOD2, catalase and GPx-1:
  - a. HiD higher vs. AI in males but not SOD2 and catalase in females
  - b. DEF lower vs. AI in both males but not GPx1 in females
3. For TNF- $\alpha$  and IL-6:
  - a. HiD lower vs. AI in males but not females
  - b. DEF higher vs. AI in males and females

TNF-  $\alpha$  and IL-6 are released by both neurons and microglia during spinal cord damage to initiate a pronounced inflammatory response in the spinal cord (87)

4. Because IL-10 is an anti-inflammatory cytokine, we expect:
  - a. HiD higher vs. AI in males but not females.

- b. DEF lower vs. AI in both males and females.

Because of the effects of toxicity in female HiD mice, damage and thus inflammation will be higher in the animal, inhibiting the release of the pro-inflammatory IL-10.

5. Ratio of Bax/Bcl-2 and cleaved/pro-caspase (CASP3):
  - a. HiD lower vs. AI in males but not females
  - b. DEF higher vs. AI in males and females

Based on studies by Parkhomenko et al (229), higher CASP3 was observed in HiD female *gastrocnemius* mice which was likely due to toxicity. These results are predicted to also be observed in the spinal cord because of previous studies by Gianforcaro et al who found a 31% greater disease severity prior to disease onset and reduced food intake (absolute and corrected for body weight) in HiD females (228)

6. GDNF:
  - a. HiD higher vs. AI
  - b. DEF lower vs. AI

7. ChAT and SMI-36/SMI-32 ratio:
  - a. HiD higher vs. AI in males but not females
  - b. DEF lower vs. AI in males and females

As a result of a predicted increase in apoptosis in HiD females and DEF mice, neuronal count is predicted to be lower in these groups.

## **Pilot Studies**

In 2013, we published a paper investigating the influence of vitamin D supplementation and deficiency on disease severity and progression as well as functional outcomes (226, 228) but not molecular outcome measures. In addition, no other study has investigated the impact of vitamin D on the spinal cords of ALS mice. Hence, this study was established as a pilot, because -1- females showed differing results than males when supplemented with 50x AI, -2- vitamin D's effect is tissue-specific (changes in one tissue may not be reflected through changes in other tissues. Indeed, the results in the CNS in these studies did not translate exactly to the changes observed in muscle cells. This is due to the fact that calcidiol is not converted to calcitriol in the muscle, whereas it is in the spinal cord), and -3- the evidence that there is sexual dimorphism in ALS, independent of the toxic effects of 50x AI vitamin D. Given the above, it is evident that the interaction between vitamin D and the mouse model of ALS presents with a complex disease that is difficult to elucidate without a pilot study. Also, since there are several molecular pathways contributing to the pathophysiology of ALS, and since vitamin D influences several cellular processes throughout the body, it was not possible to run a large study and analyze dozens of outcome measures to elucidate the many pathways common to both ALS and vitamin D function without first conducting a pilot study. Based on the findings in these pilot studies, we have paved the way for us and other researchers to be more specific with sample analysis in future studies. In addition, no other study has investigated the impact of vitamin D on the spinal cords of ALS mice. Hence for all these reasons, and notwithstanding our 2013 publication, these are pilot studies.

***Statistically***, P values are set by investigators in an arbitrary fashion (please consult with a statistician about this matter). There is no excellent reason why some disciplines use P values of 0.05, whereas others use P values of 0.10 or even 0.15. The reasons are all excellent, and no reason is better than the other. It is customary in the life sciences discipline to use a P value of 0.10 for pilot studies to avoid type II error. The results of our current studies are not artifactual, and the choice of a P value of 0.10 for these pilot studies does not lead to inaccurate conclusions.

***Ethically***, pilot studies are important to move scientific discovery forward. *In vivo* studies are costly and involve stringent ethical standards. To include a high number of animals that may yield insignificant results without *a priori* understanding which molecular pathways are involved is not only unethical but also irresponsible. Our pilot studies contribute to science vis-à-vis vitamin D's role in ALS specifically, and neurodegenerative diseases in general. As well, our studies are proof-of-concept that present molecular biologists, nutrition physiologists and clinicians with a new potential therapeutic as well as the specific pathways that they would need to investigate when conducting *in vitro*, animal and human studies. This is a major discovery for a fatal disease that hitherto has no cure or even an effective drug (Riluzole has been mediocre at best, and has proven to be inefficacious, and very costly). So far, vitamin D has proven to be a promising, accessible, inexpensive, potential therapeutic for ALS, and probably other neurodegenerative diseases.

The purpose of our studies was to investigate the effect of vitamin D on the spinal cord of G93A mice and stimulate further scientific exploration, with future studies consisting of higher number of subjects. Pilot studies usually entail smaller sample sizes. However, a

smaller sample size results in higher variability, causing an increase in P values. With the use of  $P = 0.10$ , we were able to draw attention to all notable differences in outcome measures. Statistically, any P value is arbitrary and does not affect the final conclusions drawn for the obtained results. The results of our current studies are not artifactual and our choice of  $P = 0.10$  did not lead to inaccurate conclusions. Actually, choosing a P value of 0.05 in a pilot study would result in type II error, and hence to inaccurate conclusions.

**MANUSCRIPT #1:**

**VITAMIN D<sub>3</sub> SUPPLEMENTATION AT 50X THE ADEQUATE INTAKE  
ATTENUATES DISEASE PATHOPHYSIOLOGY IN THE SPINAL CORD OF  
MALE, BUT IS TOXIC IN FEMALE, G93A MOUSE MODEL OF  
AMYOTROPHIC LATERAL SCLEROSIS**

**Moghimi E, Gianforcaro A, Solomon JA, Hamadeh MJ. Vitamin D3  
supplementation at 50x the adequate intake attenuates disease pathophysiology in  
the spinal cord of male, but is toxic in female, G93A mouse model of amyotrophic  
lateral sclerosis. PLoS One 2015 (*in revision*).**

**Vitamin D<sub>3</sub> at 50X the adequate intake attenuates disease pathophysiology in the spinal cord of the male, but is toxic in female, G93A mouse model of amyotrophic lateral sclerosis**

Elnaz Moghimi, Alexandro Gianforcaro, Jesse A Solomon and Mazen J Hamadeh

*<sup>1</sup>School of Kinesiology and Health Science, Faculty of Health, York University, Toronto, Ontario, Canada, <sup>2</sup>Muscle Health Research Centre, York University, Toronto, Ontario, Canada*

**First Author:**

Elnaz Moghimi

**Corresponding Author:**

Mazen J. Hamadeh

**Keywords:** Vitamin D, hypervitaminosis D, amyotrophic lateral sclerosis, spinal cord, motor neurons, neuroprotection, oxidative stress, inflammation, antioxidant capacity, apoptosis, neurotrophic factors, neuron damage

## Abstract

**Background:** Vitamin D<sub>3</sub> (D<sub>3</sub>) at 50x the adequate intake (AI) improves paw grip endurance in G93A mice. However, apoptosis increases in female *quadriceps*, indicating a threshold of toxicity. ALS is a neuromuscular disease characterized by progressive degeneration of upper and lower motor neurons. **Objective:** We analyzed the spinal cords of G93A mice following dietary D<sub>3</sub> supplementation at 50x the AI for oxidative damage (4-HNE, 3-NY), antioxidant enzymes (SOD2, catalase, GPx1), inflammation (TNF- $\alpha$ , IL-6, IL-10), apoptosis (Bax/Bcl-2 ratio, cleaved/pro-caspase 3 ratio), neurotrophic factor (GDNF), and neuron damage (ChAT, SMI-36/SMI-32 ratio). **Methods:** Beginning at age 25 d, 41 G93A mice were provided food *ad libitum* with either adequate (AI; 1 IU D<sub>3</sub>/g feed; 12 M, 11 F) or high (HiD; 50 IU D<sub>3</sub>/g feed; 10 M, 8 F) D<sub>3</sub>. At age 113 d, the spinal cords were analyzed for protein content. Because this was a pilot study, differences were considered significant at  $P \leq 0.10$ . **Results:** HiD females had 14% higher 3-NY ( $P = 0.065$ ), 21% lower catalase ( $P < 0.001$ ), 18% higher GPx1 ( $P = 0.101$ ), 21% higher TNF- $\alpha$  ( $P = 0.003$ ), 13% lower IL-10 ( $P = 0.042$ ), 13% higher cleaved/pro-caspase 3 ratio ( $P = 0.010$ ) and 18% lower ChAT ( $P = 0.024$ ) vs. AI. HiD males had 16% lower 3-NY ( $P = 0.073$ ), 24% lower IL-6 ( $P = 0.085$ ), 26% lower cleaved/pro-caspase 3 ratio ( $P = 0.009$ ) and 19% lower SMI-36/SMI-32 ( $P = 0.098$ ) vs. AI. **Conclusion:** In G93A mice, dietary D<sub>3</sub> at 50x AI is toxic in the spinal cord of females but attenuates disease pathophysiology in males. This is in accord with results in the *quadriceps*, as well as functional and disease severity outcomes. Future studies need to identify the sex-specific therapeutic dose of D<sub>3</sub> for ALS.

## Introduction

Amyotrophic lateral sclerosis (ALS), also known as Lou Gehrig's disease is the most commonly occurring adult-onset motor neuron disease of unknown cause (1, 2) and is typically diagnosed between 45 and 60 years of age (3, 4). It is characterized by degeneration of upper and lower motor neurons, resulting in skeletal muscle atrophy (5) and death by respiratory failure within 3-5 years of initial symptoms (6-8). 90% of cases are of unknown etiology (sporadic ALS; sALS) (3, 9), whereas the other 10% have inherited genetic mutations (3, 10) (familial ALS; fALS), ~12% of these cases being a result of a mutation in the  $\text{Cu}^{2+}/\text{Zn}^{2+}$  super-oxide dismutase 1 (SOD1) gene (11-14). The most commonly used animal model of ALS is the G93A mouse model (15) that transgenically overexpresses the mutant SOD1 gene (10). Their disease pathology and neurodegenerative patterns closely resemble that which is found in ALS patients (10). On a cellular level, excessive stimulation of glutamate receptors (16) leads to a large influx of calcium ion into the post synaptic neuron, resulting in a destructive cascade of membrane, cytoplasmic and nuclear events (17). These include oxidative damage (18, 19), oxidative stress (20, 21), inflammation (22), compromised neurotrophic factor release (22) and apoptosis (13).

The only available therapy for ALS is the antiglutamatergic drug, riluzole, even though nutrition-based interventions have shown differing levels of improvements in animal models of ALS (23). Daily 100 mg oral consumption of the drug may extend life for approximately 2-3 months and may increase the likelihood of survival in the first year by 9% (24). However, riluzole is very expensive, costing approximately \$10,000/year in

the US and £4056/year in the UK (25) Thus, alternative therapies need to be investigated.

Vitamin D is a fat-soluble vitamin with hormone-like properties that is essential for health, growth and development (26). Vitamin D<sub>3</sub> and/or its metabolites [calcidiol (25(OH)D<sub>3</sub>) and calcitriol (1,25(OH)<sub>2</sub>D<sub>3</sub>)] can protect dopaminergic neurons against the neurotoxic effects of glutamate and dopaminergic toxins (27), and has anti-inflammatory and modulatory effects on CNS components such as neurotrophins and growth factors (28). Vitamin D treatment can improve compromised functional outcomes and muscle physiology in humans and rodents, whereas vitamin D receptor (VDR) knockout mice have loss of motor function and muscle mass (29). Vitamin D reduces the expression of biomarkers associated with oxidative stress and inflammation in diseases that share common pathophysiologies with ALS.

In response to oxidative stress and inflammation, vitamin D also increases antioxidant capacity in a multitude of associated disease pathologies. In human prostate cancer cell cultures, the SOD gene is highly induced by calcitriol (30, 31). In phenobarbital induced rat hepatocarcinogenesis, supplementation with calcitriol increases SOD activity levels and prevents DNA damage (32). In the arterial walls of rabbits, injection with high doses of calcitriol (10 000 IU/kg) increased antioxidant activity (SOD, GPx and catalase) and decreased lipid peroxidation (33). Administration of 5000 IU/kg bwt/d calcitriol to diabetic rats enhanced SOD, catalase and GPx (207, 52 and 72%, respectively) in the liver and kidneys compared to diabetic controls (34).

In a retrospective study by Karam *et al* in ALS patients, supplementation with 2000 IU of vitamin D<sub>3</sub>/day for 9 months improved ALS functional rating scale score (ALSFRS-R) (35). We have previously shown the benefits of 10x and 50x the adequate intake (AI) of vitamin D<sub>3</sub> (D<sub>3</sub>) supplementation in G93A mice (36-40). Functionally, D<sub>3</sub> supplementation improved motor performance (37) and paw grip endurance (PaGE) (36, 37), and in their *quadriceps* D<sub>3</sub> supplementation increased antioxidant capacity (40) vs. AI. However, the underlying mechanisms in the spinal cord for the above observations have not been delineated.

Based on our previous studies in the G93A mouse model of ALS (28-30, 32) and those in ALS patients (35), the objective of this study was to examine the effects of high levels of vitamin D<sub>3</sub> supplementation (50 IU/g feed) vs. adequate intake (1 IU/g feed) on spinal cord biomarkers of oxidative damage, antioxidant enzymes, inflammation, apoptosis, neurotrophic factors and neuron damage in the G93A transgenic mouse model of ALS.

## **Methods**

### **Ethical Statement**

The experimental protocol that was used in this study followed the guidelines of the Canadian Council of Animal Care and was approved by York University Animal Research Ethics Board (protocol # 2007-9). All the necessary steps were taken to minimize suffering and distress to the mice in the study.

### **Animals**

Male B6SJL-TgN(SOD1-G93A)<sup>1</sup>Gur hemizygous mice (No. 002726) were harem-bred with non-affected female B6SJL control mice (No. 100012; Jackson Laboratory, Bar Harbor, ME). We identified the presence of the human-derived G93A transgene by using polymerase chain reaction (PCR) amplification of DNA extracted from ear tissue as outlined by Sigma-Aldrich (XNAT REDEExtract-N-Amp Tissue PCR Kit; XNAT-1KT). All breeding mice were housed 3 females per 1 male, and consumed Research Diet AIN-93G (1 IU D<sub>3</sub>/g feed; Research Diet, New Brunswick, NJ). All animals were housed individually at age 25 d in a 12 h light/dark cycle.

### **Study Design**

41 (22 M, 19 F) G93A mice consumed a diet that contained an adequate intake of vitamin D<sub>3</sub> (1 IU/g feed; Research Diet AIN-93G; Product # D10012G; Research Diets Inc, New Brunswick NJ [38]) *ad libitum* after weaning (21 d). At age 25 d, the mice were individually caged and divided into one of two groups: 1) adequate vitamin D<sub>3</sub> (AI; 1 IU D<sub>3</sub>/g feed; 12 M, 11 F; Research Diet AIN-93G) or 2) high vitamin D<sub>3</sub> (HiD; 50 IU D<sub>3</sub>/g feed; 10 M, 8 F; product # D10030802; Research Diets Inc, New Brunswick, NJ) (Table 1).

When the mice reached a clinical score (CS; disease severity) of 3.0, food and calorie-free gel (Harlan-Gel, Harlan Teklad, Madison WI) were placed on the floor of the cage to fulfill ethics requirements. Endpoint was determined as previously described by Solomon *et al* 2011 (41). The calorie-free gel contained synthetic polymers (WATER LOCK<sup>®</sup> superabsorbent polymer G-400, G-430, G-500, G-530; 95% by weight) and methanol (4.5% by weight). A summary of food intake, vitamin D<sub>3</sub> intake and body weight of the G93A mice can be found in Table 1.2. Two researchers who were blinded to the diets conducted all measurements.

**Table 1.1** Nutrient content of the adequate intake (AI) and high (HiD) vitamin D<sub>3</sub> diets

Nutrient	Diet	
	AI	HiD
Energy (kcal/g)	4	4
Carbohydrate (%)	64	64
Protein (%)	20	20
Fat (%)	7	7
Vitamin D <sub>3</sub> (IU/g)	1 <sup>a</sup>	50 <sup>a,b</sup>
Calcium (%)	0.5 <sup>c</sup>	0.5 <sup>c</sup>
Vitamin mix V10037 (mg/g)	10	10
Mineral mix S100022G (mg/g)	35	35

Diets provided by Research Diets (based on AIN-93G; New Brunswick, NJ; AI product # D10012G; HiD product # D08080101;).

<sup>a</sup>, included in vitamin mix V10037

<sup>b</sup>, additional vitamin D<sub>3</sub> was added to reach 50 IU/g feed.

<sup>c</sup>, included in mineral mix S100022G (42)

\* table adopted from Gianforcaro *et al*, PLoS ONE 2013 (36)

**Table 1.2** Food intake, vitamin D<sub>3</sub> intake and body weight of G93A mice.

Measurements	Males		Females	
	AI (n=12)	HiD (n=10)	AI (n=11)	HiD (n=8)
Food intake (g/d)*	3.5±0.1	3.4±0.1	3.4±0.1	3.1±0.1
Food intake (mg/g b.wt./d)*	151.5±5.4	155.2±4.8	195.0±6.7	171.5±5.4
Vitamin D <sub>3</sub> intake (IU D <sub>3</sub> /d)	3.5±0.1	168.2±4.6	3.4±0.1	153.2±5.0
Vitamin D <sub>3</sub> intake (IU D <sub>3</sub> /g b.wt./d)	0.152±0.005	7.759±0.239	0.195±0.007	8.574±0.269
Body weight (g)*	23.1±0.4	21.8±0.6	17.6±0.3	17.9±0.4

AI, adequate intake, n=23; HiD, high vitamin D<sub>3</sub>, n=18; b.wt.: body weight. HiD females consumed 11% less absolute feed (P = 0.041) and 12% less feed corrected for body weight vs. AI females (P=0.020). HiD males consumed 4% less absolute feed vs. AI males (P = 0.047). HiD males consumed 10% more absolute feed (P = 0.042) but 10% less feed corrected for body weight (P = 0.037) vs. HiD females. Males (153.2±3.6 mg/g b.wt./d) consumed 17% less food corrected for body weight vs. females (185.1±5.2 mg/g b.wt./d) (P<0.0001). Males (22.5 ±0.4 g) had 27% higher body weight vs. females (17.8±0.2 g) (P<0.0001). HiD males had 22% higher body weight (P<0.0001) vs. HiD females. HiD males had 6% lower body weight (P = 0.081) vs. AI males. HiD mice (3.2±0.1 g) had 7% less absolute food intake vs. AI mice (3.5 ± 0.1 g) (P = 0.062). Data are means ±SEM.

### Tissue Collection

At age 113 d, mice were sacrificed and spinal cords were harvested. The mice were placed under anaesthesia with gaseous isoflurane as the tissue was collected and placed in individual sterile polyethylene tubes for immediate freezing in liquid nitrogen. Samples were stored at -80°C.

### Spinal Cord Homogenization

Spinal cords were weighed, and minced with a glass-Teflon Port-Evenhejm homogenizer (5% wt/vol) in radioimmunoprecipitation assay (RIPA) buffer (1:20) containing 50 mM tris HCL 8.0 (Bioshop, TRS002.500, Burlington, Ontario), 150 mM

NaCl (BioBasic Canada, 7647145, Markham, Ontario), 0.1% SDS (Bioshop, SDS001.500, Burlington, Ontario), 0.5% sodium deoxycholate (Bioship, DCA333.50, Burlington, Ontario), 1% NP-40 (Thermo Scientific, 28324, Rockford, Illinois), 5 mM EDTA pH 8.0 (Bioshop, EDT001.500, Burlington, Ontario) and 1 mM PMSF (Sigma-Aldrich, 93482, St. Louis, Missouri). The protease inhibitor cocktail (Roche, 11836153001, Mannheim, Germany) was added to the buffer in accordance to manufacturer's instructions (1:100) prior to homogenization. Mouse spinal cord was homogenized for about 40 grinds using constant force to ensure consistency and homogeneity of samples. Homogenates were divided in roughly equal volumes in eppendorf tubes and were placed on a shaker at 4°C for 30 minutes. The homogenates were then centrifuged at (600 g) for 20 min at 4°C. The resulting supernatant was decanted, put into newly labeled eppendorf tubes and immediately stored at -80°C. The protein concentration was determined using the BCA Protein Assay technique (43). The supernatant concentration was measured at 562 nm using an ultraviolet spectrophotometer (Cecil 9200 Super Aquarius, Cambridge, UK). Protein concentrations were presented as mg/ml.

### **Western Blot**

Equal amounts of protein were size-separated by 12.5% sodium dodecyl sulfate-polyacrylamide gel electrophoresis (SDS-PAGE) and were transferred to nitrocellulose membranes (#165-3322, Bio-Rad Mini-PROTEAN 2 electrophoresis system, Mississauga, ON, Canada) at 100 V for 2 h. The membranes were blocked in 3% fat free milk (SMI-36), 5% fat free milk (SOD2, catalase, TNF- $\alpha$ , IL-6) or 5% BSA (4-HNE, 3-NY, GPx1, IL-10, Bax, Bcl-2, pro-caspase 3, cleaved caspase 3, GDNF, ChAT, SMI-32)

diluted in Tris-buffered saline with tween (1%) for 2 h at room temperature and incubated with primary antibodies in 3% fat free milk (SMI36), 5% fat free milk (catalase, TNF-  $\alpha$ , IL-6), 1% BSA (SOD2, cleaved caspase 3, GDNF, ChAT), 3% BSA (IL-10, SMI32) or 5% BSA (4-HNE, 3-NY, GPx1, Bax, Bcl-2, pro-caspase 3) against 4-HNE (1:800; Abcam, ab46545), 3-NY (1:1000; Abcam, ab110282), SOD2 (1:8000; Abcam, ab13533), catalase (1:3500; Abcam, ab1877-10), GPx1 (1:800; Abcam, 22604), TNF-  $\alpha$  (1:2000; Abcam, ab9739) IL-6 (1:1000; Abcam, ab6672), IL-10 (1:2000; Abcam, ab9969), Bax (1:1000; Cell Signaling Technology, 2772), Bcl-2 (1:1000; Cell Signaling Technology, 2870), pro-caspase 3 (1:1000; Millipore, 04-440), cleaved caspase 3 (1:1000; Millipore, 04-439), GDNF (1:1000; Abcam, a18956), ChAT (1:1000; Abcam, ab85609), SMI-32 (1:1000; Abcam, ab28029) and SMI-36 (1:1000; Abcam, ab24572), overnight at 4°C. Equal loading was verified by ponceau staining, as well as probing for glyceraldehyde 3-phosphate dehydrogenase (GAPDH; 1:100,000; MAB374, Millipore). The antigen-antibody complexes were detected by incubating the membranes in anti-rabbit (1: 5000; Novus Biologicals, NB730-H) or anti-mouse (1:5000; Novus Biologicals, NB7539) HRP conjugated secondary antibodies at room temperature for 2 h in 3% fat free milk (SMI36), 5% fat free milk (4-HNE, catalase, TNF-  $\alpha$ , IL-6), 1% BSA (SOD2, cleaved caspase 3, GDNF, ChAT), 3% BSA (IL-10, SMI32) or 5% BSA (3-NY, GPx1, Bax, Bcl-2, pro-caspase 3). Immunoreactive proteins were visualized with enhanced chemiluminescence (sc-2048, Santa Cruz Biotechnology), and scanned using Kodak Imaging Station 4000MM Pro (Carestream Health, Inc. Rochester, NY, USA). Protein intensity was standardized to GAPDH and analyzed using Carestream MI (v 5.0.2.30,

NY, USA). Representative western blot bands for the biomarkers are found in supplementary figure S1.1 in Appendix A.

### **Calculations**

Human equivalent dosage (HED) was calculated according to the US FDA (44):

$$\text{HED} = \text{Animal dose (mg/kg)} \times [\text{animal weight (kg)} \div \text{human weight (kg)}]^{0.33}.$$

### **Statistical analysis**

We established planned comparisons between HiD vs. AI. A one-tailed independent t-test was used to determine differences between the diets within each sex, because we hypothesized *a priori* that absolute and body weight-adjusted spinal cord weight, antioxidant activity, neurotrophic factors and neuronal count would be higher in HiD males vs. AI but not females whereas oxidative damage, inflammation and apoptosis would be lower in HiD males vs. AI but not females. These are based on studies conducted by us and other researchers (23, 29, 34, 36-41, 45-49). For all other outcome measures, a two-tailed analysis was performed. All statistical analyses were completed using GraphPad Prism 6 for Macintosh (GraphPad Software Inc, La Jolla, CA). Data were presented as means  $\pm$  standard error of mean (SEM). Significance was set to  $P \leq 0.10$ , since this was a pilot study.

## **Results**

### **Oxidative Damage**

#### 4-HNE

There was no significant difference in 4-HNE protein content between the diets or between the sexes (Figure 1.1A and 1.1B).

#### 3-NY

HiD females had 14% higher 3-NY protein content vs. AI females ( $P = 0.065$ ) (Figure 1.1C). HiD males had 16% lower 3-NY protein content vs. AI males ( $P = 0.073$ ) (Figure 1.1D). AI males had 18% higher 3-NY protein content vs. AI females ( $P = 0.073$ ). HiD males had 14% lower 3-NY protein content vs. HiD females ( $P = 0.069$ ).

### **Antioxidant Enzymes**

#### SOD2

There was no significant difference in SOD2 protein content between the diets or between the sexes (Figure 1.2A and 1.2B)

#### Catalase

HiD mice had 12% lower catalase protein content vs. AI ( $P = 0.097$ ). HiD females had 21% lower catalase protein content vs. AI females ( $P < 0.0001$ ) (Figure 1.2C). HiD males had 34% higher catalase protein content vs. HiD females ( $P = 0.013$ ).

#### GPx1

HiD mice had 13% higher GPx1 protein content vs. AI ( $P = 0.088$ ). HiD females had 18% higher GPx1 protein content vs. AI females ( $P = 0.101$ ) (Figure 1.2E). AI males had 10% higher GPx1 protein content vs. AI females ( $P = 0.054$ ).

## **Inflammation**

### *TNF- $\alpha$*

HiD mice had 16% higher TNF- $\alpha$  protein content vs. AI (P = 0.015). HiD females had 21% higher TNF- $\alpha$  protein content vs. AI females (P = 0.003) (Figure 1.3A).

### *Il-6*

HiD males had 24% lower IL-6 protein content vs. AI males (P = 0.085) (Figure 1.3D).

AI males had 14% lower IL-6 protein content vs. AI females (P = 0.075). HiD males had 38% lower IL-6 protein content vs. HiD females (P = 0.034).

### *IL-10*

HiD females had 13% lower IL-10 protein content vs. AI females (P = 0.042) (Figure 1.3E). AI males had 11% lower IL-10 protein content vs. AI females (P = 0.074).

## **Apoptosis**

### *Bax*

There was no significant difference in Bax protein content between the diets or between the sexes. (Figure 1.4A and 1.4B).

### *Bcl-2*

There was no significant difference in Bcl-2 protein content between the diets (Figure 1.4C and 1.4D). AI males had 14% higher Bcl-2 protein content vs. AI females (P = 0.048).

### *Bax/Bcl-2 ratio*

There was no significant difference in Bax/Bcl-2 protein content between the diets or between the sexes (Figure 1.4E and 1.4F).

## **Caspase 3**

### Pro-caspase 3

HiD mice had 12% higher pro-caspase 3 protein content vs. AI (P = 0.003). HiD males had 22% higher pro-caspase 3 protein content vs. AI males (P = 0.036) (Figure 1.5B). HiD males had 17% higher pro-caspase 3 protein content vs. HiD females (P = 0.095).

### Cleaved caspase 3

HiD females had 15% higher cleaved caspase 3 protein content vs. AI females (P = 0.014) (Figure 5C). HiD males had 12% lower cleaved caspase 3 protein content vs. AI males (P = 0.063) (Figure 5D). HiD males had 27% lower cleaved caspase 3 protein content vs. HiD females (P < 0.001).

### Cleaved/pro-caspase 3

HiD females had 13% higher cleaved/pro-caspase 3 protein content vs. AI females (P = 0.010) (Figure 1.5E). HiD males had 26% lower cleaved/pro-caspase 3 protein content vs. AI males (P = 0.009) (Figure 1.5F). HiD males had 35% lower cleaved/pro-caspase 3 vs. HiD females (P < 0.0001).

## **Neurotrophic Factor**

### GDNF

There was no significant difference in GDNF protein content between the diets or between the sexes (Figure 1.6A and 1.6B).

## **Neuron Damage**

### ChAT

HiD females had 18% lower ChAT protein content vs. AI females (P = 0.024) (Figure 1.7A). AI males had 23% lower ChAT protein content vs. AI females (P = 0.005)

### SMI-32

There was no significant difference in SMI-32 protein content between the diets (Figure 1.7C and 1.7D). AI males had 15% lower SMI-32 protein content vs. AI females (P = 0.039).

### SMI-36

There was no significant difference in spinal cord SMI-36 protein content between the diets (figure 1.7E and 1.7F). AI males had 13% lower spinal cord SMI-36 protein content vs. AI females (P = 0.016). HiD males had 13% lower SMI-36 vs. HiD females (P = 0.008).

### SMI-36/SMI-32

HiD males had 19% lower spinal cord SMI-36/SMI-32 protein content vs. AI males (P = 0.098) (Figure 1.7H).

### **Spinal cord weights**

Absolute spinal cord weight was not different between the diets (Table 1.3). Between the sexes, AI males had 15% lighter absolute spinal cord weight vs. AI females (P = 0.065) (Table 1.3). HiD males had 19% heavier body weight-adjusted spinal cord weight vs. AI males (P = 0.076) (Table 1.3; Figure 8B). Between the sexes, AI males had 33% lighter body weight-adjusted spinal cord weight vs. AI females (P = 0.001) (Table 1.3; Figure 8C), and HiD males had 18% lighter body weight-adjusted spinal cord weight vs. HiD females (P = 0.045) (Table 1.3; Figure 8D).

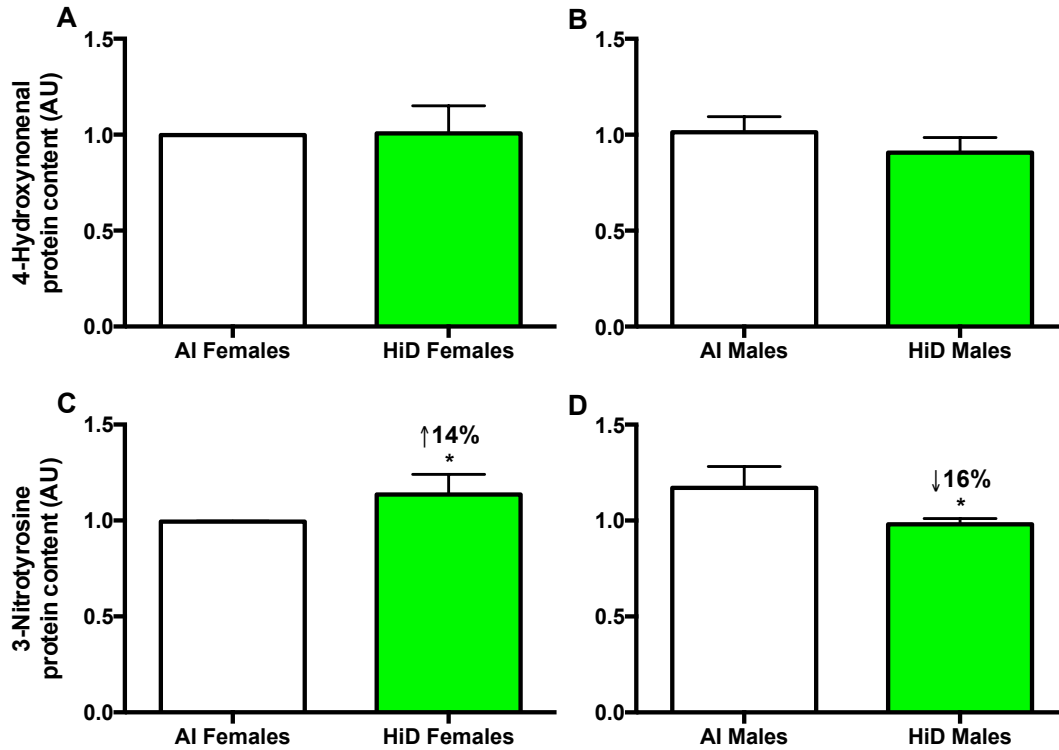


**Figure 1.1 Oxidative damage in HiD vs. AI G93A mice.**

4-HNE (A and B) and 3-NY (C and D) protein content (arbitrary units; AU) in spinal cord of 41 G93A mice: 23 adequate vitamin D<sub>3</sub> intake (AI; 1 IU D<sub>3</sub>/g feed; 12 M, 11 F) and 18 high vitamin D<sub>3</sub> intake (HiD; 50 IU D<sub>3</sub>/g feed; 10 M, 8 F). *4-Hydroxynonenal (4-HNE, A and B)*: There was no significant difference in 4-HNE protein content between the diets or between the sexes. *3-Nitrotyrosine (3-NY, C and D)*: HiD females had 14% higher 3-NY protein content vs. AI females (P = 0.065). HiD males had 16% lower 3-NY protein content vs. AI males (P = 0.073). AI males had 18% higher 3-NY protein content vs. AI females (P = 0.073). HiD males had 14% lower 3-NY protein content vs. HiD females (P = 0.069). Data presented as means ± SEM.

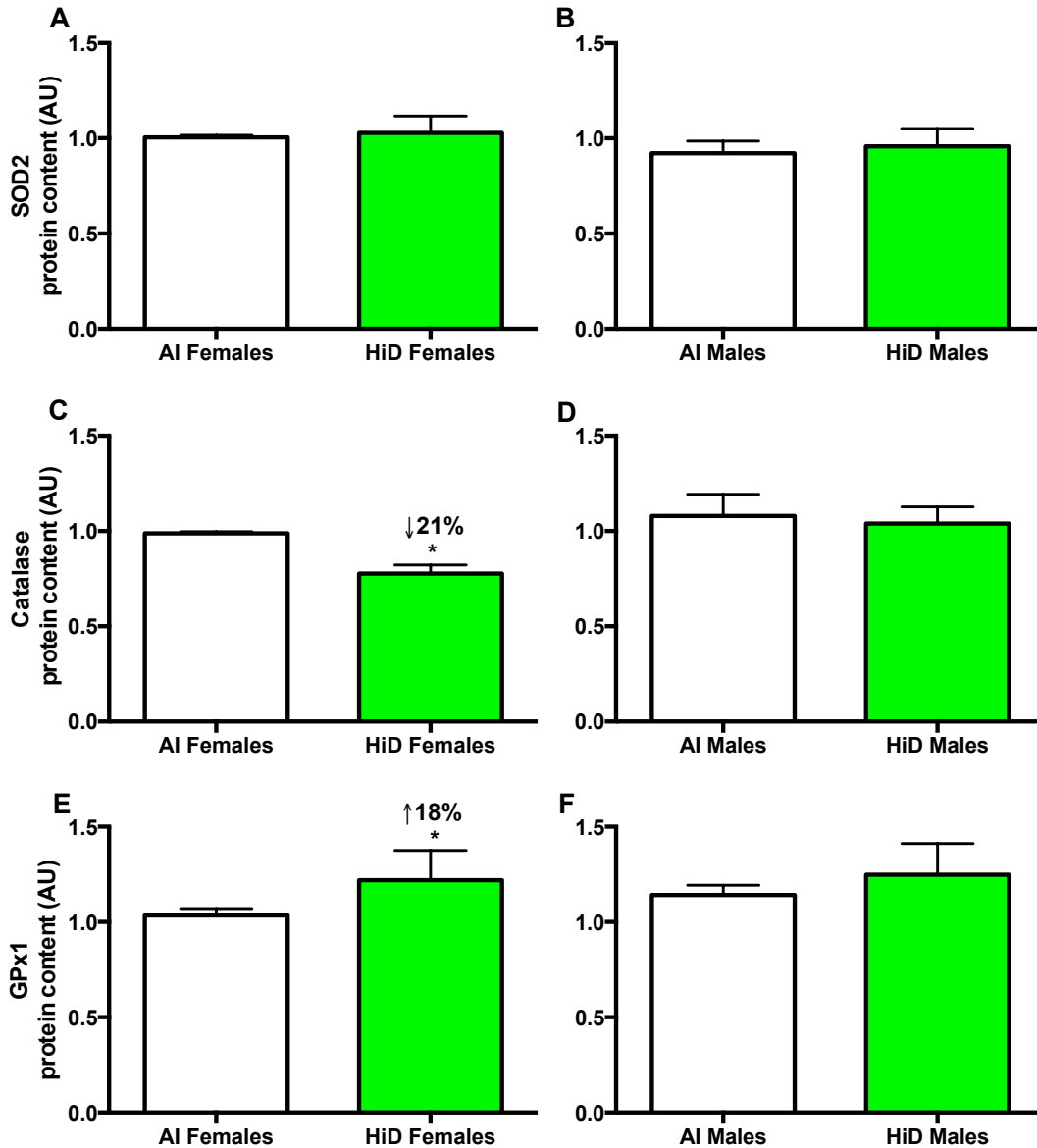


**Figure 1.2 Antioxidant enzymes in HiD vs. AI G93A mice.**

SOD2 (A and B), catalase (C and D) and GPx1 (E and F) protein content (arbitrary units; AU) in spinal cord of 41 G93A mice: 23 adequate vitamin D<sub>3</sub> intake (AI; 1 IU D<sub>3</sub>/g feed; 12 M, 11 F) and 18 high vitamin D<sub>3</sub> intake (HiD; 50 IU D<sub>3</sub>/g feed; 10 M, 8 F). *SOD2 (A and B)*: There was no significant difference in SOD2 protein content between the diets or between the sexes. *Catalase (C and D)*: HiD mice had 12% lower catalase protein content vs. AI (P = 0.097). HiD females had 21% lower catalase protein content vs. AI females (P < 0.0001). HiD males had 34% higher catalase protein content vs. HiD females (P = 0.013). *GPx1 (E and F)*: HiD mice had 13% higher GPx1 protein content vs. AI (P = 0.088). HiD females had 18% higher GPx1 protein content vs. AI females (P = 0.101). AI males had 10% higher GPx1 protein content vs. AI females (P = 0.054). Data presented as means ± SEM.

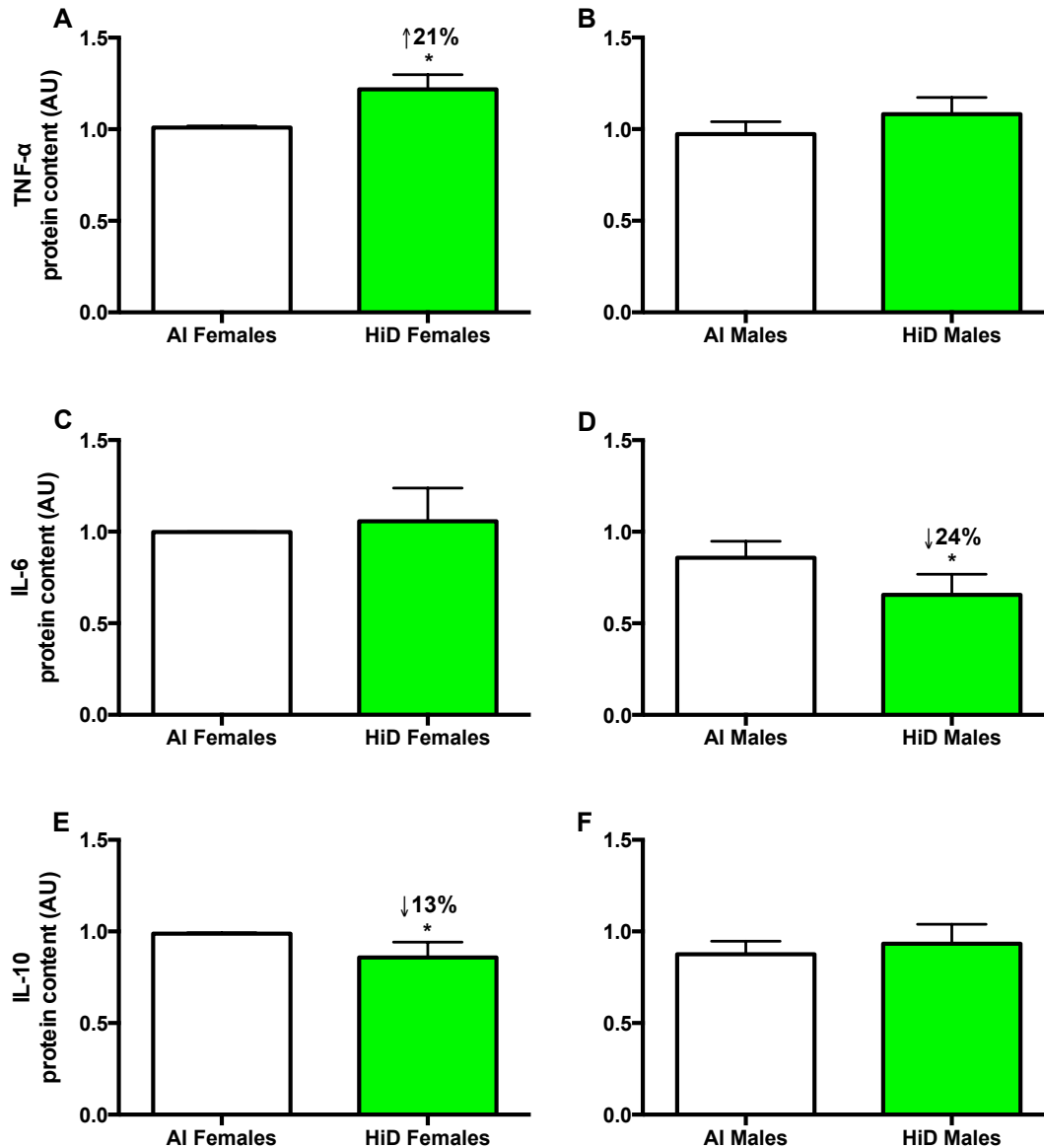


**Figure 1.3 Inflammation in HiD vs. AI G93A mice.**

TNF- $\alpha$  (A and B), IL-6 (C and D) and IL-10 (E and F) protein content (arbitrary units; AU) in spinal cord of 41 G93A mice: 23 adequate vitamin D<sub>3</sub> intake (AI; 1 IU D<sub>3</sub>/g feed; 12 M, 11 F) and 18 high vitamin D<sub>3</sub> intake (HiD; 50 IU D<sub>3</sub>/g feed; 10 M, 8 F). *TNF- $\alpha$*  (A and B): HiD mice had 16% higher TNF- $\alpha$  protein content vs. AI (P = 0.015). HiD females had 21% higher TNF- $\alpha$  protein content vs. AI females (P = 0.003). *IL-6* (C and D): HiD males had 24% lower IL-6 protein content vs. AI males (P = 0.085). AI males had 14% lower IL-6 protein content vs. AI females (P = 0.075). HiD males had 38% lower IL-6 protein content vs. HiD females (P = 0.034). *IL-10* (E and F): HiD females had 13% lower IL-10 protein content vs. AI females (P = 0.042). AI males had 11% lower IL-10 protein content vs. AI females (P = 0.074). Data presented as means  $\pm$  SEM.

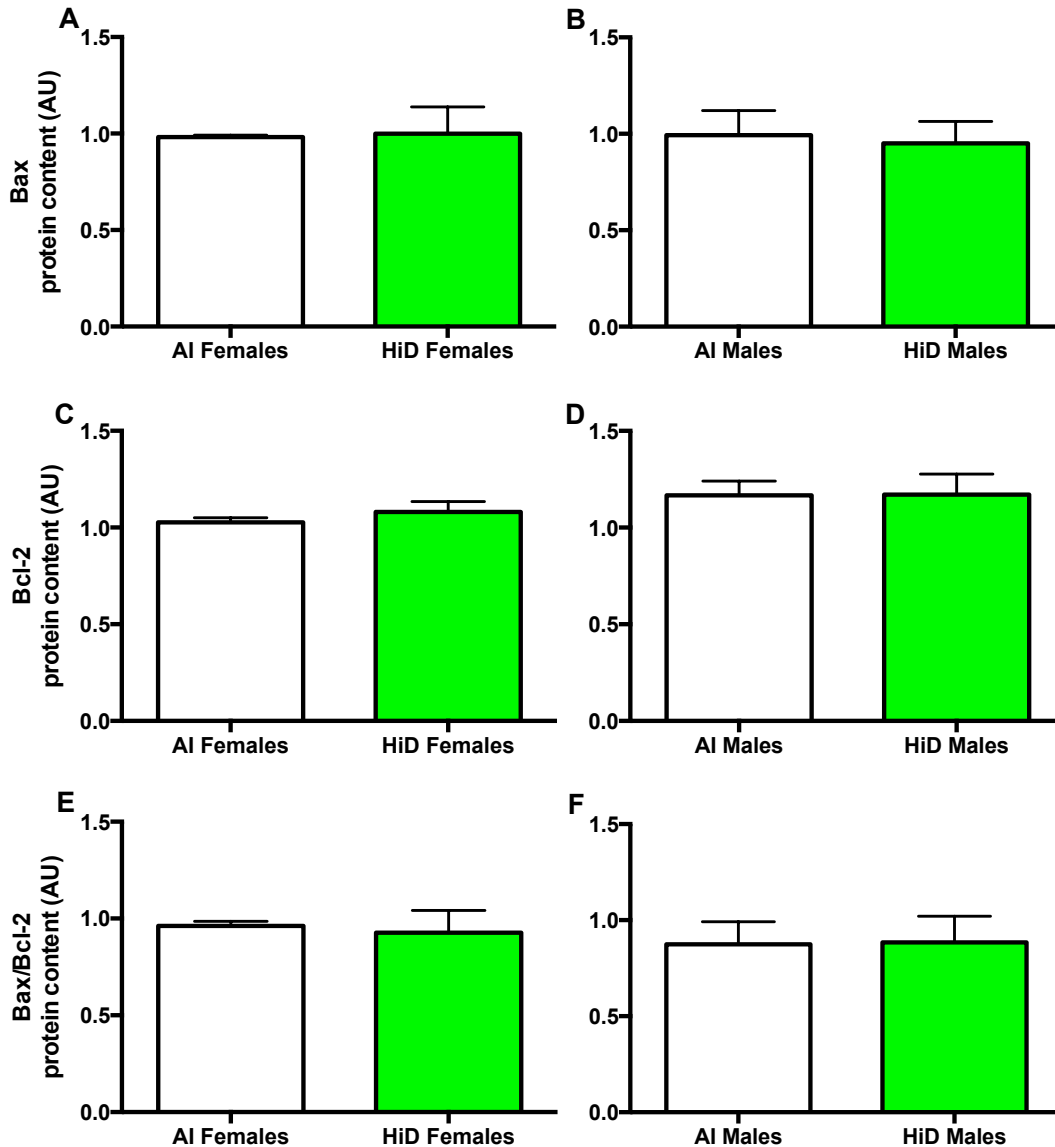


**Figure 1.4 Bax/Bcl-2 in HiD vs. AI G93A mice.**

Bax (panel A and B), Bcl-2 (C and D) and Bax/Bcl-2 ratio (panel E and F) protein content (arbitrary units; AU) in spinal cord of 41 G93A mice: 23 adequate vitamin D<sub>3</sub> intake (AI; 1 IU D<sub>3</sub>/g feed; 12 M, 11 F) and 18 high vitamin D<sub>3</sub> intake (HiD; 50 IU D<sub>3</sub>/g feed; 10 M, 8 F). Bax (A and B): There was no significant difference in Bax protein content between the diets or between the sexes. Bcl-2 (C and D): There was no significant difference in Bcl-2 protein content between the diets. AI males had 14% higher Bcl-2 protein content vs. AI females (P = 0.048). Bax/Bcl-2 ratio (E and F): There was no significant difference in Bax/Bcl-2 protein content between the diets or between the sexes. Data presented as means ± SEM.

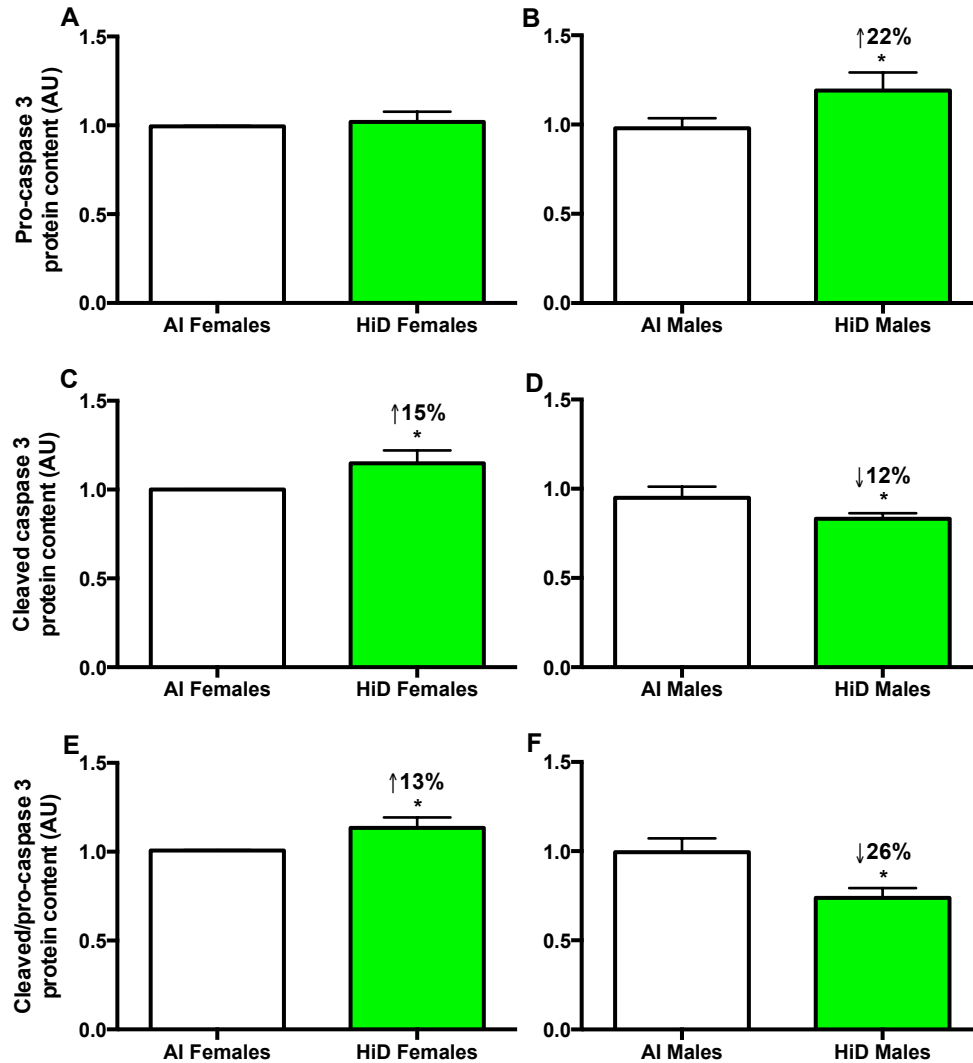


**Figure 1.5 Caspase 3 in HiD vs. AI G93A mice.**

Pro-caspase 3 (A and B), cleaved caspase 3 (C and D) and cleaved/pro-caspase 3 ratio (E and F) protein content (arbitrary units; AU) in spinal cord of 41 G93A mice: 23 adequate vitamin D<sub>3</sub> intake (AI; 1 IU D<sub>3</sub>/g feed; 12 M, 11 F) and 18 high vitamin D<sub>3</sub> intake (HiD; 50 IU D<sub>3</sub>/g feed; 10 M, 8 F). *Pro-caspase 3 (A and B)*: HiD mice had 12% higher pro-caspase 3 protein content vs. AI (P = 0.003). HiD males had 22% higher pro-caspase 3 protein content vs. AI males (P = 0.036). HiD males had 17% higher pro-caspase 3 protein content vs. HiD females (P = 0.095). *Cleaved caspase 3 (C and D)*: HiD females had 15% higher cleaved caspase 3 protein content vs. AI females (P = 0.014). HiD males had 12% lower cleaved caspase 3 protein content vs. AI males (P = 0.063). HiD males had 27% lower cleaved caspase 3 protein content vs. HiD females (P < 0.001). *Cleaved/pro-caspase 3 ratio (E and F)*: HiD females had 13% higher cleaved/pro-caspase 3 protein content vs. AI females (P = 0.010). HiD males had 26% lower cleaved/pro-caspase 3 protein content vs. AI males (P = 0.009). HiD males had 35% lower cleaved/pro-caspase 3 vs. HiD females (P < 0.0001). Data presented as means ± SEM.

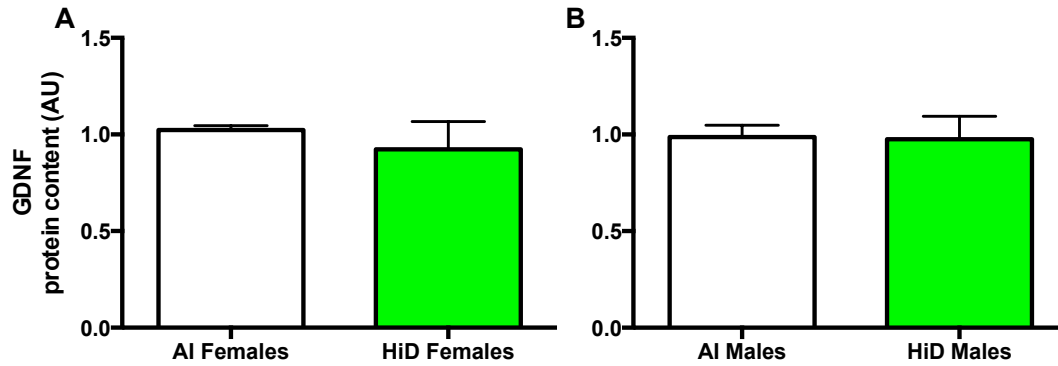


**Figure 1.6 Neurotrophic factor in HiD vs. AI G93A mice.**

GDNF protein content (A and B) (arbitrary units; AU) in spinal cord of 41 G93A mice: 23 adequate vitamin D<sub>3</sub> intake (AI; 1 IU D<sub>3</sub>/g feed; 12 M, 11 F) and 18 high vitamin D<sub>3</sub> intake (HiD; 50 IU D<sub>3</sub>/g feed; 10 M, 8 F). There was no significant difference in GDNF protein content between the diets or between the sexes. Data presented as means ± SEM.

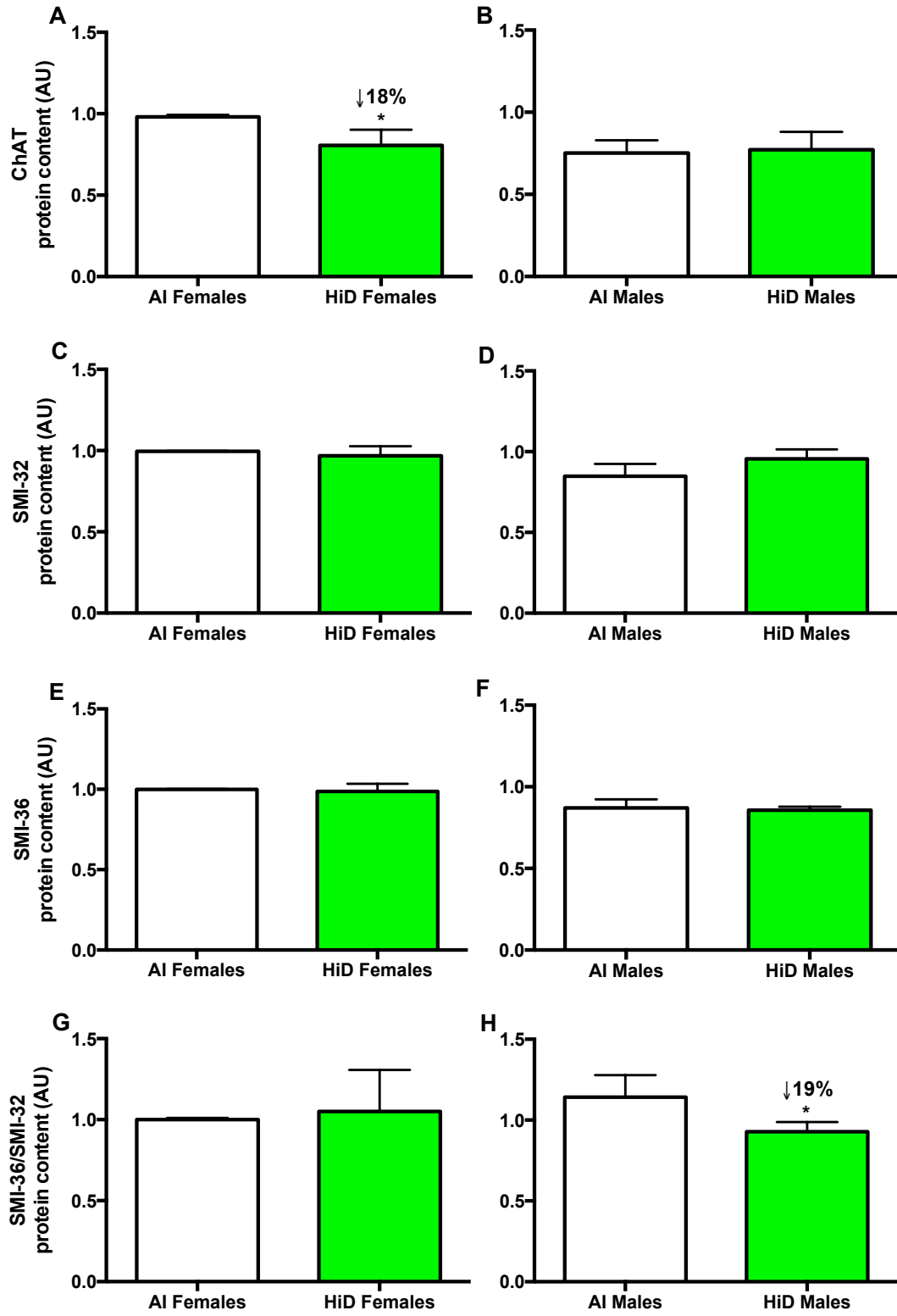


**Figure 1.7 Neuron damage in HiD vs. AI G93A mice.**

ChAT (A and B), SMI-32 (C and D), SMI-36 (E and F) and SMI-36/SMI-32 ratio (G and H) protein content (arbitrary units; AU) in spinal cord of 41 G93A mice: 23 adequate vitamin D<sub>3</sub> intake (AI; 1 IU D<sub>3</sub>/g feed; 12 M, 11 F) and 18 high vitamin D<sub>3</sub> intake (HiD; 50 IU D<sub>3</sub>/g feed; 10 M, 8 F). ChAT (A and B): HiD females had 18% lower ChAT protein content vs. AI females (P = 0.024). AI males had 23% lower ChAT protein content vs. AI females (P = 0.005). SMI-32 (C and D): There was no significant difference in SMI-32 protein content between the diets. AI males had 15% lower SMI-32 protein content vs. AI females (P = 0.039). SMI-36 (E and F): There was no significant difference in spinal cord SMI-36 protein content between the diets. AI males had 13% lower spinal cord SMI-36 protein content vs. AI females (P = 0.016). HiD males had 13% lower SMI-36 vs. HiD females (P = 0.008). SMI-36/SMI-32 ratio (G and H): HiD males had 19% lower spinal cord SMI-36/SMI-32 protein content vs. AI males (P = 0.098). Data presented as means ± SEM.

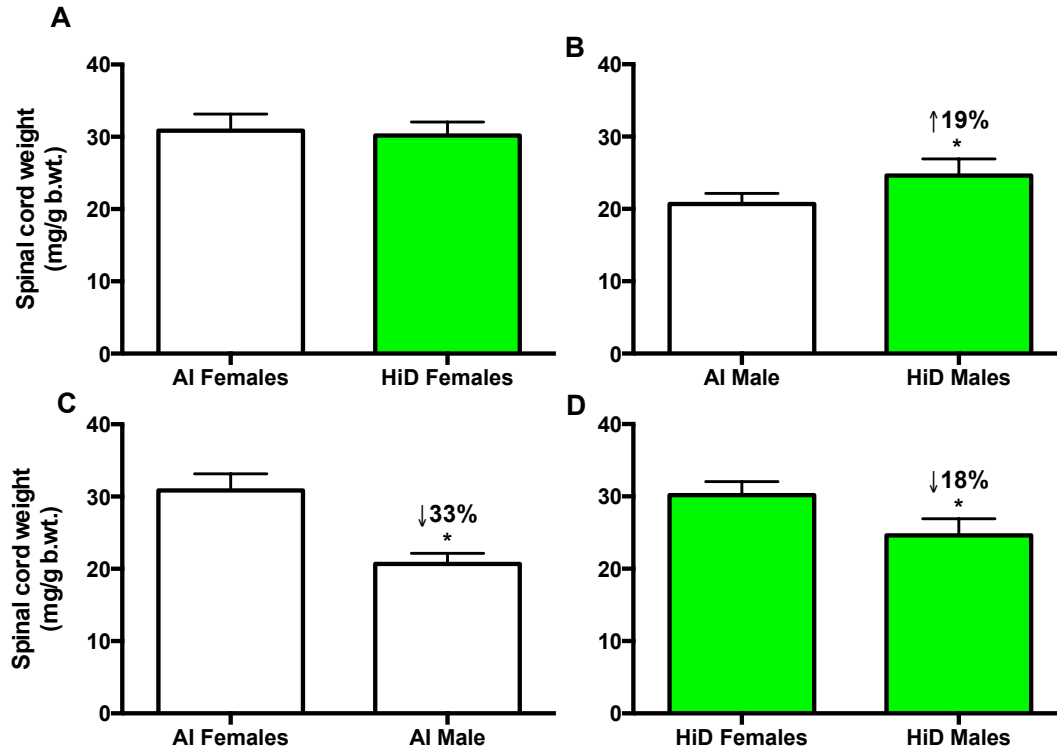


**Figure 1.8 Body weight-adjusted spinal cord weights at 113 d.**

Body weight-adjusted spinal cord weight (mg/g b.wt.) of 41 G93A mice: 23 adequate vitamin D<sub>3</sub> intake (AI; 1 IU D<sub>3</sub>/g feed; 12 M, 11 F) and 18 high vitamin D<sub>3</sub> intake (HiD; 50 IU D<sub>3</sub>/g feed; 10 M, 8 F). *Between the diets (A and B)*: HiD males had 19% heavier body weight-adjusted spinal cord weight vs. AI males ( $P = 0.076$ ). *Between the sexes (C and D)*: AI males had 33% lighter body weight-adjusted spinal cord weight vs. AI females ( $P = 0.001$ ), and HiD males had 18% lighter body weight-adjusted spinal cord weight vs. HiD females ( $P = 0.045$ ). Data presented as means  $\pm$  SEM.

**Table 1.3. Spinal cord weight between the diets and sexes at 113 d.**

Spinal cord weights	Females			Males			Within-AI between-sex differences	Within-HiD between-sex differences
	AI	HiD	P value	AI	HiD	P value	P value	P value
<b>Absolute spinal cord weight (mg)</b>	583±43	576±30	NS	494±37	546±48	NS	P = 0.065	NS
<b>Body weight-adjusted spinal cord weight (mg/g b.wt.)</b>	31±2	30±2	NS	21±2	25±2	P = 0.076	P = 0.001	P = 0.045

Data are means ± SEM.

AI, adequate intake; HiD, high vitamin D<sub>3</sub>

AI Males, n = 12; AI Females, n = 11

HiD Males, n = 10; HiD Females, n = 8

## Discussion

We investigated the effects of dietary vitamin D<sub>3</sub> supplementation at 50x the rodent AI on markers of oxidative damage, antioxidant enzymes, inflammation, apoptosis, growth factors and neuron damage in the spinal cord of G93A mice, a rodent model of ALS. Dietary D<sub>3</sub> at 50x the AI improved disease pathophysiology in male mice by lowering protein damage, inflammation and apoptosis compared to AI males. On the contrary, females supplemented with 50x AI of D<sub>3</sub> had reached the threshold of toxicity. HiD females had higher protein damage, lower antioxidant capacity and higher inflammation, apoptosis and neuron damage, compared to AI females. The optimal therapeutic dose of vitamin D<sub>3</sub> differs between males and females.

In the present study, females consuming 50 IU of vitamin D<sub>3</sub>/g feed may have reached the threshold of toxicity due to the exacerbation of their disease pathophysiology. In a mouse model of experimental autoimmune encephalomyelitis (EAE; a rodent model of multiple sclerosis- MS) consuming 40 IU/d of vitamin D<sub>3</sub>, females had ~67% greater calcitriol concentration vs. males 70-84 d post-supplementation despite having similar serum values (50). The study also reported ~4 fold lower calcitriol deactivating enzyme (CYP24A1) mRNA transcripts in females compared to males. A synergy exists between vitamin D<sub>3</sub> and estrogen, which is also found in the spinal cord. Estrogen causes estrogen receptor-mediated down-regulation of CYP24A1 transcription to increase net calcitriol concentration, and thus enhances vitamin D function. As well, estrogen up-regulates VDR to enhance vitamin D potency, and, in turn, calcitriol uses VDR-mediated up-regulation of estrogen synthase to enhance endogenous estrogen synthesis (51).

Many studies have shown that females have higher serum vitamin D<sub>3</sub> levels compared to males (52-54). Estrogen plays a strong role in stimulating calcitriol in females (55-57). Gray *et al* showed that serum calcitriol levels fluctuate during the menstrual cycle, increasing 2-fold from the early follicular phase (low estrogen) to menstruation (high estrogen) (56). Moreover, post-menopausal women have lower calcitriol levels compared to their pre-menopausal state (57), but increase their status by >50% when subjected to estrogen therapy (58, 59). In the CNS, basal calcitriol levels are higher in females vs. males, because of the females' ability to synthesize more calcitriol (50). As such, the presence of estrogen indicates that therapeutic vitamin D levels must differ between males and females, and that a specific dosage in males does not have the same impact in females.

Though calcitriol has many beneficial effects on motor neurons, toxic levels pose a great concern because it can result in hypercalcemia (60) in a disease model that already suffers from intracellular hypercalcemia-induced damage. Despite the fact that vitamin D increases the activity of calcium buffering proteins such as calbindin d-28k and parvalbumin (61, 62), toxicity can cause excessive calcium accumulation. A dysregulation in calcium homeostasis is toxic for motor neurons (63), and in sALS patients intracellular calcium levels are well above normal (64). In motor neurons, high intracellular calcium levels can increase free radical production (65), which leads to neuron damage and subsequently death. It is important to investigate the influence of vitamin D analogs on ALS pathophysiology, given that analogs mimic the beneficial effects of vitamin D without the dangers of hypercalcemia (66).

Vitamin D plays an important role in protecting the cell from oxidative stress. Protein damage, marked by 3-NY protein content, was 16% lower in HiD males vs. AI males. Calcitriol is protective against ultraviolet ray-induced increases in 3-NY in keratinocytes (67). This is due to calcitriol's ability to lower the formation of nitric oxide (NO) products and increase p53 protein, which aids in DNA repair (68). Conversely, AI males had 18% higher 3-NY protein content vs. AI females. In females, 17 $\beta$ -estradiol's antioxidative effect reduces 3-NY immunoreactivity (69). Brain cell cultures of mice exposed to 17 $\beta$ -estradiol significantly reduced 3-NY levels regardless of whether or not they were exposed to superoxide (70). Estrogen inhibits nitric oxide synthase (NOS) activity, thereby reducing peroxynitrite and subsequently 3-NY generation (71). However, HiD females had 14% higher 3-NY levels compared to HiD males, in accord with the presence of toxicity. Increased concentrations of 3-NY have been found in the spinal cord of both sALS and fALS patients (72). In HiD females, heightened oxidative stress brought about by hypervitaminosis D increased protein damage as marked by elevated 3-NY protein content.

In terms of antioxidant capacity, catalase was 21% lower in HiD females vs. AI females. Generally, catalase activity is high in the liver and kidneys, and low in the brain and skeletal muscle (73). The sharp decrease in catalase in HiD females may be due to the increase in the pro-inflammatory TNF- $\alpha$ . A strong link between catalase and TNF- $\alpha$  has been observed (74). Catalase neutralizes the oxidative effects of free radicals, but when inflammation exceeds its capabilities, the enzyme no longer functions properly and thus tissue damage occurs (75). Yasmineh *et al*'s study on rats showed that injection of 100  $\mu$ g/kg/day of human recombinant TNF- $\alpha$  for 5 days decreased the catalase enzyme

activity of the liver between 21-56% when compared to rats without injections (74). A study has shown that a decrease in catalase enzyme activity is due to a reduction in catalase protein (76). Interestingly, our study showed a 21% increase in TNF-  $\alpha$  and a 21% decrease in catalase, corresponding to the pattern observed in the study by Yasmineh *et al.* This increase in TNF-  $\alpha$  also confirms the presence of heightened oxidative stress. In insulin-resistant adipocytes, reactive oxidative species (ROS) production is increased when treated with TNF-  $\alpha$  (77). A decrease in catalase may be a result of inflammation-induced damage to the peroxisomes, where most of the catalase resides. In rat liver, TNF-  $\alpha$  suppresses protein expression of both catalase and peroxisomal proteins (78). Singh *et al* showed that the spinal cord of EAE mice have impaired peroxisomal function due to increased inflammation (79). This was marked by 37% reduction in catalase enzyme activity, underscoring the importance of peroxisome integrity to catalase function.

There was 18% higher GPx1 protein content in HiD females vs. AI females. Under physiological conditions, vitamin D has an inverse relationship with GPx1 and a positive association with glutathione reductase (GR) activity (80). This relationship is due to reduced glutathione's (GSH) role in maintaining intracellular redox balance. Hence, increasing the activity of GR and decreasing GPx1 function allow vitamin D to enhance the GSH pool. Thus, an upregulation of GPx1 activity may be an indicator of excessive cellular damage. Female hypertensive Wister rats had increased GPx1 activity and lower GSH levels (81). In many cancers, GPx1 has been shown to further induce malignancy and promote tumor progression (82). In breast cancer patients, high expression of GPx1 was associated with high rates of patient mortality and shorter overall

survival (83). This may be due to nuclear factor-kappa B (NF- $\kappa$ B). In ALS, activated microglia use the NF- $\kappa$ B pathway to induce mitochondrial dysfunction inhibition of SOD2 and motor neuron death (84, 85). When bound to the promoter region of GPx1, NF- $\kappa$ B upregulates its function and expression upstream (82). Vitamin D and VDR inhibit NF- $\kappa$ B expression and thus decrease GPx1 levels (43, 44). In females, estrogen increases the conversion of calcidiol to calcitriol (86), which heightens the ability of the vitamin to inhibit the NF- $\kappa$ B pathway, thereby reducing GPx1 levels. However, under toxic conditions, the excessive oxidative damage likely surpasses vitamin D's ability to efficiently regulate GPx1. Toxicity, and thus heightened oxidative damage, may result in an adaptive increase in GPx1 levels to compensate for the elevated cellular damage. The 10% higher GPx1 levels in AI males vs. AI females indicate that at adequate non-toxic levels, vitamin D has a stronger ability in increasing GPx1 in males vs. females.

As well as heightened inflammation, HiD females also had lower anti-inflammatory cytokine, as marked by a 13% lower IL-10 compared to AI females. In patients with neuromyelitis optica, a CNS inflammatory syndrome, upregulation of oxidative stress resulted in lower IL-10 levels (87). This indicates that a more inflammatory milieu is present in HiD females, likely due to the excessive oxidative stress brought about by hypervitaminosis D. Patients with advanced chronic heart failure, a disease marked by excessive inflammation, have a high TNF- $\alpha$ /IL-10 ratio (88). This pattern was also observed in renal tissue of rats with systematic inhibition of NOS (89). It is important to note that it is not NOS inhibition itself that downregulates IL-10 production, but rather the subsequent deficiency in NO. NOS inhibition has been shown to reduce IL-10 levels, which lead to increases in TNF- $\alpha$  levels (89), similar to our

observation in the current study. Normally, TNF-  $\alpha$  is suppressed by IL-10 production, not NOS inhibition. IL-10 knockout mice had increased endothelial NOS production which did not impact TNF- $\alpha$  levels (89). The exact mechanistic link between IL-10 and NO has not been well established. Within the spinal cord, inhibition of NOS is important for neuroprotection and thus motor function of spinal cord injury (SCI) rats (90). NO-related toxicity occurs when NOS produces NO that reacts with superoxide to produce peroxynitrite which nitrates tyrosine residues and upregulates 3-NY production (91). Upregulation of 3-NY levels in HiD females in the current study may confirm the presence of NO-related toxicity. In the CNS, calcitriol inhibits the synthesis of inducible NOS as a means of enhancing neuroprotection (90). Despite the toxicity, the excessive calcitriol in the spinal cord of HiD females may have inhibited NOS as a means of reducing oxidative damage, resulting in lower IL-10 levels. The 11% lower IL-10 protein content in AI males compared to AI females may be an indicator that oxidative damage is higher in males, and hence NOS inhibition is higher, vs. females. Indeed, 3-NY and TNF- $\alpha$  protein levels were higher in AI males compared to AI females, suggesting higher susceptibility of AI males to neuron damage.

HiD males had 24% lower IL-6 compared to AI males. Overall, males had lower IL-6 protein content compared to females, where AI and HiD males had 14% and 38% lower IL-6 levels, respectively, compared to their female counterparts. Studies show that testosterone maintains low IL-6 levels (92-94). However, lower IL-6 protein content in HiD males vs. AI males indicates that vitamin D also reduces inflammation. Vitamin D downregulates IL-6 production in human monocytes (95). 800 IU/d vitamin D<sub>3</sub> supplementation in colorectal adenoma patients showed a 32% decrease in plasma IL-6

levels (96). Vitamin D's action in lowering IL-6 levels may be mediated through its action on transforming growth factor beta (TGF- $\beta$ 1). TGF- $\beta$ 1 is a potent modulator of cell growth (97). Exogenous TGF- $\beta$ 1 protects neurons, including motor neurons, from damage occurring both *in vitro* and *in vivo* (98). TGF- $\beta$ 1 can reduce the inflammatory effects of IL-6 (99) by protecting neurons from Ca<sup>2+</sup>-mediated neural degeneration (100). In EAE mice, supplementation with vitamin D<sub>3</sub> increases the number of transcripts of TGF- $\beta$ 1 mRNA in affected CNS tissue (101).

With respect to apoptosis, opposing results were observed between the sexes. HiD females had 13% higher cleaved/pro-caspase 3 ratio compared to AI females, whereas HiD males had a 26% lower ratio compared to AI males. Consequently, HiD males had significantly lower apoptosis compared to HiD females. In HiD females, a higher ratio was due to a 15% increase in cleaved caspase 3. Hypervitaminosis D increases premature aging in mutant mice, a process associated with heightened oxidative stress (102). In HiD females, greater 3-NY indicates the presence of oxidative stress. High oxidative stress induces activation of caspase 3 in the spinal cord of mSOD1 mice (103). As well, excessive oxidative stress in HiD females may have led to glutathione depletion, due to high GPx1 levels, which is associated with activation of caspase 3 (104). In the high-copy G93A mouse, depletion of GSH in the spinal cord and motor neurons correlates with apoptosis-inducing factor translocation, caspase-3 activation and motor neuron degeneration during disease onset and progression (105). Conversely, HiD males had lower cleaved/pro-caspase 3 compared to AI males. Vitamin D has been shown to reduce activated caspase 3 in the spinal cord of EAE mice (105). In HiD males, the downregulation of microglial activation, and thus oxidative damage and inflammation,

may have resulted in reduction of apoptosis. In cultured neurons of the rat hippocampus, vitamin D<sub>3</sub> treatment lowered microglial activation by downregulating inflammation, marked by lower IFN $\gamma$  and IL-1 $\beta$  levels (106). Calcitriol can also modulate oxidative stress by enhancing intracellular GSH pools to lower nitrite production (107).

With respect to neuron damage, HiD females had 18% lower ChAT compared to AI females. This may be due to higher peroxynitrite levels, marked by increased 3-NY levels. Cholinergic synaptosomes purified from *Torpedo marmorata* showed that peroxynitrite inhibits acetylcholine synthesis (108). Interestingly, the inhibition of ChAT by peroxynitrite coincided with the appearance of nitrotyrosine and was evident at concentrations as low as 50-100  $\mu$ M peroxynitrite. This confirms that damage and atrophy of motor neurons is strongly associated with nitration-induced protein damage. AI males had 23% lower ChAT and 15% lower SMI-32 compared to AI females, indicating higher neuron damage. In mSOD1 mice, onset, disease progression and survival are dependent on sex; males lose body weight more rapidly following disease onset and die before females (109, 110). A reduction in body weight reflects muscle atrophy brought about by neuron degeneration. As with higher motor neuron count in AI females, it is possible that damaged motor neurons are also more prevalent. This explains why SMI-36 levels were 13% lower in AI males vs. AI females. HiD males had 19% lower SMI-36/SMI-32 ratio, a proxy measure of motor neuron damage (111), compared to AI males. With lower apoptosis, it is evident that motor neuron integrity is maintained, hence the lower SMI-36/SMI-32 ratio.

On a tissue level, HiD males had 19% heavier body weight-adjusted spinal cord weights compared to AI males. This confirms vitamin D's protective effects on a cellular

level, retaining the integrity of the spinal cord and thus lowering the rate of degeneration. The protective effects of estrogen were also confirmed since both AI and HiD males had 33% and 18% lighter body weight-adjusted spinal cord weight compared to their female counterparts, respectively. These results contrast with our previous study that found no difference in body weight-adjusted brain weights between the diets and sexes (36). Correlational analysis showed that there was no association between body weight-adjusted brain weights (36) and body weight-adjusted spinal cord weights. This confirms that ALS pathology within the CNS is mainly localized to the spinal cord.

This study outlines the beneficial effects of vitamin D at the molecular level in males at non-toxic dosages and the detrimental effects in females that reached the threshold of toxicity. The study also supports the attenuation of the decline in paw grip endurance (PaGE) in the HiD mice observed in our previous studies (36, 37). It is important to note that females were not considered to be in a fully toxic state as previous studies in the same mouse model observed greater paw grip endurance (PaGE) compared to AI females (36). Supraphysiological concentrations of calcitriol in the spinal cord may have induced mild toxicity as evidenced by greater disease severity prior to onset and decreased food intake (36). As well, oxidative damage in the spinal cord of HiD females may explain the increase in Bax/Bcl2 ratio in the *quadriceps* of these mice compared to AI females (38). However, the damaging effects of D<sub>3</sub> toxicity in HiD females and the beneficial effects in HiD males were more exaggerated in the spinal cord than in the skeletal muscle of the same G93A mice (38, 39). This is because vitamin D has a tissue-specific effect in the CNS vs. skeletal muscle, since calcidiol is the active vitamin D metabolite in skeletal muscle (112), whereas in the CNS it is calcitriol (113). Skeletal muscle cannot convert

calcidiol to calcitriol (114). In the current study, HiD females consumed ~150 IU vitamin D<sub>3</sub>/d (8.6 IU/g b.wt./d), which seemed to induce hypercalcitriol toxicity both at the functional and cellular levels. Functionally, there was greater disease severity prior to disease onset and decreased food intake (36). Whereas at the cellular level, increased apoptosis was observed in the *quadriceps* of HiD females vs. AI females (38), and in the spinal cord there was increased inflammation and apoptosis and lower antioxidant capacity. The improved PaGE in HiD mice is most probably due to the higher antioxidant capacity and lower inflammation in the *quadriceps* compared to AI mice. G93A mice that were fed 10x AI vitamin D<sub>3</sub>/g feed not only had an improvement in their PaGE but also in their motor performance (37), corresponding to 8257 IU/d for an 80 kg man and 8785 IU/d for a 70 kg woman. The vitamin D<sub>3</sub> intake in this study corresponds to 40,037 IU/d for an 80 kg man and 38,062 IU/d for a 70 kg woman. We previously hypothesized that the optimal therapeutic vitamin D dosage, both functionally and cellularly, lies between 10x and 50x AI vitamin D (29, 36, 37). Karam *et al*'s retrospective study in ALS patients showed that supplementation with 2000 IU of vitamin D<sub>3</sub>/day for 9 months improved ALS functional rating scale score (ALSF<sub>RS</sub>-R) (35). Based on our hypothesis and given the fact that there were no side effects in humans following supplementation with 10 000 IU/d dosages in patients with MS for 12 weeks (115) and up to 40 000 IU/d for 28 weeks (116), ALS patients in Karam *et al*'s study may have shown greater improvements in their ALSF<sub>RS</sub>-R had they been supplemented with dosages between 10 000-40 000 IU/d.

In conclusion, the present study demonstrates that at non-toxic levels, dietary vitamin D<sub>3</sub> supplementation can lower oxidative damage, inflammation and apoptosis in

the G93A mouse model of ALS. However, when the threshold of toxicity is reached, disease pathophysiology is exacerbated. As well, there is a clear sexual dimorphism where at a similar high vitamin D dose females are at higher risk of reaching toxicity compared to males (117).

### **Acknowledgements**

We thank Sanjeef Thampinathan, Mahshad Kolahdouzan and Safoura Sadeghimehr for assisting in lab analysis, data entry and literature search.

### **Author Contributions**

Conceived and designed the experiments: MJH AG JAS. Performed the experiments: EM. Analyzed the data: EM. Contributed reagents/materials/analysis tools: MJH. Wrote the paper: EM MJH.

## References

1. Nishitoh H, Kadowaki H, Nagai A, Maruyama T, Yokota T, Fukutomi H, Noguchi T, Matsuzawa A, Takeda K, Ichijo H. ALS-linked mutant SOD1 induces ER stress- and ASK1-dependent motor neuron death by targeting Derlin-1. *Genes Dev* 2008;22:1451-64.
2. de Almeida JL, Silvestre R, Pinto A, de Carvalho M. Exercise and amyotrophic lateral sclerosis. *Neurological Sciences* 2012;33:9-15.
3. Robberecht W, Philips T. The changing scene of amyotrophic lateral sclerosis. *Nat Rev Neurosci* 2013;14:248-64.
4. Dadon-Nachum M, Melamed E, Offen D. The "dying-back" phenomenon of motor neurons in ALS. *J Mol Neurosci* 2011;43:470-7.
5. Wijesekera LC, Leigh PN. Amyotrophic lateral sclerosis. *Orphanet J Rare Dis* 2009;4:3,1172-4-3.
6. Jennum P, Ibsen R, Pedersen SW, Kjellberg J. Mortality, health, social and economic consequences of amyotrophic lateral sclerosis: a controlled national study. *J Neurol* 2013;260:785-93.
7. Tripodoro VA, De Vito EL. Management of dyspnea in advanced motor neuron diseases. *Curr Opin Support Palliat Care* 2008;2:173-9.
8. Lechtzin N. Respiratory effects of amyotrophic lateral sclerosis: problems and solutions. *Respir Care* 2006;51:871,81; discussion 881-4.
9. Gros-Louis F, Gaspar C, Rouleau GA. Genetics of familial and sporadic amyotrophic lateral sclerosis. *Biochim Biophys Acta* 2006;1762:956-72.
10. Berthod F, Gros-Louis F. In Vivo and In Vitro Models to Study Amyotrophic Lateral Sclerosis.
11. Rosen DR, Siddique T, Patterson D, Figlewicz DA, Sapp P, Hentati A, Donaldson D, Goto J, O'Regan JP, Deng HX. Mutations in Cu/Zn superoxide dismutase gene are associated with familial amyotrophic lateral sclerosis. *Nature* 1993;362:59-62.
12. Mitchell JD. Amyotrophic lateral sclerosis: toxins and environment. *Amyotroph Lateral Scler Other Motor Neuron Disord* 2000;1:235-50.
13. Bruijn LI, Miller TM, Cleveland DW. Unraveling the mechanisms involved in motor neuron degeneration in ALS. *Annu Rev Neurosci* 2004;27:723-49.
14. Renton AE, Chio A, Traynor BJ. State of play in amyotrophic lateral sclerosis genetics. *Nat Neurosci* 2014;17:17-23.

15. Gurney ME, Pu H, Chiu AY, Dal Canto MC, Polchow CY, Alexander DD, Caliendo J, Hentati A, Kwon YW, Deng HX. Motor neuron degeneration in mice that express a human Cu,Zn superoxide dismutase mutation. *Science* 1994;264:1772-5.
16. Foran E, Trotti D. Glutamate transporters and the excitotoxic path to motor neuron degeneration in amyotrophic lateral sclerosis. *Antioxid Redox Signal* 2009;11:1587-602.
17. Mark LP, Prost RW, Ulmer JL, Smith MM, Daniels DL, Strottmann JM, Brown WD, Haccin-Bey L. Pictorial review of glutamate excitotoxicity: fundamental concepts for neuroimaging. *AJNR Am J Neuroradiol* 2001;22:1813-24.
18. Trumbull KA, Beckman JS. A role for copper in the toxicity of zinc-deficient superoxide dismutase to motor neurons in amyotrophic lateral sclerosis. *Antioxid Redox Signal* 2009;11:1627-39.
19. Pedersen WA, Fu W, Keller JN, Markesbery WR, Appel S, Smith RG, Kasarskis E, Mattson MP. Protein modification by the lipid peroxidation product 4-hydroxynonenal in the spinal cords of amyotrophic lateral sclerosis patients. *Ann Neurol* 1998;44:819-24.
20. Nguyen D, Alavi MV, Kim KY, Kang T, Scott RT, Noh YH, Lindsey JD, Wissinger B, Ellisman MH, Weinreb RN, et al. A new vicious cycle involving glutamate excitotoxicity, oxidative stress and mitochondrial dynamics. *Cell Death Dis* 2011;2:e240.
21. Schubert D, Piasecki D. Oxidative glutamate toxicity can be a component of the excitotoxicity cascade. *J Neurosci* 2001;21:7455-62.
22. Zhao L, Hart S, Cheng JG, Melenhorst JJ, Bierie B, Ernst M, Stewart C, Schaper F, Heinrich PC, Ullrich A, et al. Mammary gland remodeling depends on gp130 signaling through Stat3 and MAPK. *J Biol Chem* 2004;279:44093-100.
23. Patel BP, Hamadeh MJ. Nutritional and exercise-based interventions in the treatment of amyotrophic lateral sclerosis. *Clinical Nutrition* 28:604-17.
24. Deng Y, Xu Z, Xu B, Tian Y, Xin X, Deng X, Gao J. The protective effect of riluzole on manganese caused disruption of glutamate-glutamine cycle in rats. *Brain Res* 2009;1289:106-17.
25. Miller RG, Mitchell JD, Moore DH. Riluzole for amyotrophic lateral sclerosis (ALS)/motor neuron disease (MND). *Cochrane Database Syst Rev* 2012;3:CD001447.
26. Summerday NM, Brown SJ, Allington DR, Rivey MP. Vitamin D and multiple sclerosis: review of a possible association. *J Pharm Pract* 2012;25:75-84.
27. Ibi M, Sawada H, Nakanishi M, Kume T, Katsuki H, Kaneko S, Shimohama S, Akaike A. Protective effects of 1 alpha,25-(OH)(2)D(3) against the neurotoxicity of glutamate and reactive oxygen species in mesencephalic culture. *Neuropharmacology* 2001;40:761-71.
28. Pierrot-Deseilligny C. Clinical implications of a possible role of vitamin D in multiple sclerosis. *J Neurol* 2009;256:1468-79.

29. Gianforcaro A, Hamadeh MJ. Vitamin D as a potential therapy in amyotrophic lateral sclerosis. *CNS Neurosci Ther* 2014;20:101-11.
30. Halicka HD, Zhao H, Li J, Traganos F, Studzinski GP, Darzynkiewicz Z. Attenuation of constitutive DNA damage signaling by 1,25-dihydroxyvitamin D<sub>3</sub>. *Aging (Albany NY)* 2012;4:270-8.
31. Lambert JR, Kelly JA, Shim M, Huffer WE, Nordeen SK, Baek SJ, Eling TE, Lucia MS. Prostate derived factor in human prostate cancer cells: gene induction by vitamin D via a p53-dependent mechanism and inhibition of prostate cancer cell growth. *J Cell Physiol* 2006;208:566-74.
32. Banakar MC, Paramasivan SK, Chattopadhyay MB, Datta S, Chakraborty P, Chatterjee M, Kannan K, Thygarajan E. 1alpha, 25-dihydroxyvitamin D<sub>3</sub> prevents DNA damage and restores antioxidant enzymes in rat hepatocarcinogenesis induced by diethylnitrosamine and promoted by phenobarbital. *World J Gastroenterol* 2004;10:1268-75.
33. Harbuzova VI. Intensity of lipid peroxidation and antioxidant enzyme activity in arterial and venous walls during hypervitaminosis D. *Fiziol Zh* 2002;48:87-90.
34. Hamden K, Carreau S, Jamoussi K, Miladi S, Lajmi S, Aloulou D, Ayadi F, Elfeki A. 1Alpha,25 dihydroxyvitamin D<sub>3</sub>: therapeutic and preventive effects against oxidative stress, hepatic, pancreatic and renal injury in alloxan-induced diabetes in rats. *J Nutr Sci Vitaminol (Tokyo)* 2009;55:215-22.
35. Karam C, Barrett MJ, Imperato T, Macgowan DJ, Scelsa S. Vitamin D deficiency and its supplementation in patients with amyotrophic lateral sclerosis. *J Clin Neurosci* 2013;
36. Gianforcaro A, Solomon JA, Hamadeh MJ. Vitamin D(3) at 50x AI attenuates the decline in paw grip endurance, but not disease outcomes, in the G93A mouse model of ALS, and is toxic in females. *PLoS One* 2013;8:e30243.
37. Gianforcaro A, Hamadeh MJ. Dietary vitamin D<sub>3</sub> supplementation at 10x the adequate intake improves functional capacity in the G93A transgenic mouse model of ALS, a pilot study. *CNS Neurosci Ther* 2012;18:547-57.
38. Taheri-Shalmani S, Shahsavar S, Gianforcaro A, Solomon JA, Hamadeh MJ. Dietary vitamin D<sub>3</sub> supplementation at 50x the adequate intake decreases calbindin d28k and endoplasmic reticulum stress and increases apoptosis, suggesting toxicity, in the female transgenic G93A mouse model of amyotrophic lateral sclerosis. *The FASEB Journal* 2013;27:644.1.
39. Parkhomenko E, Milionis A, Gianforcaro A, Solomon JA, Hamadeh MJ. Dietary vitamin D<sub>3</sub> at 50x the adequate intake increases apoptosis in the quadriceps of the female G93A mouse model of amyotrophic lateral sclerosis: a pilot study. *The FASEB Journal* 2012;26:255.7.
40. Parkhomenko EA, Gianforcaro A, Solomon JA, Hamadeh MJ. Dietary vitamin D<sub>3</sub> at 50 fold the adequate intake increases antioxidant capacity and decreases inflammation in the G93A mouse model of ALS. *Canadian Nutrition Society* 2011;329.

41. Solomon JA, Tarnopolsky MA, Hamadeh MJ. One universal common endpoint in mouse models of amyotrophic lateral sclerosis. *PLoS One* 2011;6:e20582.
42. Bieri, J,G. Stoewsand, G,S. Briggs, G,M.Phillips, R,W. Woodard, J,C. Knapka, J,J. Report of the American Institute of Nutrition ad hoc Committee on Standards for Nutritional Studies. *J Nutr* 1977;107:1340-8.
43. Sapan CV, Lundblad RL, Price NC. Colorimetric protein assay techniques. *Biotechnol Appl Biochem* 1999;29 ( Pt 2):99-108.
44. Food and Drug Administration, ed. Estimating the safe starting dose in clinical trials for therapeutics in adult healthy volunteers. . Rockville, Maryland, USA: U.S.: Food and Drug Administration, 2005.
45. Wang Y, Chiang YH, Su TP, Hayashi T, Morales M, Hoffer BJ, Lin SZ. Vitamin D(3) attenuates cortical infarction induced by middle cerebral arterial ligation in rats. *Neuropharmacology* 2000;39:873-80.
46. Milionis A, Parkhomenko E, Solomon JA, Gianforcaro A, Hamadeh MJ. Dietary vitamin D3 restriction differentially alters quadriceps contractile proteins in both sexes in the transgenic G93A mouse model of amyotrophic lateral sclerosis: a pilot study. *The FASEB Journal* 2012;26:255.8.
47. Parkhomenko EA, Gianforcaro A, Solomon JA, Hamadeh MJ. Vitamin D deficiency improves antioxidant capacity in males and attenuates the sexual dichotomy in the G93A mouse model of amyotrophic lateral sclerosis: is the female sex at D<sub>3</sub> disadvantage? *Canadian Nutrition Society* 2011;328:
48. Shahsavari S, Taheri-Shalmani S, Solomon JA, Gianforcaro A, Hamadeh MJ. Sexual dichotomy in calcium buffering capacity may be dependent on the severity of endoplasmic reticulum stress in the skeletal muscle of the vitamin D3 deficient transgenic G93A mouse model of amyotrophic lateral sclerosis. *The FASEB Journal* 2013;27:644.2.
49. Solomon JA, Gianforcaro A, Hamadeh MJ. Vitamin D3 deficiency differentially affects functional and disease outcomes in the G93A mouse model of amyotrophic lateral sclerosis. *PLoS One* 2011;6:e29354.
50. Spach KM, Hayes CE. Vitamin D3 confers protection from autoimmune encephalomyelitis only in female mice. *J Immunol* 2005;175:4119-26.
51. Nashold FE, Spach KM, Spanier JA, Hayes CE. Estrogen controls vitamin D3-mediated resistance to experimental autoimmune encephalomyelitis by controlling vitamin D3 metabolism and receptor expression. *J Immunol* 2009;183:3672-81.
52. Genzen JR, Gosselin JT, Wilson TC, Racila E, Krasowski MD. Analysis of vitamin D status at two academic medical centers and a national reference laboratory: Result patterns vary by age, gender, season, and patient location. *BMC Endocrine Disorders* 2013;13:

53. Martini LA, Verly E, Jr, Marchioni DM, Fisberg RM. Prevalence and correlates of calcium and vitamin D status adequacy in adolescents, adults, and elderly from the Health Survey-Sao Paulo. *Nutrition* 2013;29:845-50.
54. Naugler C, Zhang J, Henne D, Woods P, Hemmelgarn BR. Association of vitamin D status with socio-demographic factors in Calgary, Alberta: an ecological study using Census Canada data. *BMC Public Health* 2013;13:316,2458-13-316.
55. Spach KM, Hayes CE. Vitamin D3 confers protection from autoimmune encephalomyelitis only in female mice. *J Immunol* 2005;175:4119-26.
56. Gray TK, McAdoo T, Hatley L, Lester GE, Thierry M. Fluctuation of serum concentration of 1,25-dihydroxyvitamin D3 during the menstrual cycle. *Am J Obstet Gynecol* 1982;144:880-4.
57. Lerchbaum E. Vitamin D and menopause--a narrative review. *Maturitas* 2014;79:3-7.
58. van Hoof HJ, van der Mooren MJ, Swinkels LM, Rolland R, Benraad TJ. Hormone replacement therapy increases serum 1,25-dihydroxyvitamin D: A 2-year prospective study. *Calcif Tissue Int* 1994;55:417-9.
59. Cheema C, Grant BF, Marcus R. Effects of estrogen on circulating "free" and total 1,25-dihydroxyvitamin D and on the parathyroid-vitamin D axis in postmenopausal women. *J Clin Invest* 1989;83:537-42.
60. Selby PL, Davies M, Marks JS, Mawer EB. Vitamin D intoxication causes hypercalcaemia by increased bone resorption which responds to pamidronate. *Clin Endocrinol (Oxf)* 1995;43:531-6.
61. Celio MR. Calbindin D-28k and parvalbumin in the rat nervous system. *Neuroscience* 1990;35:375-475.
62. Garcia-Segura LM, Baetens D, Roth J, Norman AW, Orci L. Immunohistochemical mapping of calcium-binding protein immunoreactivity in the rat central nervous system. *Brain Res* 1984;296:75-86.
63. Appel SH, Beers D, Siklos L, Engelhardt JI, Mosier DR. Calcium: the Darth Vader of ALS. *Amyotroph Lateral Scler Other Motor Neuron Disord* 2001;2 Suppl 1:S47-54.
64. Siklos L, Engelhardt J, Harati Y, Smith RG, Joo F, Appel SH. Ultrastructural evidence for altered calcium in motor nerve terminals in amyotrophic lateral sclerosis. *Ann Neurol* 1996;39:203-16.
65. Dykens JA. Isolated cerebral and cerebellar mitochondria produce free radicals when exposed to elevated  $Ca^{2+}$  and  $Na^{+}$ : implications for neurodegeneration. *J Neurochem* 1994;63:584-91.
66. Verhaar HJ, Samson MM, Jansen PA, de Vreede PL, Manten JW, Duursma SA. Muscle strength, functional mobility and vitamin D in older women. *Aging (Milano)* 2000;12:455-60.

67. Sequeira VB, Rybchyn MS, Gordon-Thomson C, Tongkao-on W, Mizwicki MT, Norman AW, Reeve VE, Halliday GM, Mason RS. Opening of Chloride Channels by 1 $\alpha$ ,25-Dihydroxyvitamin D<sub>3</sub> Contributes to Photoprotection against UVR-Induced Thymine Dimers in Keratinocytes. *J Invest Dermatol* 2013;133:776-82.
68. Gupta R, Dixon KM, Deo SS, Holliday CJ, Slater M, Halliday GM, Reeve VE, Mason RS. Photoprotection by 1,25 dihydroxyvitamin D<sub>3</sub> is associated with an increase in p53 and a decrease in nitric oxide products. *J Invest Dermatol* 2007;127:707-15.
69. Tripanichkul W, Sripanichkulchai K, Duce JA, Finkelstein DI. 17 $\beta$ -Estradiol reduces nitrotyrosine immunoreactivity and increases SOD1 and SOD2 immunoreactivity in nigral neurons in male mice following MPTP insult. *Brain Res* 2007;1164:24-31.
70. Rao AK, Dietrich AK, Ziegler YS, Nardulli AM. 17 $\beta$ -Estradiol-mediated increase in Cu/Zn superoxide dismutase expression in the brain: a mechanism to protect neurons from ischemia. *J Steroid Biochem Mol Biol* 2011;127:382-9.
71. Chakrabarti S, Cheung CC, Davidge ST. Estradiol attenuates high glucose-induced endothelial nitrotyrosine: role for neuronal nitric oxide synthase. *Am J Physiol Cell Physiol* 2012;302:C666-75.
72. Cluskey S, Ramsden DB. Mechanisms of neurodegeneration in amyotrophic lateral sclerosis. *Molecular Pathology* 2001;54:386-92.
73. Deisseroth A, Dounce AL. Catalase: Physical and chemical properties, mechanism of catalysis, and physiological role. *Physiol Rev* 1970;50:319-75.
74. Yasmineh WG, Parkin JL, Caspers JI, Theologides A. Tumor necrosis factor/cachectin decreases catalase activity of rat liver. *Cancer Res* 1991;51:3990-5.
75. Grisham MB, Granger DN. Neutrophil-mediated mucosal injury. Role of reactive oxygen metabolites. *Dig Dis Sci* 1988;33:6S-15S.
76. Kaplan JH, Groves JN. Liver and blood cell catalase activity of tumor-bearing mice. *Cancer Res* 1972;32:1190-4.
77. Houstis N, Rosen ED, Lander ES. Reactive oxygen species have a causal role in multiple forms of insulin resistance. *Nature* 2006;440:944-8.
78. Beier K, Volkl A, Fahimi HD. Suppression of peroxisomal lipid beta-oxidation enzymes of TNF- $\alpha$ . *FEBS Lett* 1992;310:273-6.
79. Singh I, Paintlia AS, Khan M, Stanislaus R, Paintlia MK, Haq E, Singh AK, Contreras MA. Impaired peroxisomal function in the central nervous system with inflammatory disease of experimental autoimmune encephalomyelitis animals and protection by lovastatin treatment. *Brain Res* 2004;1022:1-11.

80. Saedisomeolia A, Taheri E, Djalali M, Djazayeri A, Qorbani M, Rajab A, Larijani B. Vitamin D status and its association with antioxidant profiles in diabetic patients: A cross-sectional study in Iran. *Indian J Med Sci* 2013;67:29-37.
81. Barp J, Sartorio CL, Campos C, Llesuy SF, Araujo AS, Bello-Klein A. Influence of ovariectomy on cardiac oxidative stress in a renovascular hypertension model. *Can J Physiol Pharmacol* 2012;90:1229-34.
82. Gan X, Chen B, Shen Z, Liu Y, Li H, Xie X, Xu X, Li H, Huang Z, Chen J. High GPX1 expression promotes esophageal squamous cell carcinoma invasion, migration, proliferation and cisplatin-resistance but can be reduced by vitamin D. *Int J Clin Exp Med* 2014;7:2530-40.
83. Jardim BV, Moschetta MG, Leonel C, Gelaleti GB, Regiani VR, Ferreira LC, Lopes JR, Zuccari DA. Glutathione and glutathione peroxidase expression in breast cancer: an immunohistochemical and molecular study. *Oncol Rep* 2013;30:1119-28.
84. Frakes AE, Ferraiuolo L, Haidet-Phillips AM, Schmelzer L, Braun L, Miranda CJ, Ladner KJ, Bevan AK, Foust KD, Godbout JP, et al. Microglia induce motor neuron death via the classical NF-kappaB pathway in amyotrophic lateral sclerosis. *Neuron* 2014;81:1009-23.
85. Keeney JT, Forster S, Sultana R, Brewer LD, Latimer CS, Cai J, Klein JB, Porter NM, Butterfield DA. Dietary vitamin D deficiency in rats from middle to old age leads to elevated tyrosine nitration and proteomics changes in levels of key proteins in brain: implications for low vitamin D-dependent age-related cognitive decline. *Free Radic Biol Med* 2013;65:324-34.
86. Gallagher JC, Riggs BL, DeLuca HF. Effect of estrogen on calcium absorption and serum vitamin D metabolites in postmenopausal osteoporosis. *J Clin Endocrinol Metab* 1980;51:1359-64.
87. Penton-Rol G, Cervantes-Llanos M, Martinez-Sanchez G, Cabrera-Gomez JA, Valenzuela-Silva CM, Ramirez-Nunez O, Casanova-Orta M, Robinson-Agramonte MA, Lopategui-Cabezas I, Lopez-Saura PA. TNF-alpha and IL-10 downregulation and marked oxidative stress in Neuromyelitis Optica. *J Inflamm (Lond)* 2009;6:18,9255-6-18.
88. Stumpf C, Lehner C, Yilmaz A, Daniel WG, Garlachs CD. Decrease of serum levels of the anti-inflammatory cytokine interleukin-10 in patients with advanced chronic heart failure. *Clin Sci* 2003;105:45-50.
89. Singh P, Castillo A, Majid DS. Decrease in IL-10 and increase in TNF-alpha levels in renal tissues during systemic inhibition of nitric oxide in anesthetized mice. *Physiol Rep* 2014;2:e00228.
90. Sharma HS, Badgaiyan RD, Alm P, Mohanty S, Wiklund L. Neuroprotective effects of nitric oxide synthase inhibitors in spinal cord injury-induced pathophysiology and motor functions: an experimental study in the rat. *Ann N Y Acad Sci* 2005;1053:422-34.
91. Urushitani M, Shimohama S. The role of nitric oxide in amyotrophic lateral sclerosis. *Amyotroph Lateral Scler Other Motor Neuron Disord* 2001;2:71-81.

92. Maggio M, Basaria S, Ble A, Lauretani F, Bandinelli S, Ceda GP, Valenti G, Ling SM, Ferrucci L. Correlation between testosterone and the inflammatory marker soluble interleukin-6 receptor in older men. *J Clin Endocrinol Metab* 2006;91:345-7.
93. Coletta RD, Reynolds MA, Martelli-Junior H, Graner E, Almeida OP, Sauk JJ. Testosterone stimulates proliferation and inhibits interleukin-6 production of normal and hereditary gingival fibromatosis fibroblasts. *Oral Microbiol Immunol* 2002;17:186-92.
94. Bobjer J, Katrinaki M, Tsatsanis C, Lundberg Giwercman Y, Giwercman A. Negative association between testosterone concentration and inflammatory markers in young men: a nested cross-sectional study. *PLoS One* 2013;8:e61466.
95. Dickie LJ, Church LD, Coulthard LR, Mathews RJ, Emery P, McDermott MF. Vitamin D3 down-regulates intracellular Toll-like receptor 9 expression and Toll-like receptor 9-induced IL-6 production in human monocytes. *Rheumatology (Oxford)* 2010;49:1466-71.
96. Hopkins MH, Owen J, Ahearn T, Fedirko V, Flanders WD, Jones DP, Bostick RM. Effects of supplemental vitamin D and calcium on biomarkers of inflammation in colorectal adenoma patients: a randomized, controlled clinical trial. *Cancer Prev Res (Phila)* 2011;4:1645-54.
97. Danielpour D, Dart LL, Flanders KC, Roberts AB, Sporn MB. Immunodetection and quantitation of the two forms of transforming growth factor-beta (TGF-beta 1 and TGF-beta 2) secreted by cells in culture. *J Cell Physiol* 1989;138:79-86.
98. Houi K, Kobayashi T, Kato S, Mochio S, Inoue K. Increased plasma TGF-beta1 in patients with amyotrophic lateral sclerosis. *Acta Neurol Scand* 2002;106:299-301.
99. Letterio JJ, Roberts AB. Transforming growth factor-beta1-deficient mice: identification of isoform-specific activities in vivo. *J Leukoc Biol* 1996;59:769-74.
100. Ilzecka J, Stelmasiak Z, Dobosz B. Transforming growth factor-Beta 1 (tgf-Beta 1) in patients with amyotrophic lateral sclerosis. *Cytokine* 2002;20:239-43.
101. Cantorna MT, Woodward WD, Hayes CE, DeLuca HF. 1,25-dihydroxyvitamin D3 is a positive regulator for the two anti-encephalitogenic cytokines TGF-beta 1 and IL-4. *J Immunol* 1998;160:5314-9.
102. Razzaque MS, Lanske B. Hypervitaminosis D and premature aging: lessons learned from Fgf23 and Klotho mutant mice. *Trends Mol Med* 2006;12:298-305.
103. Wootz H, Hansson I, Korhonen L, Napankangas U, Lindholm D. Caspase-12 cleavage and increased oxidative stress during motoneuron degeneration in transgenic mouse model of ALS. *Biochem Biophys Res Commun* 2004;322:281-6.
104. Mytilineou C, Kramer BC, Yabut JA. Glutathione depletion and oxidative stress. *Parkinsonism Relat Disord* 2002;8:385-7.

105. Zhu Y, Qin Z, Gao J, Yang M, Qin Y, Shen T, Liu S. Vitamin D Therapy in Experimental Allergic Encephalomyelitis Could be Limited by Opposing Effects of Sphingosine 1-Phosphate and Gelsolin Dysregulation. *Mol Neurobiol* 2014;50:733-43.
106. Moore M, Piazza A, Nolan Y, Lynch MA. Treatment with dexamethasone and vitamin D3 attenuates neuroinflammatory age-related changes in rat hippocampus. *Synapse* 2007;61:851-61.
107. Garcion E, Sindji L, Leblondel G, Brachet P, Darcy F. 1,25-dihydroxyvitamin D3 regulates the synthesis of gamma-glutamyl transpeptidase and glutathione levels in rat primary astrocytes. *J Neurochem* 1999;73:859-66.
108. Guermontprez L, Ducrocq C, Gaudry-Talarmain YM. Inhibition of acetylcholine synthesis and tyrosine nitration induced by peroxynitrite are differentially prevented by antioxidants. *Mol Pharmacol* 2001;60:838-46.
109. Cervetto C, Frattaroli D, Maura G, Marcoli M. Motor neuron dysfunction in a mouse model of ALS: gender-dependent effect of P2X7 antagonism. *Toxicology* 2013;311:69-77.
110. Suzuki M, Tork C, Shelley B, McHugh J, Wallace K, Klein SM, Lindstrom MJ, Svendsen CN. Sexual dimorphism in disease onset and progression of a rat model of ALS. *Amyotroph Lateral Scler* 2007;8:20-5.
111. Lariviere RC, Julien JP. Functions of intermediate filaments in neuronal development and disease. *J Neurobiol* 2004;58:131-48.
112. Birge SJ, Haddad JG. 25-Hydroxycholecalciferol Stimulation of Muscle Metabolism. *J Clin Invest* 1975;56:1100-7.
113. Shea MK, Booth SL, Massaro JM, Jacques PF, D'Agostino RB S, Dawson-Hughes B, Ordovas JM, O'Donnell CJ, Kathiresan S, Keaney JF, Jr, et al. Vitamin K and vitamin D status: associations with inflammatory markers in the Framingham Offspring Study. *Am J Epidemiol* 2008;167:313-20.
114. Zhang ZL, Ding XF, Tong J, Li BY. Partial rescue of the phenotype in 1alpha-hydroxylase gene knockout mice by vitamin D3 injection. *Endocr Res* 2011;36:101-8.
115. Burton JM, Kimball S, Vieth R, Bar-Or A, Dosch HM, Cheung R, Gagne D, D'Souza C, Ursell M, O'Connor P. A phase I/II dose-escalation trial of vitamin D3 and calcium in multiple sclerosis. *Neurology* 2010;74:1852-9.
116. Kimball SM, Ursell MR, O'Connor P, Vieth R. Safety of vitamin D3 in adults with multiple sclerosis. *Am J Clin Nutr* 2007;86:645-51.
117. Moghimi E, Solomon J, Gianforcaro A, Hamadeh M. Dietary D<sub>3</sub> restriction exacerbates disease pathophysiology in the spinal cord of the G93A mouse model of amyotrophic lateral sclerosis. *PLoS One* 2015;10 (in press).

**MANUSCRIPT #2:**

**DIETARY D<sub>3</sub> RESTRICTION EXACERBATES DISEASE  
PATHOPHYSIOLOGY IN THE SPINAL CORD OF THE G93A MOUSE MODEL  
OF AMYOTROPHIC LATERAL SCLEROSIS**

**Moghimi E, Solomon JA, Gianforcaro A, Hamadeh MJ. Dietary vitamin D3 restriction exacerbates disease pathophysiology in the spinal cord of the G93A mouse model of amyotrophic lateral sclerosis. PLoS One 2015 (*accepted for publication* on March 22, 2015).**

**Dietary D<sub>3</sub> restriction exacerbates disease pathophysiology in the spinal cord of the G93A mouse model of amyotrophic lateral sclerosis**

Elnaz Moghimi , Jesse A Solomon, Alexandro Gianforcaro and Mazen J Hamadeh

*<sup>1</sup>School of Kinesiology and Health Science, Faculty of Health, York University, Toronto, Ontario, Canada, <sup>2</sup>Muscle Health Research Centre, York University, Toronto, Ontario, Canada*

**First Author:**

Elnaz Moghimi

**Corresponding Author:**

Mazen J. Hamadeh

**Keywords:** Vitamin D, hypovitaminosis D, amyotrophic lateral sclerosis, spinal cord, motor neurons, neuroprotection, oxidative stress, inflammation, antioxidant capacity, apoptosis, neurotrophic factors, neuron damage

## **Abstract**

**Background:** Dietary vitamin D<sub>3</sub> (D<sub>3</sub>) restriction reduces paw grip endurance and motor performance in G93A mice, and increases inflammation and apoptosis in the quadriceps of females. ALS, a neuromuscular disease, causes progressive degeneration of motor neurons in the brain and spinal cord.

**Objective:** We analyzed the spinal cords of G93A mice following dietary D<sub>3</sub> restriction at 2.5% the adequate intake (AI) for oxidative damage (4-HNE, 3-NY), antioxidant enzymes (SOD2, catalase, GPx1), inflammation (TNF- $\alpha$ , IL-6, IL-10), apoptosis (bax/bcl-2 ratio, cleaved/pro-caspase 3 ratio), neurotrophic factor (GDNF) and neuron damage (ChAT, SMI-36/SMI-32 ratio).

**Methods:** Beginning at age 25 d, 42 G93A mice were provided food *ad libitum* with either adequate (AI; 1 IU D<sub>3</sub>/g feed; 12 M, 11 F) or deficient (DEF; 0.025 IU D<sub>3</sub>/g feed; 10 M, 9 F) D<sub>3</sub>. At age 113 d, the spinal cords were analyzed for protein content. Differences were considered significant at  $P \leq 0.10$ , since this was a pilot study.

**Results:** DEF mice had 16% higher 4-HNE ( $P = 0.056$ ), 12% higher GPx1 ( $P = 0.057$ ) and 23% higher Bax/Bcl2 ratio ( $P = 0.076$ ) vs. AI. DEF females had 29% higher GPx1 ( $P = 0.001$ ) and 22% higher IL-6 ( $P = 0.077$ ) vs. AI females. DEF males had 23% higher 4-HNE ( $P = 0.066$ ) and 18% lower SOD2 ( $P = 0.034$ ) vs. AI males. DEF males had 27% lower SOD2 ( $P = 0.004$ ), 17% lower GPx1 ( $P = 0.070$ ), 29% lower IL-6 ( $P = 0.023$ ) and 22% lower ChAT ( $P = 0.082$ ) vs. DEF females.

**Conclusion:** D<sub>3</sub> deficiency exacerbates disease pathophysiology in the spinal cord of G93A mice, the exact mechanisms are sex-specific. This is in accord with our previous results in the *quadriceps*, as well as functional and disease outcomes.

## Introduction

Amyotrophic lateral sclerosis (ALS), also known as Lou Gehrig's disease, is the most commonly occurring adult-onset motor neuron disease of unknown cause (1, 2) and is typically diagnosed between 45 and 60 years of age (3, 4). It is characterized by degeneration of upper and lower motor neurons, resulting in skeletal muscle atrophy (5) and death by respiratory failure within 3-5 years of initial symptoms (6-8). 90% of cases are of unknown etiology (sporadic ALS) (3, 9), whereas the other 10% have inherited genetic mutations (3, 10) (familial ALS), ~12% of these cases being a result of a mutation in the  $\text{Cu}^{2+}/\text{Zn}^{2+}$  super-oxide dismutase 1 (SOD1) gene (11-14). The most commonly used animal model of ALS is the G93A mouse model (15) that transgenically overexpresses the mutant SOD1 gene (10). Their disease pathology and neurodegenerative patterns closely resemble that which is found in ALS patients (10). On a cellular level, excessive stimulation of glutamate receptors (16) leads to a large influx of calcium ion into the post synaptic neuron, resulting in a destructive cascade of membrane, cytoplasmic and nuclear events (17). These include oxidative damage (18, 19), oxidative stress (20, 21), inflammation (22), compromised neurotrophic factor release (22) and apoptosis (13).

Some nutrition-based interventions have shown effectiveness in mitigating ALS disease severity in animal models of ALS (23). Vitamin D is a fat-soluble vitamin with hormone-like properties that is essential for health, growth and development (24). Vitamin D<sub>3</sub> and/or its metabolites [calcidiol (25(OH)D<sub>3</sub>) and calcitriol (1,25(OH)<sub>2</sub>D<sub>3</sub>)] can protect dopaminergic neurons against the neurotoxic effects of glutamate and dopaminergic toxins (25), and has anti-inflammatory and modulatory effects on CNS

components such as neurotrophins and growth factors (26). Vitamin D treatment can improve compromised functional outcomes and muscle physiology in humans and rodents, whereas vitamin D receptor (VDR) knockout mice have loss of motor function and muscle mass (27). Vitamin D reduces the expression of biomarkers associated with oxidative stress and inflammation in diseases that share common pathophysiologies with ALS. Vitamin D deficiency has been associated with the development of inflammatory and immune diseases such as type II diabetes (28), multiple sclerosis (29), dementia and Alzheimer's disease (30). A deficiency in vitamin D reduces the amount of calcium buffering protein, thus leading to higher lipid peroxidation and protein damage (31). When investigating the effects of vitamin D on biomarkers of oxidative stress in obese children aged 7-14 y, obese children with 25(OH)D insufficiency (serum calcidiol <50 nmol/L) had significantly elevated 3-nitrotyrosine (3-NY) levels, a marker of protein damage, vs. non-deficient obese children (serum calcidiol >50 nmol/L) (32). A partial correlation analysis showed an inverse relationship between 25(OH)D and 3-NY ( $r = -0.424$ ,  $P = 0.001$ ).

A retrospective study in ALS patients found that those with serum calcidiol levels <25 nmol/L increased their death rate by 6 fold and their rate of decline by 4 times, and were associated with a marked shorter life expectancy compared to patients with serum calcidiol levels >75 nmol/L (33). We have previously demonstrated the detrimental effects of vitamin D<sub>3</sub> restriction in the G93A mouse model of ALS (34-37). Dietary vitamin D<sub>3</sub> at 2.5% the adequate intake (AI) resulted in lower paw grip endurance (PaGE) and motor performance (37), and in the *quadriceps* of female G93A resulted in increased inflammation (35) and apoptosis (36), when compared to their AI counterparts.

Does vitamin D<sub>3</sub> restriction directly impact the CNS? And, if it does, will vitamin D<sub>3</sub> deficiency explain the functional outcomes in our previous study (37). Hence, the objective of this study was to investigate the effects of vitamin D deficiency via dietary restriction (0.025 IU/g feed) vs. adequate intake (1 IU/g feed) on oxidative damage, antioxidant capacity, inflammation, apoptosis, neurotrophic factor and neuron damage in the spinal cord of the G93A transgenic mouse model of ALS.

## **Methods**

### **Ethical Statement**

The experimental protocol used in this study followed the guidelines of the Canadian Council of Animal Care and was approved by York University Animal Research Ethics Board (protocol # 2007-9). All the necessary steps were taken to minimize suffering and distress to the mice in the study.

### **Animals**

Male B6SJL-TgN(SOD1-G93A)1Gur hemizygous mice (No. 002726) were harem-bred with non-affected female B6SJL control mice (No. 100012; Jackson Laboratory, Bar Harbor, ME). We identified the presence of the human-derived G93A transgene by using polymerase chain reaction (PCR) amplification of DNA extracted from ear tissue as outlined by Sigma-Aldrich (XNAT REDEExtract-N-Amp Tissue PCR Kit; XNAT-1KT). All breeding mice were housed 3 females per 1 male, and consumed Research Diet AIN-93G (1 IU D<sub>3</sub>/g feed; Research Diet, New Brunswick, NJ). All animals were housed individually at age 25 d in a 12 h light/dark cycle.

## Study Design

42 (22 M, 20 F) G93A mice consumed a diet that contained an adequate intake of vitamin D<sub>3</sub> (1 IU/g feed; Research Diet AIN-93G; Product # D10012G; Research Diets Inc, New Brunswick NJ [38]) *ad libitum* after weaning (21 d). At age 25 d, the mice were individually caged and divided into one of two groups: 1) adequate vitamin D<sub>3</sub> (AI; 1 IU D<sub>3</sub>/g feed; 12 M, 11 F; Research Diet AIN-93G) or 2) deficient vitamin D<sub>3</sub> (DEF; 1/40 IU D<sub>3</sub>/g feed; 10 M 9 F; Product #D10030801; Research Diets Inc, New Brunswick, NJ) (Table 1).

When the mice reached a clinical score (CS; disease severity) of 3.0, food and calorie-free gel (Harlan-Gel, Harlan Teklad, Madison WI) were placed on the floor of the cage to fulfill ethics requirements. Endpoint was determined as previously described by Solomon *et al* 2011 (38). The calorie-free gel contained synthetic polymers (WATER LOCK<sup>®</sup> superabsorbent polymer G-400, G-430, G-500, G-530; 95% by weight) and methanol (4.5% by weight). A summary of food intake, vitamin D<sub>3</sub> intake and body weight of the G93A mice can be found in Table 2.2. Two researchers who were blinded to the diets conducted all measurements.

**Table 2.1** Nutrient content of the adequate intake (AI) and deficient (DEF) vitamin D<sub>3</sub> diets

Nutrient	Diet	
	AI	DEF
Energy (kcal/g)	4	4
Carbohydrate (%)	64	64
Protein (%)	20	20
Fat (%)	7	7
Vitamin D <sub>3</sub> (IU/g)	1 <sup>a</sup>	0.025 <sup>b</sup>
Calcium (%)	0.5 <sup>c</sup>	0.5 <sup>d</sup>
Vitamin mix V10037 (mg/g)	10	10
Mineral mix S100022G (mg/g)	35	35

Diets provided by Research Diets (based on AIN-93G; New Brunswick, NJ; AI product # D10012G; HiD product # D08080101;).

<sup>a</sup>, included in vitamin mix V10037

<sup>b</sup>, included in vitamin mix V13203 (39)

<sup>c</sup>, included in mineral mix S100022G (40)

\* table adopted from Solomon *et al*, PLoS ONE 2011 (37).

**Table 2.2** Food intake, vitamin D<sub>3</sub> intake and body weight of G93A mice.

Measurements	Males		Females	
	AI (n=12)	DEF (n=10)	AI (n=11)	DEF (n=9)
Food intake (g/d)*	3.5±0.1	4.2±0.3	3.4±0.1	3.3±0.1
Food intake (mg/g b.wt./d)*	151.5±5.4	188.3±12.9	195.0±6.7	182.2±6.4
Vitamin D <sub>3</sub> intake (IU D <sub>3</sub> /d)	3.494±0.136	0.104±0.007	3.4±0.1	0.08±0.001
Vitamin D <sub>3</sub> intake (IU D <sub>3</sub> /g b.wt./d)	0.1515±0.0054	0.0048±0.0004	0.1950±0.0067	0.0046±0.0002
Body weight (g)*	23.1±0.4	22.1±0.6	17.6±0.3	18.1±0.4

AI, adequate intake, n=23; DEF, deficient vitamin D<sub>3</sub>, n=19; b.wt.: body weight. DEF males consumed 19% more absolute feed (P = 0.038) and 24% more feed corrected for body weight (P = 0.011) vs. AI males. DEF males consumed 26% more absolute feed (P = 0.016) vs. DEF females. Males (168.2±7.5 mg/g b.wt./d) consumed 12% less feed corrected for body weight vs. females (189.2±4.8 mg/g b.wt./d) (P = 0.027). DEF males had 22% higher body weight vs. DEF females (P<0.0001). Males (22.7±0.4 g) had 27% higher body weight vs. females (17.9±0.2 g) (P<0.0001). Data are means ±SEM.

### Tissue Collection

At age 113 d, mice were sacrificed and spinal cords were harvested. The mice were placed and kept under anesthesia with gaseous isoflurane as the tissue was collected and placed in individual sterile polyethylene tubes for immediate freezing in liquid nitrogen. Samples were stored at -80°C.

### Spinal Cord Homogenization

Spinal cords were weighed, and minced with a glass-Teflon Port-Evenhejm homogenizer (5% wt/vol) in radioimmunoprecipitation assay (RIPA) buffer (1:20) containing 50 mM tris HCL 8.0 (Bioshop, TRS002.500, Burlington, Ontario), 150 mM

NaCl (BioBasic Canada, 7647145, Markham, Ontario), 0.1% SDS (Bioshop, SDS001.500, Burlington, Ontario), 0.5% sodium deoxycholate (Bioship, DCA333.50, Burlington, Ontario), 1% NP-40 (Thermo Scientific, 28324, Rockford, Illinois), 5 mM EDTA pH 8.0 (Bioshop, EDT001.500, Burlington, Ontario) and 1 mM PMSF (Sigma-Aldrich, 93482, St. Louis, Missouri). The protease inhibitor cocktail (Roche, 11836153001, Mannheim, Germany) was added to the buffer in accordance to manufacturer's instructions (1:100) prior to homogenization. Mouse spinal cord was homogenized for about 40 grinds using constant force to ensure consistency and homogeneity of samples. Homogenates were divided in roughly equal volumes in eppendorf tubes and were placed on a shaker at 4°C for 30 minutes. The homogenates were then centrifuged at (600 g) for 20 min at 4°C. The resulting supernatant was decanted, put into newly labeled eppendorf tubes and immediately stored at -80°C. The protein concentration was determined using the BCA Protein Assay technique (41). The supernatant concentration was measured at 562 nm using an ultraviolet spectrophotometer (Cecil 9200 Super Aquarius, Cambridge, UK). Protein concentrations were presented as mg/ml.

### **Western Blot**

Equal amounts of protein were size-separated by 12.5% sodium dodecyl sulfate-polyacrylamide gel electrophoresis (SDS-PAGE) and were transferred to nitrocellulose membranes (#165-3322, Bio-Rad Mini-PROTEAN 2 electrophoresis system, Mississauga, ON, Canada) at 100 V for 2 h. The membranes were blocked in 3% fat free milk (SMI-36), 5% fat free milk (SOD2, catalase, TNF- $\alpha$ , IL-6) or 5% BSA (4-HNE, 3-NY, GPx1, IL-10, Bax, Bcl-2, pro-caspase 3, cleaved caspase 3, GDNF, ChAT, SMI-32)

diluted in Tris-buffered saline with tween (1%) for 2 h at room temperature and incubated with primary antibodies in 3% fat free milk (SMI36), 5% fat free milk (catalase, TNF-  $\alpha$ , IL-6), 1% BSA (SOD2, cleaved caspase 3, GDNF, ChAT), 3% BSA (IL-10, SMI32) or 5% BSA (4-HNE, 3-NY, GPx1, Bax, Bcl-2, pro-caspase 3) against 4-HNE (1:800; Abcam, ab46545), 3-NY (1:1000; Abcam, ab110282), SOD2 (1:8000; Abcam, ab13533), catalase (1:3500; Abcam, ab1877-10), GPx1 (1:800; Abcam, 22604), TNF-  $\alpha$  (1:2000; Abcam, ab9739) IL-6 (1:1000; Abcam, ab6672), IL-10 (1:2000; Abcam, ab9969), Bax (1:1000; Cell Signaling Technology, 2772), Bcl-2 (1:1000; Cell Signaling Technology, 2870), pro-caspase 3 (1:1000; Millipore, 04-440), cleaved caspase 3 (1:1000; Millipore, 04-439), GDNF (1:1000; Abcam, a18956), ChAT (1:1000; Abcam, ab85609), SMI-32 (1:1000; Abcam, ab28029) and SMI-36 (1:1000; Abcam, ab24572), overnight at 4°C. Equal loading was verified by ponceau staining, as well as probing for glyceraldehyde 3-phosphate dehydrogenase (GAPDH; 1:100,000; MAB374, Millipore). The antigen-antibody complexes were detected by incubating the membranes in anti-rabbit (1: 5000; Novus Biologicals, NB730-H) or anti-mouse (1:5000; Novus Biologicals, NB7539) HRP conjugated secondary antibodies at room temperature for 2 h in 3% fat free milk (SMI36), 5% fat free milk (4-HNE, catalase, TNF-  $\alpha$ , IL-6), 1% BSA (SOD2, cleaved caspase 3, GDNF, ChAT), 3% BSA (IL-10, SMI32) or 5% BSA (3-NY, GPx1, Bax, Bcl-2, pro-caspase 3). Immunoreactive proteins were visualized with enhanced chemiluminescence (sc-2048, Santa Cruz Biotechnology), and scanned using Kodak Imaging Station 4000MM Pro (Carestream Health, Inc. Rochester, NY, USA). Protein intensity was standardized to GAPDH and analyzed using Carestream MI (v 5.0.2.30,

NY, USA). Representative western blot bands for the biomarkers are found in supplementary figure S2.1 in Appendix B.

### **Calculations**

Human equivalent dosage (HED) was calculated according to the US FDA (40):

$$\text{HED} = \text{Animal dose (mg/kg)} \times [\text{animal weight (kg)} \div \text{human weight (kg)}]^{0.33}.$$

### **Statistical analysis**

We established planned comparisons between HiD vs. AI. A one-tailed independent t-test was used to determine differences between the diets within each sex, because we hypothesized *a priori* that absolute and body weight-adjusted spinal cord weight, antioxidant activity, neurotrophic factors and neuronal count would be higher in HiD males vs. AI but not females whereas oxidative damage, inflammation and apoptosis would be lower in HiD males vs. AI but not females. These are based on studies conducted by us and other researchers (23,27,32,34-38,41-45). For all other outcome measures, a two-tailed analysis was performed. All statistical analyses were completed using GraphPad Prism 6 for Macintosh (GraphPad Software Inc, La Jolla, CA). Data were presented as means  $\pm$  standard error of mean (SEM). Significance was set to  $P \leq 0.10$ , since this was a pilot study.

## **Results**

### **Oxidative Damage**

#### 4-HNE

DEF mice had 16% higher 4-HNE protein content vs. AI (P = 0.056). DEF males had 23% higher 4-HNE protein content vs. AI males (P = 0.066) (Figure 2.1B).

#### 3-NY

There was no significant difference in 3-NY protein content between the diets (Figure 2.1C and 2.1D). AI males had 18% higher 3-NY protein content vs. AI females (P = 0.073). Data presented as means  $\pm$  SEM.

### **Antioxidant Enzymes**

#### SOD2

DEF males had 18% lower SOD2 protein content vs. AI males (P = 0.034) (Figure 2.2B). DEF males had 27% lower SOD2 protein content vs. DEF females (P = 0.004).

#### Catalase

There was no significant difference in catalase protein content between the diets or between the sexes (Figure 2.2C and 2.2D)

#### GPx1

DEF mice had 12% higher GPx1 protein content vs. AI (P = 0.057). DEF females had 29% higher GPx1 protein content vs. AI females (P = 0.001) (Figure 2.2E). AI males had 10% higher GPx1 protein content vs. AI females (P = 0.054). DEF males had 17% lower GPx1 protein content vs. DEF females (P = 0.070).

### **Inflammation**

#### TNF- $\alpha$

There was no significant difference in TNF- $\alpha$  protein content between the diets or between the sexes (Figure 2.3A and 2.3B).

#### IL-6

DEF females had 22% higher IL-6 protein content vs. AI females (P = 0.077) (Figure 2.3C). AI males had 14% lower IL-6 protein content vs. AI females (P = 0.075). DEF males had 29% lower IL-6 protein content vs. DEF females (P = 0.023).

#### IL-10

There was no significant difference in IL-10 protein content between the diets (Figure 2.3E and 2.3F). AI males had 11% lower IL-10 protein content vs. AI females (P = 0.074).

### **Apoptosis**

#### Bax

There was no significant difference in Bax protein content between the diets or between the sexes (Figure 2.4A and 2.4B).

#### Bcl-2

There was no significant difference in Bcl-2 protein content between the diets (Figure 2.4C and 2.4D). AI males had 14% higher Bcl-2 protein content vs. AI females (P = 0.048).

#### Bax/Bcl-2 ratio

DEF mice had 23% higher Bax/Bcl-2 protein content vs. AI (P = 0.076).

### **Caspase 3**

#### Pro-caspase 3

There was no significant difference in pro-caspase protein content between the diets or between the sexes (Figure 2.5A and 2.5B).

#### Cleaved caspase 3

There was no significant difference in cleaved caspase 3 protein content between the diets or between the sexes (Figure 2.5C and 2.5D).

#### Cleaved/pro-caspase 3

There was no significant difference in cleaved/pro-caspase 3 protein content between the diets or between the sexes (Figure 2.5E and 2.5F).

### **Neurotrophic Factor**

#### GDNF

There was no significant difference in GDNF protein content between the diets or between the sexes (Figure 2.6A and 2.6B).

### **Neuron Damage**

#### ChAT

There was no significant difference in ChAT protein content between the diets (Figure 2.7A and 2.7B). AI males had 23% lower ChAT protein content vs. AI females (P = 0.005). DEF males had 22% lower ChAT protein content vs. DEF females (P = 0.082)

#### SMI-32

There was no significant difference in SMI-32 protein content between the diets (Figure 2.7C and 2.7D). AI males had 15% lower SMI-32 protein content vs. AI females (P = 0.039). DEF males had 17% lower SMI-32 protein content vs. DEF females (P = 0.046).

#### SMI-36

There was no significant difference in SMI-36 protein content between the diets (Figure 2.7E and 2.7F). AI males had 13% lower SMI-36 protein content vs. AI females (P = 0.016).

#### SMI-36/SMI-32

There was no significant difference in SMI-36/SMI-32 protein content between the diets or between the sexes (Figure 2.7G and 2.7H).

#### Spinal cord weights

Absolute spinal cord weight was not different between the diets (Table 2.3). Between the sexes, AI males had 15% lighter absolute spinal cord weight vs. AI females (P = 0.065), and DEF males had 16% lighter absolute spinal cord weight vs. DEF females (P = 0.053) (Table 2.3). There was no significant difference in body weight-adjusted spinal cord weights between the diets (Table 2.3; Figure 8A and 8B). Between the sexes, AI males had 33% lighter body weight-adjusted spinal cord weight vs. AI females (P = 0.001) (Table 2.3; Figure 8C), and DEF males had 27% lighter body weight-adjusted spinal cord weight vs. DEF females (P = 0.005) (Table 2.3; Figure 8D).

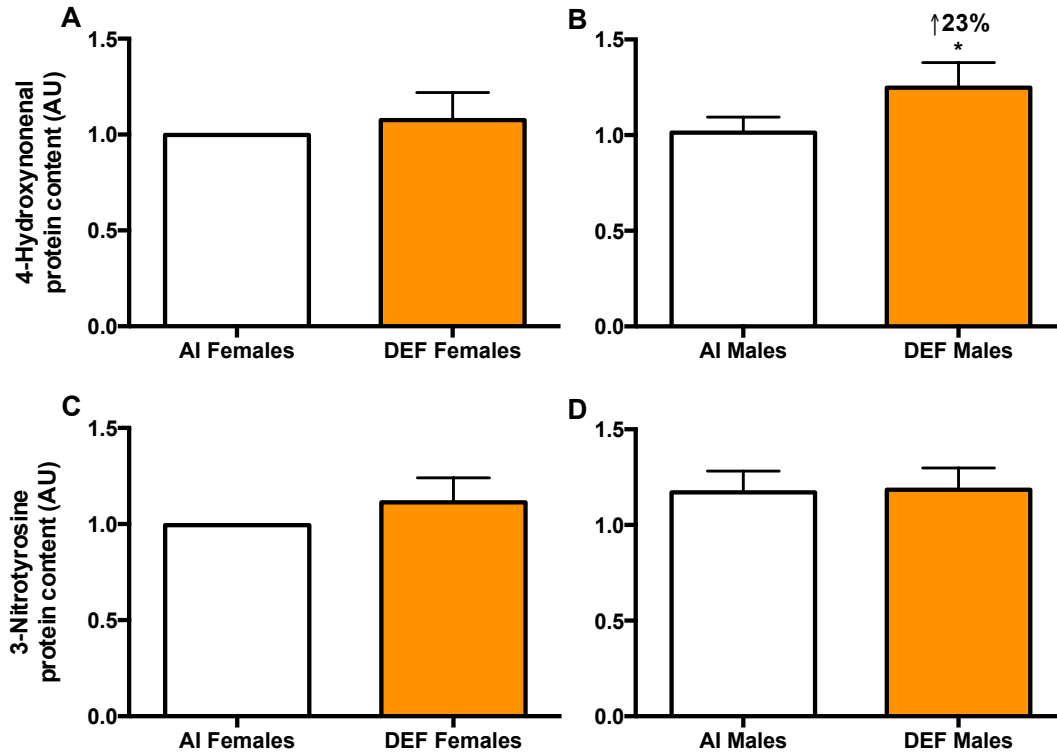


**Figure 2.1 Oxidative damage in DEF vs. AI G93A mice.**

4-HNE (A and B) and 3-NY (C and D) protein content (arbitrary units; AU) in spinal cord of 42 G93A mice: 23 adequate vitamin D<sub>3</sub> intake (AI; 1 IU D<sub>3</sub>/g feed; 12 M, 11 F) and 19 deficient vitamin D<sub>3</sub> intake (DEF; 0.025 IU D<sub>3</sub>/g feed; 10 M, 9 F). *4-Hydroxynonenal (4-HNE, A and B)*: DEF mice had 16% higher 4-HNE protein content vs. AI (P = 0.056). DEF males had 23% higher 4-HNE protein content vs. AI males (P = 0.066). *3-Nitrotyrosine (3-NY, C and D)*: There was no significant difference in 3-NY protein content between the diets. AI males had 18% higher 3-NY protein content vs. AI females (P = 0.073). Data presented as means ± SEM.

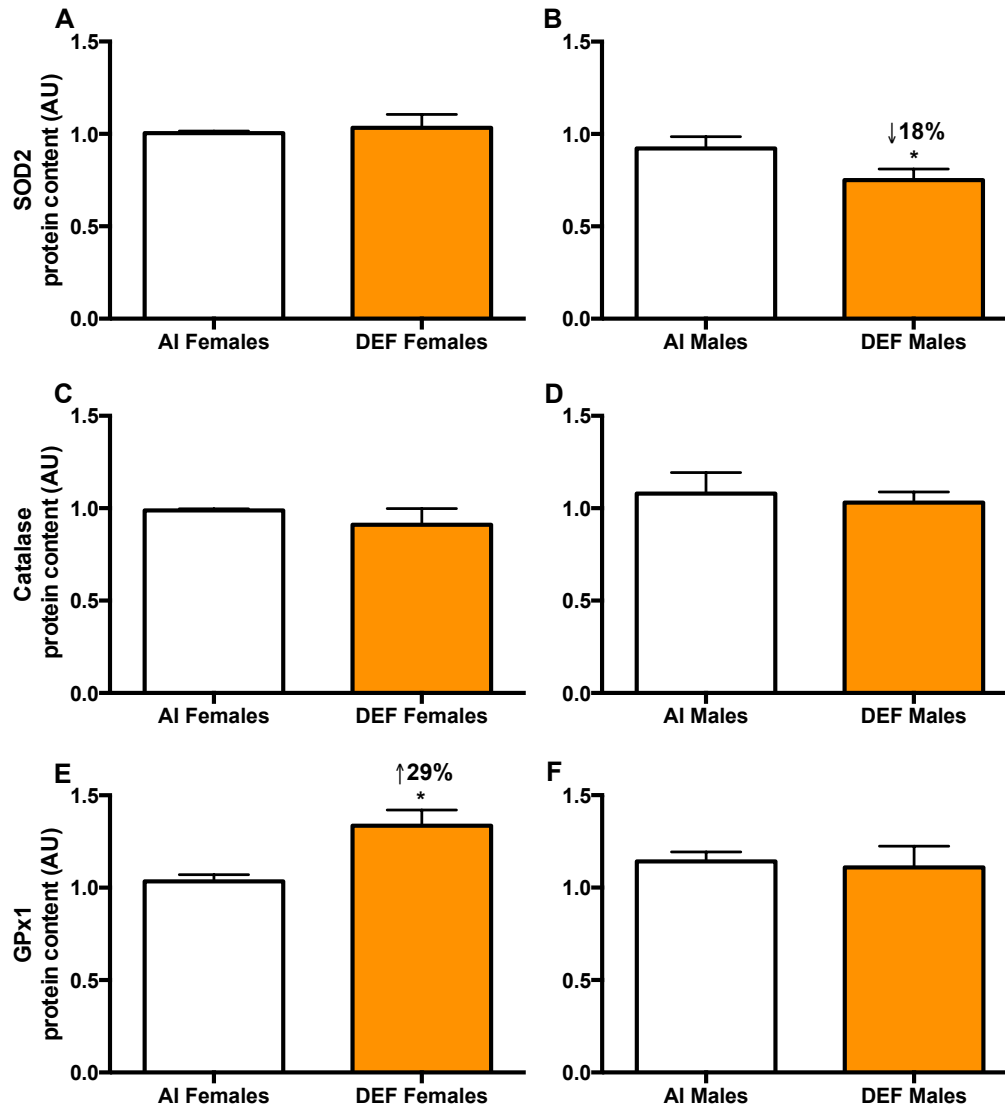


**Figure 2.2 Antioxidant enzymes in DEF vs. AI G93A mice.**

SOD2 (A and B), catalase (C and D) and GPx1 (E and F) protein content (arbitrary units; AU) in spinal cord of 42 G93A mice: 23 adequate vitamin D<sub>3</sub> intake (AI; 1 IU D<sub>3</sub>/g feed; 12 M, 11 F) and 19 deficient vitamin D<sub>3</sub> intake (DEF; 0.025 IU D<sub>3</sub>/g feed; 10 M, 9 F).

SOD2 (A and B): DEF males had 18% lower SOD2 protein content vs. AI males (P = 0.034). DEF males had 27% lower SOD2 protein content vs. DEF females (P = 0.004).

Catalase (C and D): There was no significant difference in catalase protein content

between the diets or between the sexes. GPx1 (E and F): DEF mice had 12% higher GPx1 protein content vs. AI (P = 0.057). DEF females had 29% higher GPx1 protein content vs. AI females (P = 0.001). AI males had 10% higher GPx1 protein content vs.

AI females (P = 0.054). DEF males had 17% lower GPx1 protein content vs. DEF females (P = 0.070). Data presented as means ± SEM.

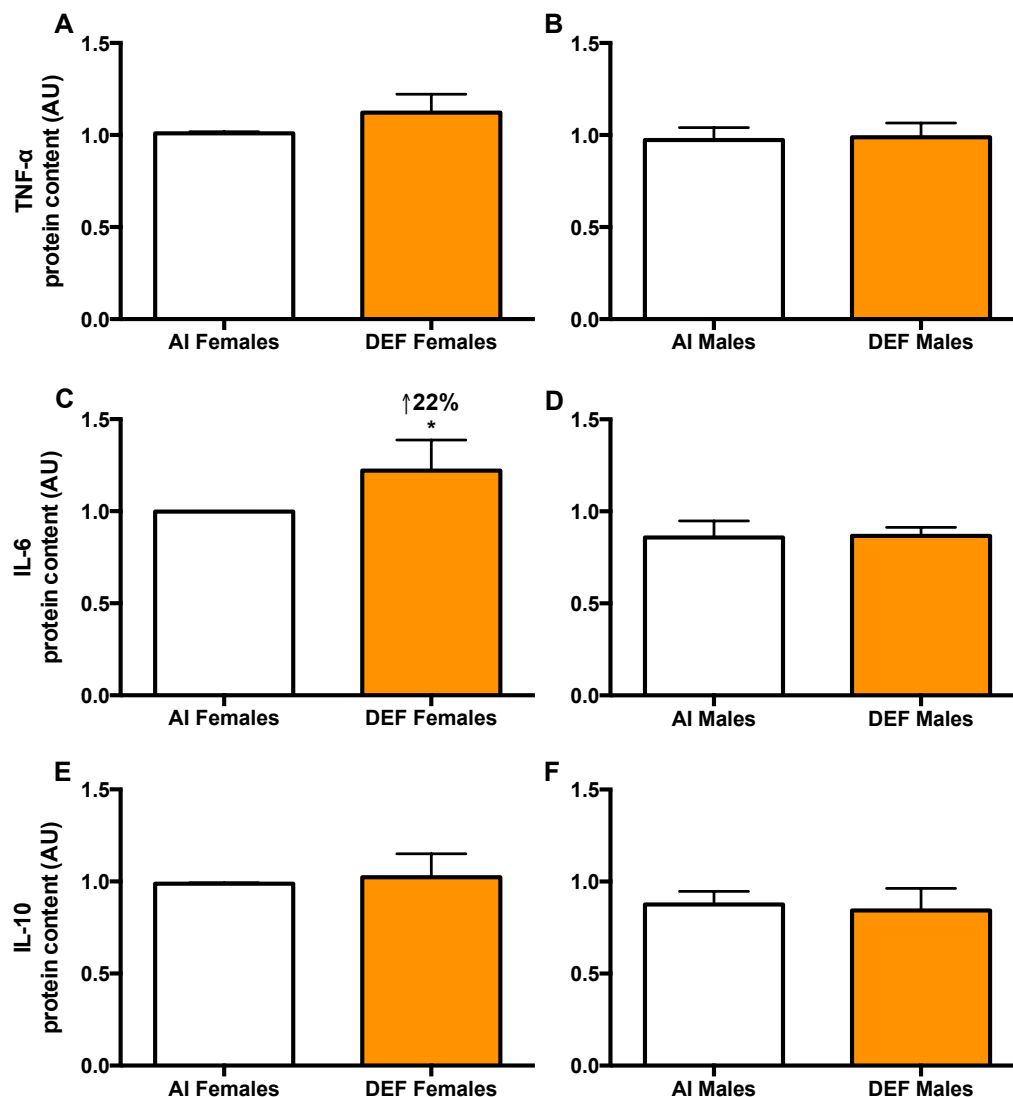


**Figure 2.3 Inflammation in DEF vs. AI G93A mice.**

TNF-  $\alpha$  (A and B), IL-6 (C and D) and IL-10 (E and F) protein content (arbitrary units; AU) in spinal cord of 42 G93A mice: 23 adequate vitamin D<sub>3</sub> intake (AI; 1 IU D<sub>3</sub>/g feed; 12 M, 11 F) and 19 deficient vitamin D<sub>3</sub> intake (DEF; 0.025 IU D<sub>3</sub>/g feed; 10 M, 9 F). *TNF- $\alpha$  (A and B):* There was no significant difference in TNF- $\alpha$  protein content between the diets or between the sexes. *IL-6 (C and D):* DEF females had 22% higher IL-6 protein content vs. AI females (P = 0.077). AI males had 14% lower IL-6 protein content vs. AI females (P = 0.075). DEF males had 29% lower IL-6 protein content vs. DEF females (P = 0.023). *IL-10 (E and F):* There was no significant difference in IL-10 protein content between the diets. AI males had 11% lower IL-10 protein content vs. AI females (P = 0.074). Data presented as means  $\pm$  SEM.

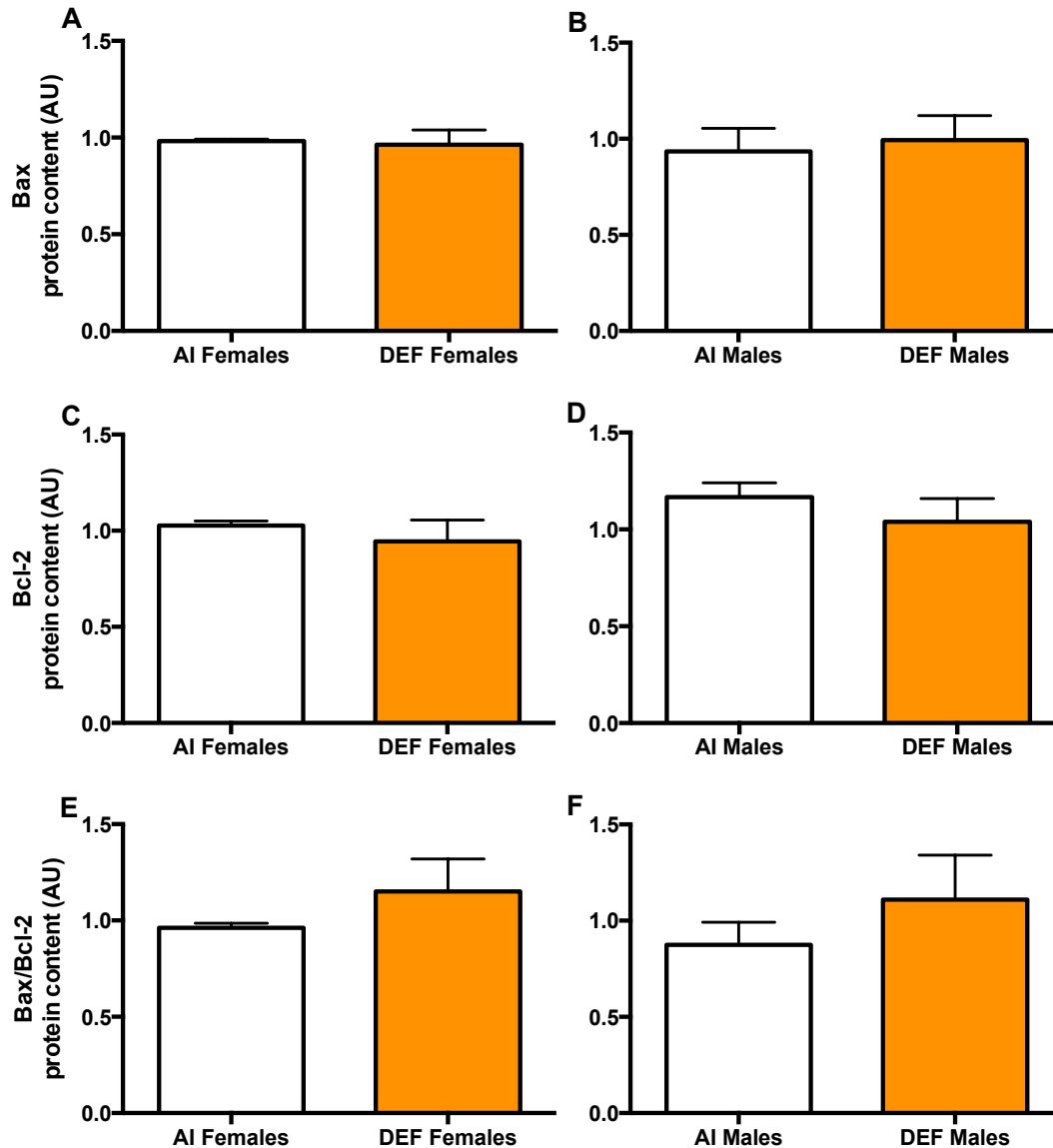


**Figure 2.4 Bax/Bcl-2 in DEF vs. AI G93A mice.**

Bax (A and B), Bcl-2 (C and D) and Bax/Bcl-2 ratio (E and F) protein content (arbitrary units; AU) in spinal cord of 42 G93A mice: 23 adequate vitamin D<sub>3</sub> intake (AI; 1 IU D<sub>3</sub>/g feed; 12 M, 11 F) and 19 deficient vitamin D<sub>3</sub> intake (DEF; 0.025 IU D<sub>3</sub>/g feed; 10 M, 9 F). Bax (A and B): There was no significant difference in Bax protein content between the diets or between the sexes. Bcl-2 (C and D): There was no significant difference in Bcl-2 protein content between the diets. AI males had 14% higher Bcl-2 protein content vs. AI females (P = 0.048). Bax/Bcl-2 ratio (E and F): DEF mice had 23% higher Bax/Bcl-2 protein content vs. AI (P = 0.076). Data presented as means ± SEM.

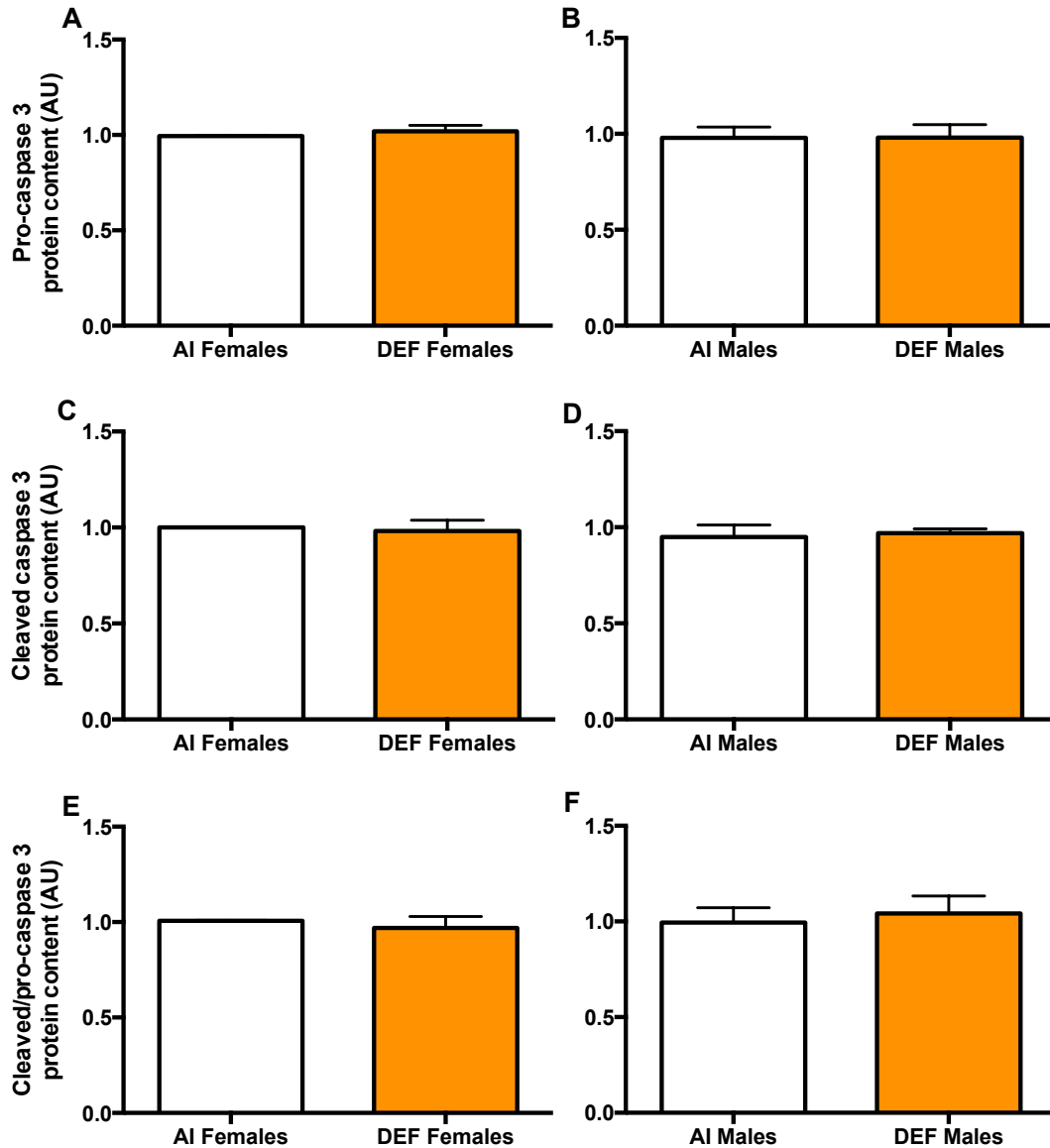


**Figure 2.5 Caspase 3 in DEF vs. AI G93A mice.**

Pro-caspase 3 (A and B), cleaved caspase 3 (C and D) and cleaved/pro-caspase 3 (E and F) protein content (arbitrary units; AU) in spinal cord of 42 G93A mice: 23 adequate vitamin D<sub>3</sub> intake (AI; 1 IU D<sub>3</sub>/g feed; 12 M, 11 F) and 19 deficient vitamin D<sub>3</sub> intake (DEF; 0.025 IU D<sub>3</sub>/g feed; 10 M, 9 F). There was no significant difference in pro-caspase 3, cleaved caspase 3 and cleaved/pro-caspase 3 protein content between the diets or between the sexes. Data presented as means  $\pm$  SEM.

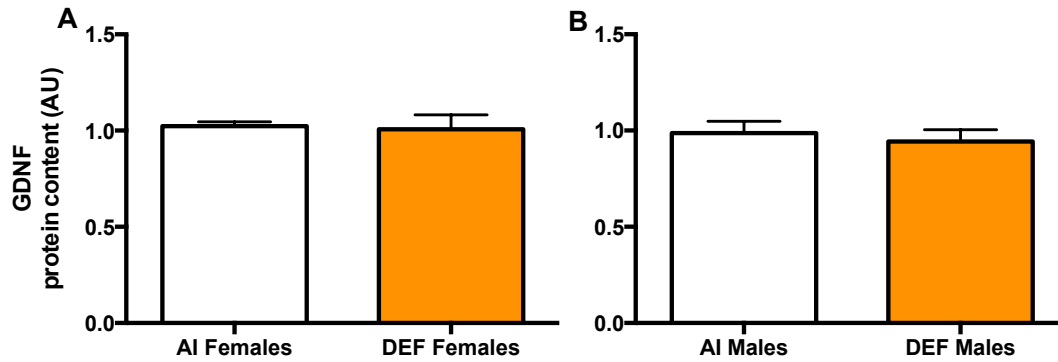


**Figure 2.6 Neurotrophic factor in DEF vs. AI G93A mice.**

GDNF protein content (A and B) (arbitrary units; AU) in spinal cord of 42 G93A mice: 23 adequate vitamin D<sub>3</sub> intake (AI; 1 IU D<sub>3</sub>/g feed; 12 M, 11 F) and 19 deficient vitamin D<sub>3</sub> intake (DEF; 0.025 IU D<sub>3</sub>/g feed; 10 M, 9 F). There was no significant difference in GDNF protein content between the diets or between the sexes. Data presented as means  $\pm$  SEM.

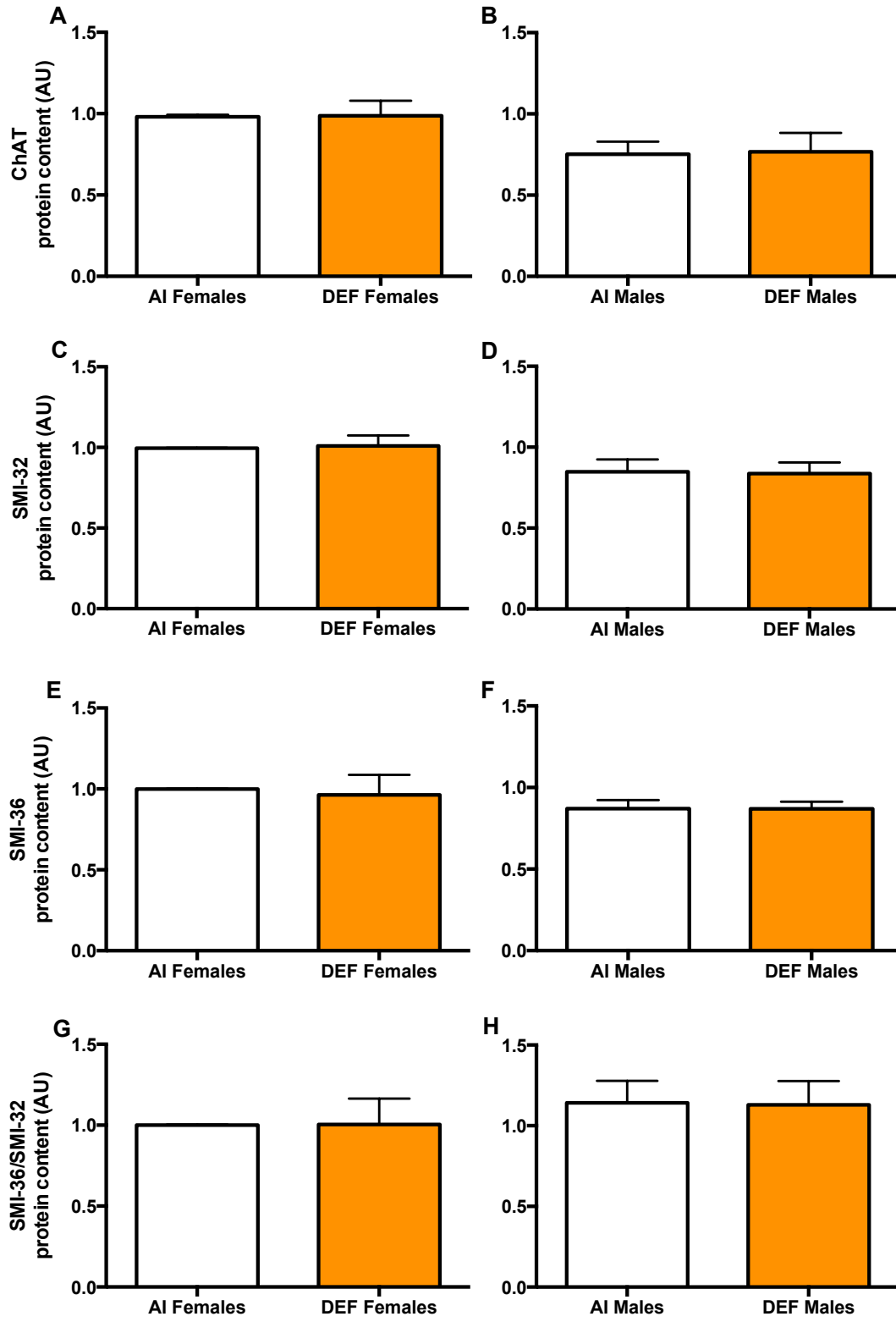


**Figure 2.7 Neuron damage in DEF vs. AI G93A mice.**

ChAT (A and B), SMI-32 (C and D), SMI-36 (E and F) and SMI-36/SMI-32 ratio (G and H) protein content (arbitrary units; AU) in spinal cord of 42 G93A mice: 23 adequate vitamin D<sub>3</sub> intake (AI; 1 IU D<sub>3</sub>/g feed; 12 M, 11 F) and 19 deficient vitamin D<sub>3</sub> intake (DEF; 0.025 IU D<sub>3</sub>/g feed; 10 M, 9 F). ChAT (A and B): There was no significant difference in ChAT protein content between the diets. AI males had 23% lower ChAT protein content vs. AI females (P = 0.005). DEF males had 22% lower ChAT protein content vs. DEF females (P = 0.082). SMI-32 (C and D): There was no significant difference in SMI-32 protein content between the diets. AI males had 15% lower SMI-32 protein content vs. AI females (P = 0.039). DEF males had 17% lower SMI-32 protein content vs. DEF females (P = 0.046). SMI-36 (E and F): There was no significant difference in SMI-36 protein content between the diets. AI males had 13% lower SMI-36 protein content vs. AI females (P = 0.016). SMI-36/SMI-32 ratio (G and H): There was no significant difference in SMI-36/SMI-32 protein content between the diets or between the sexes. Data presented as means ± SEM.

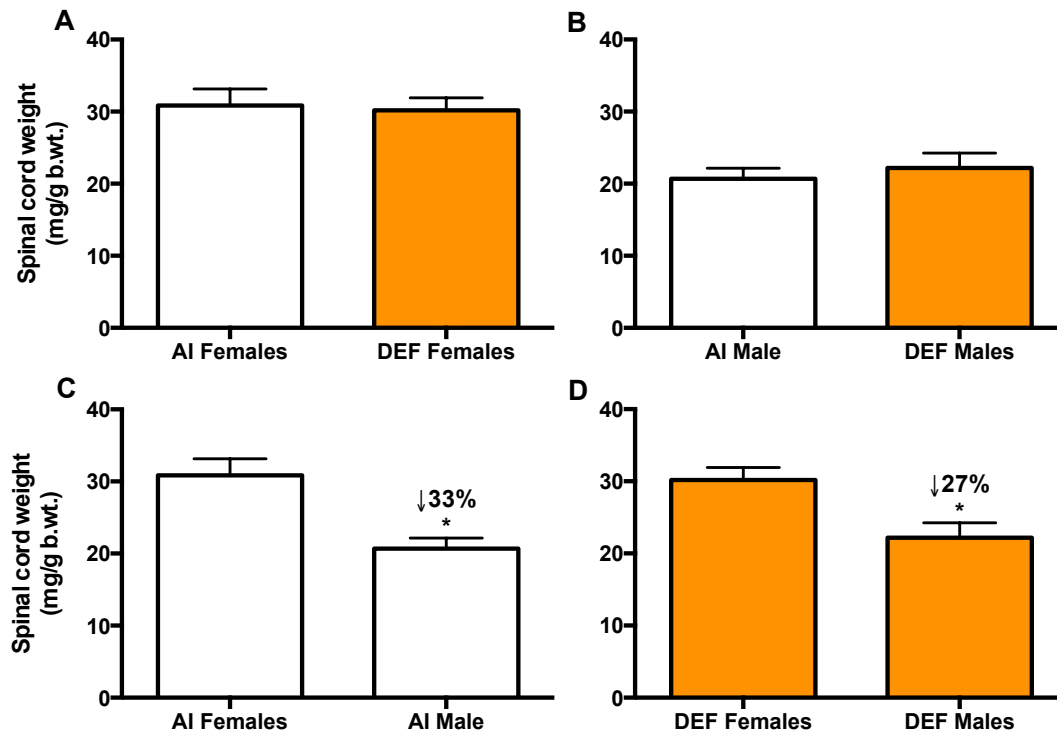


**Figure 2.8** Body weight-adjusted spinal cord weights at 113 d.

Body weight-adjusted spinal cord weight (mg/g b.wt.) of 42 G93A mice: 23 adequate vitamin D<sub>3</sub> intake (AI; 1 IU D<sub>3</sub>/g feed; 12 M, 11 F) and 19 deficient vitamin D<sub>3</sub> intake (DEF; 0.025 IU D<sub>3</sub>/g feed; 10 M, 9 F). *Between the diets (A and B)*: There was no significant difference in body weight-adjusted spinal cord weights between the diets. *Between the sexes (C and D)*: AI males had 33% lighter body weight-adjusted spinal cord weight vs. AI females (P = 0.001), and DEF males had 27% lighter body weight-adjusted spinal cord weight vs. DEF females (P = 0.005). Data presented as means ± SEM.

**Table 2.3. Spinal cord weight between the diets and sexes at 113 d.**

Spinal cord weights	Females			Males			Within-AI between-sex differences	Within-DEF between-sex differences
	AI	DEF	P value	AI	DEF	P value	P value	P value
<b>Absolute spinal cord weight (mg)</b>	583±43	581±33	NS	494±37	489±42	NS	P = 0.065	P = 0.053
<b>Body weight-adjusted spinal cord weight (mg/g b.wt.)</b>	31±2	30±5	NS	21±2	22±7	NS	P = 0.001	P = 0.005

Data are means ± SEM.

AI, adequate intake; DEF, deficient vitamin D

AI Males, n = 12; AI Females, n = 11

DEF Males, n = 10; DEF Females, n = 9

## Discussion

We investigated the effects of vitamin D deficiency, via dietary vitamin D<sub>3</sub> restriction equivalent to 2.5% the rodent AI, on markers of oxidative damage, antioxidant enzymes, inflammation, apoptosis, growth factors and neuron damage in the spinal cord of G93A mice, a rodent model of ALS. Dietary vitamin D restriction at 1/40<sup>th</sup> AI exacerbates disease pathophysiology as DEF mice displayed higher levels of lipid peroxidation and apoptosis compared to AI. DEF females had higher inflammation and a compensatory increase in the antioxidant GPx1 compared to AI females. Conversely, DEF males had reduced antioxidant capacity compared to AI males. When comparing differences between the sexes, DEF males had lower antioxidant enzymes and neuronal count compared to DEF females. The extant sexual dimorphism both in AI and DEF mice confirms that though detrimental, vitamin D deficiency negatively impacts different pathways depending on the sex, having a more deleterious effect in males compared to females.

Sexual dimorphism was observed in our current study as vitamin D deficiency caused differential results in males vs. females. Sexual dimorphism exists in a multitude of neurological and mental disorders such as multiple sclerosis (MS), Alzheimer's disease (AD), Parkinson's disease (PD) and ALS (27). ALS is predominant in males, but with increasing age the ratio of male-to-female diagnoses becomes smaller. The sex difference may be a result of different aromatase activity, the enzyme that converts testosterone into estradiol. This activity is neuroprotective (42, 43) and is higher in cortical female astrocytes than cortical male astrocytes (44). The dimorphic nature of the enzyme can protect astrocytes, as well as other CNS cell types such as neurons, from

damage in females. It has also been postulated that the presence of the sex hormone estrogen plays a role in this dimorphism. Recent clinical evidence has shown that estrogen treatment reduces the risk and delays the onset of many neurodegenerative diseases (45). In primary cultures of Wistar rat spinal cord, estradiol exerts neuroprotective effects *in vivo* (46). *In vitro*, estradiol protects cerebral neurons against glutamate excitotoxicity (46). Administration of the phytoestrogen genistein to male mSOD1 mice reduces the difference in disease onset and mortality between the sexes (prior to genistein administration, disease onset and mortality were reached sooner in males vs. females), confirming the strong role of sex hormones (47). Ovariectomy of G93A mice accelerates disease progression, and a high-dose of 17 $\beta$ -estradiol significantly slows down disease progression in these mice (48) In the presence of vitamin D<sub>3</sub>, estrogen synthesis is increased (49), allowing both estrogen and vitamin D<sub>3</sub> to exert neuroprotective effects. A confirmed synergy exists between vitamin D<sub>3</sub> and estrogen, which is also found in the spinal cord (50). Estrogen causes estrogen receptor-mediated down-regulation of CYP24A1 (calcitriol deactivating enzyme) transcription to increase net calcitriol concentration, and thus enhance vitamin D function (50). As well, estrogen up-regulates VDR to enhance vitamin D potency, and, in turn, calcitriol causes VDR-mediated up-regulation of estrogen synthase to enhance endogenous estrogen synthesis (51). As a result, basal CNS calcitriol levels are higher in females vs. males (52).

A deficiency in vitamin D reduces the amount of calcium buffering protein, thus leading to higher lipid peroxidation (31). This explains why DEF males had 23% higher 4-HNE protein content, a marker of oxidative damage, vs. AI males. This difference was

not observed in DEF females vs. AI. This is due to estrogen's protective role. Co-exposure of 17 $\beta$ -estradiol and 4-HNE in PC12 cell lines showed that estrogen was significantly effective against the cytotoxic response of 4-HNE (53). This is because 17 $\beta$ -estradiol has the ability to stabilize mitochondrial potential against oxidative stress (54). As well, estrogen works similarly to vitamin D to establish cellular calcium homeostasis. Chronic 17 $\beta$ -estradiol treatment represses glutamate receptor-mediated Ca<sup>2+</sup> influx (55). In ALS, a disruption of calcium transport can form free radicals that cause lipid peroxidation in the cell (56). Vitamin D induces the synthesis of proteins such as parvalbumin that help maintain cellular calcium homeostasis (57), thus lowering lipid peroxidation, in diabetic rats (58). Vitamin D also reduces malondialdehyde (MDA), a marker of lipid peroxidation, by stimulating the gene expression of calcium buffering proteins calbindin-D28k and calbindin-d9k (31). Obese children deficient in vitamin D (serum calcidiol <50 nmol/L) had higher lipid peroxidation as marked by increased 3-NY and MDA levels compared to non-deficient obese children (serum calcidiol >50 nmol/L) (32).

The protective role of estrogen is also a factor in why AI males had 18% higher 3-NY protein content vs. AI females. 17 $\beta$ -estradiol's antioxidative effect reduces 3-NY immunoreactivity (59). Brain cell cultures of mice exposed to 17 $\beta$ -estradiol significantly reduced 3-NY levels regardless of whether or not they have been exposed to superoxide (60). Estrogen can directly inhibit nitric oxide synthase (NOS) activity, thereby reducing peroxynitrite and subsequently 3-NY generation (61).

Vitamin D deficiency also had a negative impact on antioxidant capacity. SOD2 was 18% lower in DEF males vs. AI males. Compared to healthy individuals, SOD2

activity is lower in the brain and spinal cord of ALS patients (62). It is normally expected that in response to higher oxidative damage, antioxidant capacity increases. Thus, the exact mechanism that leads to a reduction in SOD2 activity is not well understood. It is possible that the loss of activity could be a result of post-translational modification. During CNS injury, nitric oxide (NO) is released at a high rate, which reacts with superoxide and leads to the production of nitrogenous species such as peroxynitrite (ONOO<sup>-</sup>) (63). Peroxynitrite, which is highly prevalent in ALS spinal cord, is the only known biological oxidant to inactivate enzymatic activity, nitrate important tyrosine residues and cause dityrosine formation in SOD2 (64). Higher levels of peroxynitrite lead to increased production of 3-NY (65). Compared to their female counterparts, AI and DEF males had 18% and 6% higher 3-NY levels, respectively, which could explain why SOD2 was lower in DEF males, but not DEF females, vs. AI. A reduction in SOD2 in DEF males may be related to vitamin D's impact on nuclear factor-kappa B (NF-κB). In ALS, activated microglia use the NF-κB pathway to induce mitochondrial dysfunction inhibition of SOD2 and motor neuron death (66, 67). NF-κB leads to mitochondrial dysfunction inhibition of SOD2 through nitration, by activating inducible NOS (iNOS) (68). The local conversion of calcidiol to calcitriol in the CNS is a neuroprotective response that inhibits NF-κB-related iNOS induction (69). Without the protective effects of vitamin D, this neuroprotection diminishes, which may explain the lower levels of SOD2 in DEF males.

GPx1 was 29% higher in DEF females vs. AI females. Female hypertensive Wister rats have shown increased GPx1 activity and lower reduced glutathione (GSH) levels (70). Under physiological conditions, vitamin D has an inverse relationship with

GPx1 activity and a positive association with glutathione reductase (GR) activity (71). This relationship is due to GSH's role in maintaining intracellular redox balance. Increasing the activity of GR and decreasing GPx1 function allow vitamin D to enhance the GSH pool. In vitamin D deficiency however, excessive inflammation, as reflected by high IL-6 levels, increases GPx1 activity as a means of reducing oxidative protein injury (72). This also explains why, in this study, DEF females did not have a significant increase in 3-NY vs. AI. Vitamin D deficiency increased IL-6 levels by 22% compared to AI females, thereby elevating GPx1 protein content by 29%. Thus, the adaptive increase in GPx1 may indicate heightened inflammation and cellular damage. In many cancers, including esophageal cancer, GPx1 further induces malignancy and promotes tumor progression, effects that can be reduced by vitamin D (73). In breast cancer patients, high expression of GPx1 was associated with high rate of patient mortality and shorter overall survival (74), which may be due to NF- $\kappa$ B. When bound to the promoter region of GPx1, NF- $\kappa$ B upregulates its function and expression upstream (73). Vitamin D and VDR inhibit NF- $\kappa$ B expression and thus decrease GPx1 levels (75). In females, estrogen's ability to convert calcidiol to calcitriol (76) can heighten the ability of the vitamin to inhibit the NF- $\kappa$ B pathway, thereby reducing GPx1 levels. This may explain why AI males had 10% higher GPx1 protein content than AI females.

IL-6 levels were 22% higher in DEF females vs. AI females. Damage to the CNS causes an upregulation in IL-6 and other pro-inflammatory cytokines such as TNF- $\alpha$  (77). IL-6 plays a great role in astrocyte and microglia activation, microglial proliferation as well as gliosis (78). Though it is meant to repair, gliosis can work as a double-edged sword: it can produce neurotrophic factors and protect the CNS from toxins, but it can

also produce neurotoxins such as nitric oxide, an important factor in free-radical genesis (78). Estrogen is known to regulate IL-6 expression in different cell types (79). In biliary epithelial cells, estrogen had the ability to stimulate IL-6 production in both the neoplastic and non-neoplastic cells that expressed estrogen receptor alpha (79). A study on the effects of gonadal steroids on IL-6 in peripheral blood mononuclear cells showed that 17 $\beta$ -estradiol promotes IL-6 production and release (80). As well, deficiency in vitamin D after trauma puts women at a greater risk of elevated IL-6 levels (81). This is in accord with Miller *et al*'s study that showed that women with serum 25(OH)D levels of <37.5 nmol/L at the time of hip fracture had higher serum IL-6 levels in the year after the hip fracture (81). Alternatively, testosterone maintains low IL-6 levels (82-84). This explains why we observed 14% lower IL-6 in AI males vs. AI females, and 29% lower IL-6 in DEF males vs. DEF females. Interestingly, testosterone is also negatively associated with TNF- $\alpha$  (84), whereas estradiol increases its expression (85). AI and DEF males had non-significant 4% and 12% lower TNF- $\alpha$  levels vs. their female counterparts. Higher TNF- $\alpha$  levels in DEF females reflects vitamin D's impact on this inflammatory cytokine. In females, a significant inverse association exists between 25(OH)D and TNF- $\alpha$ , whereby vitamin D deficiency increases levels of the inflammatory cytokine (86). A study in endurance-trained athletes showed that circulating TNF- $\alpha$  does not increase linearly with decreasing 25(OH)D concentration. Instead, it is abruptly higher in those that are vitamin D deficient (lower than 80 nmol/L) (87). In neuron and glial cells, matrix metalloproteinase-9 (MMP-9) regulates TNF- $\alpha$  levels and is found in high levels in damaged ALS motor neurons (88). MMPs are largely associated with inflammation and work to remodel and break down the extracellular matrix and regulate

leukocyte migration within it. Calcitriol reduces MMP-9 activity, thereby reducing TNF- $\alpha$  levels (89). Within the spinal cord of G93A mice, upregulation of the p38 mitogen activated protein kinase (p38MAPK), a signaling pathway responsible for cell death, is associated with the upregulation of TNF- $\alpha$  receptors (90). Calcitriol reduces p38MAPK activity, thereby reducing TNF- $\alpha$  levels (91, 92). In terms of anti-inflammatory cytokines, AI males had 11% lower IL-10 protein content vs. AI females. IL-10 has been shown to increase in the presence of estrogen (93). Malaria infected female mice were shown to have higher IL-10 levels compared to males (94). In terms of its relationship with inflammatory cytokines, higher IL-6 levels induce IL-10 production (95). This explains why the higher IL-10 levels we observed in females were commensurate with higher IL-6 protein content.

There was 23% higher Bax/Bcl-2 in DEF mice vs AI mice. However, this may not necessarily indicate that apoptosis was prevalent. This is because no changes in activated caspase 3 and neuron damage were observed between the diets. Though Bax/Bcl-2 ratio was elevated in DEF mice, the increase was not sufficient enough to activate caspase 3, the effector molecule in the apoptotic pathway. High Bax/Bcl-2 ratio increases the vulnerability of neurons to apoptosis (96), and is observed in neuromuscular disorders such as ALS (97). What this may indicate is that apoptotic proteins can reduce neuronal viability without leading to large-scale apoptosis. This is also confirmed in our previous study in HiD female *quadriceps* that had reached the threshold of vitamin D<sub>3</sub> toxicity. A 242% increase in Bax/Bcl-2 (98) only corresponded to an 87% increase in cleaved/pro-caspase 3 (99). Thus, a deficiency in vitamin D may increase the susceptibility of motor neurons to apoptosis without necessarily leading to large-scale apoptosis. Vitamin D has

been shown to reduce pro-apoptotic (Bax) and increase anti-apoptotic proteins (Bcl-2) (100). A reduction in calcium buffering capacity brought about by vitamin D deficiency may cause the cell to exert calcium-induced excitotoxicity, which leads to elevated levels of Bax/Bcl-2.

With respect to neuron damage, both AI and DEF males had lower ChAT (23% and 22%, respectively) and SMI-32 (15% and 17%, respectively) compared to their female counterparts, likely due to the protective effect of estrogen in females. In mSOD1 mice, onset, disease progression and survival are dependent on sex; males lose body weight more rapidly following disease onset and die sooner than females (101, 102). A reduction in body weight reflects muscle atrophy brought about by motor neuron degeneration. As with high motor neuron count in females, it is possible that damaged motor neurons are also more prevalent. This explains why SMI-36 levels were 13% lower in AI males vs. AI females. This can also explain why there was no difference in SMI-36/SMI-32 ratio between AI males and AI females, as SMI-32 and SMI-36 levels were both lower in males vs. females. Ultimately, neuron damage was not different between the diets, indicating that even though vitamin D deficiency may exacerbate disease pathophysiology, it does not have an impact on neuron damage.

On a tissue level, there was no significant difference in body weight-adjusted spinal cord weights between the diets. However, a sexual dimorphism was confirmed as AI males and DEF males had 33% and 27% lighter body weight-adjusted spinal cord weight vs. their female counterparts. This may be due to the protective effects of estrogen in the female spinal cord. These results contrast our previous study that found no difference in body weight-adjusted brain weights between the diets and sexes (103).

Correlational analysis showed that there was no association between body weight-adjusted brain weights (103) and body weight-adjusted spinal cord weights. This confirms that ALS pathology within the CNS is mainly localized to the spinal cord.

This study outlines the detrimental effects of vitamin D deficiency and confirms the lower paw grip endurance and motor performance that was observed in our previous study in the same mouse model (37). When compared to AI mice, DEF mice had 25% lower paw grip endurance (PaGE) AUC and 19% lower motor performance. Between the sexes, AI males had lower ability to move, PaGE and motor performance compared to AI females. AI males also had a higher clinical score, hastened disease onset, and reached hind limb paralysis and endpoint faster compared to AI females. The current study confirms that the functional outcomes observed are linked to neuronal damage in the spinal cord. Previous studies on spinal cord injury (SCI) rats have shown that motor performance disturbance following SCI is associated with the severity of spinal cord pathology (104). Damage in the spinal cord also reflects that in the *quadriceps*, where DEF female, but not male, G93A mice had higher inflammation and apoptosis as compared to AI females (35, 36). Despite the fact that the spinal cords of DEF females had higher inflammation, DEF male spinal cords were more susceptible to damage as marked by lower levels of SOD2 and higher levels of markers of neuron damage. We postulate that this is due to the protective effects of estrogen in females. The restricted vitamin D<sub>3</sub> intake in this study corresponds to ~25 IU/d for an 80 kg man and ~20 IU/d for a 70 kg woman. These values may be insufficient for patients with ALS. Indeed, Karam *et al*'s study on ALS patients found that supplementation with 2000 IU of vitamin D<sub>3</sub>/day for 9 months improved ALS functional rating scale score (105). A retrospective

study on ALS patients found that those with serum calcidiol levels <25 nmol/L increased their death rate by 6 fold and their rate of decline by 4 times, and were associated with a marked shorter life expectancy compared to patients with serum calcidiol levels >75 nmol/L (33). Furthermore, Guamanian Chamorros with ALS have serum calcitriol levels in the low to low-normal range (17). In humans following supplementation with 10 000 IU/d dosages in patients with MS for 12 weeks [114] and up to 40 000 IU/d for 28 weeks [115], ALS patients in Karam *et al*'s study may have shown greater improvements in their ALSFRS-R had they been supplemented with dosages between 10 000-40 000 IU/d. Based on these studies, and given our previous studies supplementing ALS mice with 10x and 50x AI, we restate our previous hypothesis that the optimal therapeutic vitamin D dosage, both functionally and cellularly, lies between 10x and 50x AI vitamin D (27, 103, 106).

In conclusion, the present study demonstrates that vitamin D deficiency exacerbates disease pathophysiology in the G93A mouse model of ALS. This is marked by increased inflammation and oxidative damage and lower antioxidant capacity. However, it is important to note that sexual dimorphism exists and that the pathways that vitamin D deficiency negatively impacts differ between males and females (107).

### **Acknowledgements**

We thank Sanjeef Thampinathan, Mahshad Kolahdouzan and Safoura Sadeghimehr for assisting in lab analysis, data entry and literature search.

### **Author Contributions**

Conceived and designed the experiments: MJH AG JAS. Performed the experiments: EM. Analyzed the data: EM. Contributed reagents/materials/analysis tools: MJH. Wrote the paper: EM MJH.

## References

1. Nishitoh H, Kadowaki H, Nagai A, Maruyama T, Yokota T, Fukutomi H, Noguchi T, Matsuzawa A, Takeda K, Ichijo H. ALS-linked mutant SOD1 induces ER stress- and ASK1-dependent motor neuron death by targeting Derlin-1. *Genes Dev* 2008;22:1451-64.
2. de Almeida JL, Silvestre R, Pinto A, de Carvalho M. Exercise and amyotrophic lateral sclerosis. *Neurological Sciences* 2012;33:9-15.
3. Robberecht W, Philips T. The changing scene of amyotrophic lateral sclerosis. *Nat Rev Neurosci* 2013;14:248-64.
4. Dadon-Nachum M, Melamed E, Offen D. The "dying-back" phenomenon of motor neurons in ALS. *J Mol Neurosci* 2011;43:470-7.
5. Wijesekera LC, Leigh PN. Amyotrophic lateral sclerosis. *Orphanet J Rare Dis* 2009;4:3,1172-4-3.
6. Jennum P, Ibsen R, Pedersen SW, Kjellberg J. Mortality, health, social and economic consequences of amyotrophic lateral sclerosis: a controlled national study. *J Neurol* 2013;260:785-93.
7. Tripodoro VA, De Vito EL. Management of dyspnea in advanced motor neuron diseases. *Curr Opin Support Palliat Care* 2008;2:173-9.
8. Lechtzin N. Respiratory effects of amyotrophic lateral sclerosis: problems and solutions. *Respir Care* 2006;51:871,81; discussion 881-4.
9. Gros-Louis F, Gaspar C, Rouleau GA. Genetics of familial and sporadic amyotrophic lateral sclerosis. *Biochim Biophys Acta* 2006;1762:956-72.
10. Berthod F, Gros-Louis F. In Vivo and In Vitro Models to Study Amyotrophic Lateral Sclerosis.
11. Rosen DR, Siddique T, Patterson D, Figlewicz DA, Sapp P, Hentati A, Donaldson D, Goto J, O'Regan JP, Deng HX. Mutations in Cu/Zn superoxide dismutase gene are associated with familial amyotrophic lateral sclerosis. *Nature* 1993;362:59-62.
12. Mitchell JD. Amyotrophic lateral sclerosis: toxins and environment. *Amyotroph Lateral Scler Other Motor Neuron Disord* 2000;1:235-50.
13. Bruijn LI, Miller TM, Cleveland DW. Unraveling the mechanisms involved in motor neuron degeneration in ALS. *Annu Rev Neurosci* 2004;27:723-49.

14. Renton AE, Chio A, Traynor BJ. State of play in amyotrophic lateral sclerosis genetics. *Nat Neurosci* 2014;17:17-23.
15. Gurney ME, Pu H, Chiu AY, Dal Canto MC, Polchow CY, Alexander DD, Caliendo J, Hentati A, Kwon YW, Deng HX. Motor neuron degeneration in mice that express a human Cu,Zn superoxide dismutase mutation. *Science* 1994;264:1772-5.
16. Foran E, Trotti D. Glutamate transporters and the excitotoxic path to motor neuron degeneration in amyotrophic lateral sclerosis. *Antioxid Redox Signal* 2009;11:1587-602.
17. Mark LP, Prost RW, Ulmer JL, Smith MM, Daniels DL, Strottmann JM, Brown WD, Haccin-Bey L. Pictorial review of glutamate excitotoxicity: fundamental concepts for neuroimaging. *AJNR Am J Neuroradiol* 2001;22:1813-24.
18. Trumbull KA, Beckman JS. A role for copper in the toxicity of zinc-deficient superoxide dismutase to motor neurons in amyotrophic lateral sclerosis. *Antioxid Redox Signal* 2009;11:1627-39.
19. Pedersen WA, Fu W, Keller JN, Markesbery WR, Appel S, Smith RG, Kasarskis E, Mattson MP. Protein modification by the lipid peroxidation product 4-hydroxynonenal in the spinal cords of amyotrophic lateral sclerosis patients. *Ann Neurol* 1998;44:819-24.
20. Nguyen D, Alavi MV, Kim KY, Kang T, Scott RT, Noh YH, Lindsey JD, Wissinger B, Ellisman MH, Weinreb RN, et al. A new vicious cycle involving glutamate excitotoxicity, oxidative stress and mitochondrial dynamics. *Cell Death Dis* 2011;2:e240.
21. Schubert D, Piasecki D. Oxidative glutamate toxicity can be a component of the excitotoxicity cascade. *J Neurosci* 2001;21:7455-62.
22. Zhao L, Hart S, Cheng JG, Melenhorst JJ, Bieri B, Ernst M, Stewart C, Schaper F, Heinrich PC, Ullrich A, et al. Mammary gland remodeling depends on gp130 signaling through Stat3 and MAPK. *J Biol Chem* 2004;279:44093-100.
23. Patel BP, Hamadeh MJ. Nutritional and exercise-based interventions in the treatment of amyotrophic lateral sclerosis. *Clinical Nutrition* 28:604-17.
24. Summerday NM, Brown SJ, Allington DR, Rivey MP. Vitamin D and multiple sclerosis: review of a possible association. *J Pharm Pract* 2012;25:75-84.
25. Ibi M, Sawada H, Nakanishi M, Kume T, Katsuki H, Kaneko S, Shimohama S, Akaike A. Protective effects of 1 alpha,25-(OH)(2)D(3) against the neurotoxicity of glutamate and reactive oxygen species in mesencephalic culture. *Neuropharmacology* 2001;40:761-71.
26. Pierrot-Deseilligny C. Clinical implications of a possible role of vitamin D in multiple sclerosis. *J Neurol* 2009;256:1468-79.

27. Gianforcaro A, Hamadeh MJ. Vitamin D as a potential therapy in amyotrophic lateral sclerosis. *CNS Neurosci Ther* 2014;20:101-11.
28. Lim S, Kim MJ, Choi SH, Shin CS, Park KS, Jang HC, Billings LK, Meigs JB. Association of vitamin D deficiency with incidence of type 2 diabetes in high-risk Asian subjects. *Am J Clin Nutr* 2013;97:524-30.
29. Knippenberg S, Bol Y, Damoiseaux J, Hupperts R, Smolders J. Vitamin D status in patients with MS is negatively correlated with depression, but not with fatigue. *Acta Neurol Scand* 2011;124:171-5.
30. Littlejohns TJ, Henley WE, Lang IA, Annweiler C, Beauchet O, Chaves PH, Fried L, Kestenbaum BR, Kuller LH, Langa KM, et al. Vitamin D and the risk of dementia and Alzheimer disease. *Neurology* 2014;83:920-8.
31. Halhali A, Figueras AG, Diaz L, Avila E, Barrera D, Hernandez G, Larrea F. Effects of calcitriol on calbindins gene expression and lipid peroxidation in human placenta. *J Steroid Biochem Mol Biol* 2010;121:448-51.
32. Codoner-Franch P, Tavaréz-Alonso S, Simo-Jorda R, Laporta-Martin P, Carratala-Calvo A, Alonso-Iglesias E. Vitamin D status is linked to biomarkers of oxidative stress, inflammation, and endothelial activation in obese children. *J Pediatr* 2012;161:848-54.
33. Camu W, Tremblier B, Plassot C, Alphantery S, Salsac C, Pageot N, Juntas-Morales R, Scamps F, Daures JP, Raoul C. Vitamin D confers protection to motoneurons and is a prognostic factor of amyotrophic lateral sclerosis. *Neurobiol Aging* 2014;35:1198-205.
34. Milionis A, Parkhomenko E, Solomon JA, Gianforcaro A, Hamadeh MJ. Dietary vitamin D3 restriction differentially alters quadriceps contractile proteins in both sexes in the transgenic G93A mouse model of amyotrophic lateral sclerosis: a pilot study. *The FASEB Journal* 2012;26:255.8.
35. Parkhomenko EA, Gianforcaro A, Solomon JA, Hamadeh MJ. Vitamin D deficiency improves antioxidant capacity in males and attenuates the sexual dichotomy in the G93A mouse model of amyotrophic lateral sclerosis: is the female sex at D<sub>3</sub> disadvantage? *Canadian Nutrition Society* 2011;328:
36. Shahsavari S, Taheri-Shalmani S, Solomon JA, Gianforcaro A, Hamadeh MJ. Sexual dichotomy in calcium buffering capacity may be dependent on the severity of endoplasmic reticulum stress in the skeletal muscle of the vitamin D3 deficient transgenic G93A mouse model of amyotrophic lateral sclerosis. *The FASEB Journal* 2013;27:644.2.
37. Solomon JA, Gianforcaro A, Hamadeh MJ. Vitamin D3 deficiency differentially affects functional and disease outcomes in the G93A mouse model of amyotrophic lateral sclerosis. *PLoS One* 2011;6:e29354.

38. Solomon JA, Tarnopolsky MA, Hamadeh MJ. One universal common endpoint in mouse models of amyotrophic lateral sclerosis. *PLoS One* 2011;6:e20582.
39. Sapan CV, Lundblad RL, Price NC. Colorimetric protein assay techniques. *Biotechnol Appl Biochem* 1999;29 ( Pt 2):99-108.
40. Food and Drug Administration, ed. Estimating the safe starting dose in clinical trials for therapeutics in adult healthy volunteers. . Rockville, Maryland, USA: U.S.: Food and Drug Administration, 2005.
41. Laird E, McNulty H, Ward M, Hoey L, McSorley E, Wallace JM, Carson E, Molloy AM, Healy M, Casey MC, et al. Vitamin D deficiency is associated with inflammation in older Irish adults. *J Clin Endocrinol Metab* 2014;99:1807-15.
42. Parkhomenko EA, Gianforcaro A, Solomon JA, Hamadeh MJ. Dietary vitamin D<sub>3</sub> at 50 fold the adequate intake increases antioxidant capacity and decreases inflammation in the G93A mouse model of ALS. *Canadian Nutrition Society* 2011;329.
43. Parkhomenko E, Milionis A, Gianforcaro A, Solomon JA, Hamadeh MJ. Dietary vitamin D<sub>3</sub> at 50x the adequate intake increases apoptosis in the quadriceps of the female G93A mouse model of amyotrophic lateral sclerosis: a pilot study. *The FASEB Journal* 2012;26:255.7.
44. Gianforcaro A, Hamadeh MJ. Dietary vitamin D<sub>3</sub> supplementation at 10x the adequate intake improves functional capacity in the G93A transgenic mouse model of ALS, a pilot study. *CNS Neurosci Ther* 2012;18:547-57.
45. Gianforcaro A, Solomon JA, Hamadeh MJ. Vitamin D(3) at 50x AI attenuates the decline in paw grip endurance, but not disease outcomes, in the G93A mouse model of ALS, and is toxic in females. *PLoS One* 2013;8:e30243.
46. Garcia-Segura LM, Veiga S, Sierra A, Melcangi RC, Azcoitia I. Aromatase: a neuroprotective enzyme. *Prog Neurobiol* 2003;71:31-41.
47. Saldanha CJ, Duncan KA, Walters BJ. Neuroprotective actions of brain aromatase. *Front Neuroendocrinol* 2009;30:106-18.
48. Liu M, Hurn PD, Roselli CE, Alkayed NJ. Role of P450 aromatase in sex-specific astrocytic cell death. *J Cereb Blood Flow Metab* 2007;27:135-41.
49. Czlonkowska A, Ciesielska A, Gromadzka G, Kurkowska-Jastrzebska I. Estrogen and cytokines production - the possible cause of gender differences in neurological diseases. *Curr Pharm Des* 2005;11:1017-30.

50. Nakamizo T, Urushitani M, Inoue R, Shinohara A, Sawada H, Honda K, Kihara T, Akaike A, Shimohama S. Protection of cultured spinal motor neurons by estradiol. *Neuroreport* 2000;11:3493-7.
51. Trieu VN, Uckun FM. Genistein is neuroprotective in murine models of familial amyotrophic lateral sclerosis and stroke. *Biochem Biophys Res Commun* 1999;258:685-8.
52. Groeneveld GJ, Van Muiswinkel FL, Sturkenboom JM, Wokke JH, Bar PR, Van den Berg LH. Ovariectomy and 17beta-estradiol modulate disease progression of a mouse model of ALS. *Brain Res* 2004;1021:128-31.
53. Kinuta K, Tanaka H, Moriwake T, Aya K, Kato S, Seino Y. Vitamin D Is an Important Factor in Estrogen Biosynthesis of Both Female and Male Gonads. *Endocrinology* 2000;141:1317-24.
54. Spach KM, Hayes CE. Vitamin D3 confers protection from autoimmune encephalomyelitis only in female mice. *J Immunol* 2005;175:4119-26.
55. Nashold FE, Spach KM, Spanier JA, Hayes CE. Estrogen controls vitamin D3-mediated resistance to experimental autoimmune encephalomyelitis by controlling vitamin D3 metabolism and receptor expression. *J Immunol* 2009;183:3672-81.
56. Spach KM, Hayes CE. Vitamin D3 confers protection from autoimmune encephalomyelitis only in female mice. *J Immunol* 2005;175:4119-26.
57. Siddiqui MA, Kashyap MP, Al-Khedhairi AA, Musarrat J, Khanna VK, Yadav S, Pant AB. Protective potential of 17beta-estradiol against co-exposure of 4-hydroxynonenal and 6-hydroxydopamine in PC12 cells. *Hum Exp Toxicol* 2011;30:860-9.
58. Wang J, Green PS, Simpkins JW. Estradiol protects against ATP depletion, mitochondrial membrane potential decline and the generation of reactive oxygen species induced by 3-nitropropionic acid in SK-N-SH human neuroblastoma cells. *J Neurochem* 2001;77:804-11.
59. Numakawa T, Matsumoto T, Numakawa Y, Richards M, Yamawaki S, Kunugi H. Protective Action of Neurotrophic Factors and Estrogen against Oxidative Stress-Mediated Neurodegeneration. *Journal of Toxicology* 2011;2011:12.
60. Parakh S, Spencer DM, Halloran MA, Soo KY, Atkin JD. Redox regulation in amyotrophic lateral sclerosis. *Oxid Med Cell Longev* 2013;2013:408681.
61. Wrzosek M, Lukaszewicz J, Wrzosek M, Jakubczyk A, Matsumoto H, Piatkiewicz P, Radziwon-Zaleska M, Wojnar M, Nowicka G. Vitamin D and the central nervous system. *Pharmacol Rep* 2013;65:271-8.

62. Hamden K, Carreau S, Jamoussi K, Miladi S, Lajmi S, Aloulou D, Ayadi F, Elfeki A. 1 $\alpha$ ,25 dihydroxyvitamin D<sub>3</sub>: therapeutic and preventive effects against oxidative stress, hepatic, pancreatic and renal injury in alloxan-induced diabetes in rats. *J Nutr Sci Vitaminol (Tokyo)* 2009;55:215-22.
63. Tripanichkul W, Sripanichkulchai K, Duce JA, Finkelstein DI. 17 $\beta$ -estradiol reduces nitrotyrosine immunoreactivity and increases SOD1 and SOD2 immunoreactivity in nigral neurons in male mice following MPTP insult. *Brain Res* 2007;1164:24-31.
64. Rao AK, Dietrich AK, Ziegler YS, Nardulli AM. 17 $\beta$ -Estradiol-mediated increase in Cu/Zn superoxide dismutase expression in the brain: a mechanism to protect neurons from ischemia. *J Steroid Biochem Mol Biol* 2011;127:382-9.
65. Chakrabarti S, Cheung CC, Davidge ST. Estradiol attenuates high glucose-induced endothelial nitrotyrosine: role for neuronal nitric oxide synthase. *Am J Physiol Cell Physiol* 2012;302:C666-75.
66. Uchino M, Ando Y, Tanaka Y, Nakamura T, Uyama E, Mita S, Murakami T, Ando M. Decrease in Cu/Zn- and Mn-superoxide dismutase activities in brain and spinal cord of patients with amyotrophic lateral sclerosis. *J Neurol Sci* 1994;127:61-7.
67. Beckman JS, Carson M, Smith CD, Koppenol WH. ALS, SOD and peroxynitrite. *Nature* 1993;364:584.
68. Macmillan-Crow LA, Cruthirds DL. Invited review: manganese superoxide dismutase in disease. *Free Radic Res* 2001;34:325-36.
69. Bishop A, Gooch R, Eguchi A, Jeffrey S, Smallwood L, Anderson J, Estevez AG. Mitigation of peroxynitrite-mediated nitric oxide (NO) toxicity as a mechanism of induced adaptive NO resistance in the CNS. *J Neurochem* 2009;109:74-84.
70. Frakes AE, Ferraiuolo L, Haidet-Phillips AM, Schmelzer L, Braun L, Miranda CJ, Ladner KJ, Bevan AK, Foust KD, Godbout JP, et al. Microglia induce motor neuron death via the classical NF- $\kappa$ B pathway in amyotrophic lateral sclerosis. *Neuron* 2014;81:1009-23.
71. Keeney JT, Forster S, Sultana R, Brewer LD, Latimer CS, Cai J, Klein JB, Porter NM, Butterfield DA. Dietary vitamin D deficiency in rats from middle to old age leads to elevated tyrosine nitration and proteomics changes in levels of key proteins in brain: implications for low vitamin D-dependent age-related cognitive decline. *Free Radic Biol Med* 2013;65:324-34.
72. Tangpong J, Cole MP, Sultana R, Estus S, Vore M, St Clair W, Ratanachaiyavong S, St Clair DK, Butterfield DA. Adriamycin-mediated nitration of manganese superoxide dismutase in the central nervous system: insight into the mechanism of chemobrain. *J Neurochem* 2007;100:191-201.

73. Garcion E, Sindji L, Montero-Menei C, Andre C, Brachet P, Darcy F. Expression of inducible nitric oxide synthase during rat brain inflammation: regulation by 1,25-dihydroxyvitamin D<sub>3</sub>. *Glia* 1998;22:282-94.
74. Barp J, Sartorio CL, Campos C, Llesuy SF, Araujo AS, Bello-Klein A. Influence of ovariectomy on cardiac oxidative stress in a renovascular hypertension model. *Can J Physiol Pharmacol* 2012;90:1229-34.
75. Saedisomeolia A, Taheri E, Djalali M, Djazayeri A, Qorbani M, Rajab A, Larijani B. Vitamin D status and its association with antioxidant profiles in diabetic patients: A cross-sectional study in Iran. *Indian J Med Sci* 2013;67:29-37.
76. Jin X, Zhang Z, Beer-Stolz D, Zimmers TA, Koniaris LG. Interleukin-6 inhibits oxidative injury and necrosis after extreme liver resection. *Hepatology* 2007;46:802-12.
77. Gan X, Chen B, Shen Z, Liu Y, Li H, Xie X, Xu X, Li H, Huang Z, Chen J. High GPX1 expression promotes esophageal squamous cell carcinoma invasion, migration, proliferation and cisplatin-resistance but can be reduced by vitamin D. *Int J Clin Exp Med* 2014;7:2530-40.
78. Jardim BV, Moschetta MG, Leonel C, Gelaleti GB, Regiani VR, Ferreira LC, Lopes JR, Zuccari DA. Glutathione and glutathione peroxidase expression in breast cancer: an immunohistochemical and molecular study. *Oncol Rep* 2013;30:1119-28.
79. Wu S, Sun J. Vitamin D, Vitamin D Receptor, and Macroautophagy in Inflammation and Infection. *Discovery Medicine* 2011;11:325-35.
80. Gallagher JC, Riggs BL, DeLuca HF. Effect of estrogen on calcium absorption and serum vitamin D metabolites in postmenopausal osteoporosis. *J Clin Endocrinol Metab* 1980;51:1359-64.
81. Woodroffe MN. Cytokine production in the central nervous system. *Neurology* 1995;45:S6-10.
82. Swartz KR, Liu F, Sewell D, Schochet T, Campbell I, Sandor M, Fabry Z. Interleukin-6 promotes post-traumatic healing in the central nervous system. *Brain Res* 2001;896:86-95.
83. Isse K, Specht SM, Lunz JG, 3rd, Kang LI, Mizuguchi Y, Demetris AJ. Estrogen stimulates female biliary epithelial cell interleukin-6 expression in mice and humans. *Hepatology* 2010;51:869-80.
84. Li ZG, Danis VA, Brooks PM. Effect of gonadal steroids on the production of IL-1 and IL-6 by blood mononuclear cells in vitro. *Clin Exp Rheumatol* 1993;11:157-62.

85. Miller RR, Hicks GE, Shardell MD, Cappola AR, Hawkes WG, Yu-Yahiro JA, Keegan A, Magaziner J. Association of serum vitamin D levels with inflammatory response following hip fracture: the Baltimore Hip Studies. *J Gerontol A Biol Sci Med Sci* 2007;62:1402-6.
86. Maggio M, Basaria S, Ble A, Lauretani F, Bandinelli S, Ceda GP, Valenti G, Ling SM, Ferrucci L. Correlation between testosterone and the inflammatory marker soluble interleukin-6 receptor in older men. *J Clin Endocrinol Metab* 2006;91:345-7.
87. Coletta RD, Reynolds MA, Martelli-Junior H, Graner E, Almeida OP, Sauk JJ. Testosterone stimulates proliferation and inhibits interleukin-6 production of normal and hereditary gingival fibromatosis fibroblasts. *Oral Microbiol Immunol* 2002;17:186-92.
88. Bobjer J, Katrinaki M, Tsatsanis C, Lundberg Giwercman Y, Giwercman A. Negative association between testosterone concentration and inflammatory markers in young men: a nested cross-sectional study. *PLoS One* 2013;8:e61466.
89. Zaldivar V, Magri ML, Zarate S, Jaita G, Eijo G, Radl D, Ferraris J, Pisera D, Seilicovich A. Estradiol increases the expression of TNF-alpha and TNF receptor 1 in lactotropes. *Neuroendocrinology* 2011;93:106-13.
90. Peterson CA, Heffernan ME. Serum tumor necrosis factor-alpha concentrations are negatively correlated with serum 25(OH)D concentrations in healthy women. *J Inflamm (Lond)* 2008;5:10,9255-5-10.
91. Willis KS, Smith DT, Broughton KS, Larson-Meyer DE. Vitamin D status and biomarkers of inflammation in runners. *Open access journal of sports medicine* 2012;3:35.
92. Kiaei M, Kipiani K, Calingasan NY, Wille E, Chen J, Heissig B, Rafii S, Lorenzl S, Beal MF. Matrix metalloproteinase-9 regulates TNF-alpha and FasL expression in neuronal, glial cells and its absence extends life in a transgenic mouse model of amyotrophic lateral sclerosis. *Exp Neurol* 2007;205:74-81.
93. Long K, Nguyen LT. Roles of vitamin D in amyotrophic lateral sclerosis: possible genetic and cellular signaling mechanisms. *Mol Brain* 2013;6:16,6606-6-16.
94. Veglianese P, Lo Coco D, Bao Cutrona M, Magnoni R, Pennacchini D, Pozzi B, Gowing G, Julien JP, Tortarolo M, Bendotti C. Activation of the p38MAPK cascade is associated with upregulation of TNF alpha receptors in the spinal motor neurons of mouse models of familial ALS. *Mol Cell Neurosci* 2006;31:218-31.
95. Ravid A, Rubinstein E, Gamady A, Rotem C, Liberman UA, Koren R. Vitamin D inhibits the activation of stress-activated protein kinases by physiological and environmental stresses in keratinocytes. *J Endocrinol* 2002;173:525-32.

96. Zhang Y, Leung DY, Richers BN, Liu Y, Remigio LK, Riches DW, Goleva E. Vitamin D inhibits monocyte/macrophage proinflammatory cytokine production by targeting MAPK phosphatase-1. *J Immunol* 2012;188:2127-35.
97. Whitacre CC. Sex differences in autoimmune disease. *Nat Immunol* 2001;2:777-80.
98. Cernetich A, Garver LS, Jedlicka AE, Klein PW, Kumar N, Scott AL, Klein SL. Involvement of gonadal steroids and gamma interferon in sex differences in response to blood-stage malaria infection. *Infect Immun* 2006;74:3190-203.
99. Steensberg A, Fischer CP, Keller C, Moller K, Pedersen BK. IL-6 enhances plasma IL-1ra, IL-10, and cortisol in humans. *Am J Physiol Endocrinol Metab* 2003;285:E433-7.
100. Oltvai ZN, Milliman CL, Korsmeyer SJ. Bcl-2 heterodimerizes in vivo with a conserved homolog, Bax, that accelerates programmed cell death. *Cell* 1993;74:609-19.
101. Gonzalez de Aguilar JL, Gordon JW, Rene F, de Tapia M, Lutz-Bucher B, Gaiddon C, Loeffler JP. Alteration of the Bcl-x/Bax ratio in a transgenic mouse model of amyotrophic lateral sclerosis: evidence for the implication of the p53 signaling pathway. *Neurobiol Dis* 2000;7:406-15.
102. Taheri-Shalmani S, Shahsavari S, Gianforcaro A, Solomon JA, Hamadeh MJ. Dietary vitamin D3 supplementation at 50x the adequate intake decreases calbindin d28k and endoplasmic reticulum stress and increases apoptosis, suggesting toxicity, in the female transgenic G93A mouse model of amyotrophic lateral sclerosis. *The FASEB Journal* 2013;27:644.1.
103. Samuel S, Sitrin MD. Vitamin D's role in cell proliferation and differentiation. *Nutr Rev* 2008;66:S116-24.
104. Cervetto C, Frattaroli D, Maura G, Marcoli M. Motor neuron dysfunction in a mouse model of ALS: gender-dependent effect of P2X7 antagonism. *Toxicology* 2013;311:69-77.
105. Suzuki M, Tork C, Shelley B, McHugh J, Wallace K, Klein SM, Lindstrom MJ, Svendsen CN. Sexual dimorphism in disease onset and progression of a rat model of ALS. *Amyotroph Lateral Scler* 2007;8:20-5.
106. Sharma HS, Badgaiyan RD, Alm P, Mohanty S, Wiklund L. Neuroprotective effects of nitric oxide synthase inhibitors in spinal cord injury-induced pathophysiology and motor functions: an experimental study in the rat. *Ann N Y Acad Sci* 2005;1053:422-34.
107. Karam C, Barrett MJ, Imperato T, Macgowan DJ, Scelsa S. Vitamin D deficiency and its supplementation in patients with amyotrophic lateral sclerosis. *J Clin Neurosci* 2013;

108. Moghimi E, Gianforcaro A, Solomon J, Hamadeh MJ. Vitamin D<sub>3</sub> at 50X the adequate intake attenuates disease pathophysiology in the spinal cord of the male, but is toxic in female, G93A mouse model of amyotrophic lateral sclerosis. PloS One 2015 (in revision).
109. Reeves PG, Nielsen FH, Fahey GC, Jr. AIN-93 purified diets for laboratory rodents: final report of the American Institute of Nutrition ad hoc writing committee on the reformulation of the AIN-76A rodent diet. J Nutr 1993;123:1939-51.
110. Bieri, J.G. Stoewsand, G.S. Briggs, G.M. Phillips, R.W. Woodard, J.C. Knapka, J.J. Report of the American Institute of Nutrition ad hoc Committee on Standards for Nutritional Studies. J Nutr 1977;107:1340-8.

## SUMMARY AND FUTURE RESEARCH

### Summary

The objective of this thesis was to determine the effects of dietary D<sub>3</sub> supplementation, restriction and adequate intake on oxidative damage, antioxidant capacity, inflammation, apoptosis, neurotrophic factor and neuron count in the spinal cord of the G93A mouse model of ALS.

### Oxidative damage

Oxidative damage was increased in HiD females, indicating the presence of vitamin D toxicity. This was observed by 14% higher 3-NY protein content in HiD females vs. AI females. However, at non-toxic levels, vitamin D can lower 3-NY production by lowering the formation of NO products and increasing p53 protein, which aids in DNA repair (230). This explains why HiD males had 16% lower 3-NY protein content compared to HID females. In females, non-toxic vitamin D levels, combined with estrogen's ability to directly inhibit NOS activity, reduces peroxynitrite and subsequently 3-NY generation (231). This is why AI males had 18% higher 3-NY protein content vs. AI females.

A deficiency in vitamin D reduces the amount of calcium buffering protein, further dysregulating calcium homeostasis, producing ROS and thus leading to higher lipid peroxidation (232). In females, estrogen can protect the from cell lipid peroxidation as co-exposure of 17 $\beta$ -estradiol and 4-HNE in PC12 cell lines showed that estrogen was significantly effective against the cytotoxic response of 4-HNE (233). As males lack high levels of estrogen, DEF males had 23% higher 4-HNE protein content vs. AI males

whereas DEF females did not exhibit any significant changes in their 4-HNE protein levels.

### **Antioxidant Capacity**

In HiD females, excessive inflammation resulted in a 21% decrease in catalase compared to AI females ( $P < 0.001$ ). This pattern is supported by studies on rat liver, where TNF- $\alpha$ , a marker of inflammation, suppresses protein expression of both catalase and peroxisomal proteins (234). However, Gpx1, a protective antioxidant with similar function as catalase was 18% higher in HiD females vs. AI females. Contrary to catalase, toxicity results in an adaptive increase in GPx1 levels to compensate for the elevated cellular damage. Physiologically, vitamin D has an inverse relationship with GPx1 and a positive association GR activity (235) in order to maintain high GSH concentrations, a regulator of intracellular redox balance. However, under vitamin D toxicity, excessive oxidative damage likely surpasses vitamin D's ability to efficiently regulate GPx1 which results in an adaptive increase in GPx1 levels. The 10% higher GPx1 levels in AI males vs. AI females indicates that at adequate, non-toxic levels, vitamin D reduces GPx1 in females vs. males, also indicating that there is lower cellular damage occurring in AI females vs. AI males.

In vitamin D deficiency, excessive inflammation in DEF females vs. AI females, as reflected by high IL-6 levels, resulted in a compensatory increase GPx1 activity (236). This further confirms that high GPx1 protein levels are an indicator of elevated intracellular oxidative damage and inflammation. In DEF males, SOD2 was 18% higher than in AI males. In ALS, activated microglia use the NF- $\kappa$ B pathway to induce mitochondrial dysfunction inhibition of SOD2 and motor neuron death (237, 238). NF-

$\kappa$ B leads to mitochondrial dysfunction inhibition of SOD2 by activating iNOS (239). iNOS releases high amounts of NO, which react with superoxide to generate the peroxynitrite necessary (240), to cease enzymatic activity and produce 3-NY (241). The local conversion of calcidiol to calcitriol in the CNS is a neuroprotective response that inhibits NF- $\kappa$ B-related iNOS induction (242). Without the protective effects of vitamin D, this neuroprotection diminishes, which may explain the lower levels of SOD2 in DEF males.

### **Inflammation**

HiD females had 21% higher TNF-  $\alpha$  levels and 13% lower anti-inflammatory cytokine IL-10 compared to AI females. This indicates that a more inflammatory milieu is present in HiD females, likely due to the excessive oxidative stress brought about by hypervitaminosis D. High TNF-  $\alpha$ /IL-10 ratio has been observed in the renal tissue of rats with systematic inhibition of NOS (243), resulting in lower NO production, lowering IL-10 levels and increasing TNF-  $\alpha$  levels (243). The 11% lower IL-10 protein content in AI males compared to AI females may be an indicator that oxidative damage is higher in males, confirmed by higher 3-NY levels. Hence NOS inhibition is higher in males vs. females. At non-toxic levels, as observed in HiD males, inflammation, marked by IL-6 levels, was 24% lower compared to AI males. 800 IU/d vitamin D<sub>3</sub> supplementation in colorectal adenoma patients showed a 32% decrease in plasma IL-6 levels (244). As well, testosterone exerts a strong anti-inflammatory effect by lowering IL-6 levels (245-247) observed by AI and HiD males having 14% and 38% lower IL-6 levels compared to their female counterparts, respectively.

The anti-inflammatory effect of testosterone was also observed in DEF males as they had 29% lower IL-6, vs. DEF females. In DEF females, IL-6 levels were 22% higher vs. AI females. Contrary to testosterone; estrogen promotes IL-6 production and release during cellular damage (248). Without vitamin D's anti-inflammatory properties, a deficiency during trauma puts women, the sex that naturally possesses high levels of IL-6, at a greater risk of elevated levels of the inflammatory cytokine (249). Our findings are in accord with Miller et al's study that showed that women with serum 25(OH)D levels of <37.5 nmol/L at the time of hip fracture, indicative of cellular damage, had higher serum IL-6 levels in the year after the hip fracture (249).

### **Apoptosis**

HiD females had 13% higher cleaved/pro-caspase 3 ratio compared to AI females due to a 15% increase in cleaved caspase 3. In HiD females, elevated 3-NY levels indicate the presence of oxidative stress which can activate caspase 3 in the spinal cord of mSOD1 mice (250). Because males did not reach the threshold of toxicity, vitamin D had a protective role in males as the HiD group had a 26% lower cleaved/pro-caspase 3 ratio compared to AI males. Vitamin D has been shown to reduce activated caspase 3 in the spinal cord of EAE mice (251). In HiD males, the downregulation of microglial activation, and thus oxidative damage and inflammation, may have resulted in reduction of apoptosis.

In DEF mice, vitamin D no longer exerted its protective effects and thus bax/bcl-2 ratio was elevated by 23% in DEF mice vs. AI. A reduction in calcium buffering capacity brought about by vitamin D deficiency may cause the cell to exert calcium-induced excitotoxicity, which leads to elevated levels of bax/bcl-2. However, this increase was

not sufficient enough to activate caspase 3, the effector molecule in the apoptotic pathway. This is also confirmed in our previous study in HiD female *quadriceps* where a 242% increase in bax/bcl-2 (252) only corresponded to an 87% increase in cleaved/pro-caspase 3 (229). Thus, a deficiency in vitamin D may increase the susceptibility of motor neurons to apoptosis without necessarily leading to large-scale apoptosis.

### **Neurotrophic Factor**

There was no significant difference in GDNF protein content between the diets and sexes in both HiD and DEF groups.

### **Neuron Damage**

HiD females had 18% lower ChAT compared to AI females. This may be due to higher peroxynitrite levels, marked by increased 3-NY levels, which inhibits acetylcholine synthesis (253). AI males had 23% lower ChAT and 15% lower SMI-32 compared to AI females, indicating higher neuron damage. In mSOD1 mice, onset, disease progression and survival are dependent on sex; males lose body weight more rapidly following disease onset and die before females (254, 255). A reduction in body weight is reflective of muscle atrophy brought about by neuron degeneration. As with increased motor neuron count in AI females, it is more likely that damaged motor neurons are also more prevalent. This explains why SMI-36 levels were 13% lower in AI males vs. AI females. Despite lower motor neurons in HiD males vs. HiD females, they had 19% lower SMI-36/SMI-32 ratio, a proxy measure of motor neuron loss (256), compared to AI males. With lower apoptosis, it is evident that motor neuron integrity is maintained, and a decrease in SMI-36/SMI-32 ratio is evident.

DEF males also had 22% lower ChAT and 17% lower SMI-32 compared to their female counterparts, likely due to the protective effect of estrogen in females. This pattern is also retained in AI males vs. AI females, indicating the presence of a sexual dimorphism due to sex hormones. Because there was no change in neuron count between the diets, our findings confirm that though vitamin D deficiency may exasperate disease pathophysiology, it does not have an impact on neuron count.

### **Future Research**

Future research need to measure the effect of D<sub>3</sub> supplementation and restriction tested in this thesis on markers related to mechanisms implicated in ALS pathophysiology. Markers of oxidative damage (4-HNE and 3-NY), antioxidant capacity (SOD2, catalase and GPx1), inflammation (TNF- $\alpha$ , IL-6, IL-10), apoptosis (caspase 3, BAX and Bcl-2), neurotrophic factor (GDNF) and neuron count (SMI-32/SMI-36) need to be measured in the brain to confirm if they follow a pattern similar to what was observed in the spinal cord.

As well, recent studies have focused on the role of endoplasmic reticulum (ER) stress in ALS pathology (252, 257). Dysregulated calcium homeostasis and oxidative stress can damage the ER, the organelle responsible for protein synthesis, folding and targeting. Studies in G93A *quadriceps* confirmed that vitamin D deficiency reduces calcium-buffering capacity and increases prolonged ER-stress-induced apoptosis in females (257). On the contrary, D<sub>3</sub> supplementation at 50x AI decreases ER stress in females (252). ER stress has also been observed in the spinal cord of ALS patients, where it is linked to protein damage, aggregation, at increased motor neuron death (258).

Thus, future studies should focus how vitamin D restriction and supplementation impacts the ER within the spinal cord, focusing on markers of intracellular calcium trafficking (parvalbumin, calretinin, calbindin d28k) and ER stress (SERCA, CHOP).

Lastly, vitamin D status and corresponding calcium concentrations should be measured to establish levels at which toxicity is induced in females, and to compare these levels with males. A therapeutic optimal dose of D<sub>3</sub> also needs to be established concerning its effects on disease pathophysiology in this model. This is accomplished by examining differential doses of D<sub>3</sub>. Since 50 IU/g feed is likely the approximate threshold for D<sub>3</sub> toxicity and 10x has produced beneficial results without toxic effects, we would recommend future experimental HiD doses to be between these amounts.

References for Introduction, Rationale, Objective, Hypotheses and Pilot Studies and Summary and Future Research

1. Bruijn LI, Miller TM, Cleveland DW. Unraveling the mechanisms involved in motor neuron degeneration in ALS. *Annu Rev Neurosci* 2004;27:723-49.
2. Robberecht W, Philips T. The changing scene of amyotrophic lateral sclerosis. *Nat Rev Neurosci* 2013;14:248-64.
3. Dadon-Nachum M, Melamed E, Offen D. The "dying-back" phenomenon of motor neurons in ALS. *J Mol Neurosci* 2011;43:470-7.
4. Nishitoh H, Kadowaki H, Nagai A, Maruyama T, Yokota T, Fukutomi H, Noguchi T, Matsuzawa A, Takeda K, Ichijo H. ALS-linked mutant SOD1 induces ER stress- and ASK1-dependent motor neuron death by targeting Derlin-1. *Genes Dev* 2008;22:1451-64.
5. de Almeida JL, Silvestre R, Pinto A, de Carvalho M. Exercise and amyotrophic lateral sclerosis. *Neurological Sciences* 2012;33:9-15.
6. Wijesekera LC, Leigh PN. Amyotrophic lateral sclerosis. *Orphanet J Rare Dis* 2009;4:3,1172-4-3.
7. Eisen A, Weber M. The motor cortex and amyotrophic lateral sclerosis. *Muscle Nerve* 2001;24:564-73.
8. Mitchell JD, Borasio GD. Amyotrophic lateral sclerosis. *Lancet* 2007;369:2031-41.
9. Brooks BR. Clinical epidemiology of amyotrophic lateral sclerosis. *Neurol Clin* 1996;14:399-420.
10. Kokubo Y, Kuzuhara S, Narita Y. Geographical distribution of amyotrophic lateral sclerosis with neurofibrillary tangles in the Kii Peninsula of Japan. *J Neurol* 2000;247:850-2.
11. Muscaritoli M, Kushta I, Molfino A, Inghilleri M, Sabatelli M, Rossi Fanelli F. Nutritional and metabolic support in patients with amyotrophic lateral sclerosis. *Nutrition* 2012;28:959-66.
12. Deng Y, Xu Z, Xu B, Tian Y, Xin X, Deng X, Gao J. The protective effect of riluzole on manganese caused disruption of glutamate-glutamine cycle in rats. *Brain Res* 2009;1289:106-17.
13. Rowland LP, Shneider NA. Amyotrophic lateral sclerosis. *N Engl J Med* 2001;344:1688-700.

14. Chou SM. Neuropathology of amyotrophic lateral sclerosis: new perspectives on an old disease. *J Formos Med Assoc* 1997;96:488-98.
15. Cleveland DW. Neuronal growth and death: order and disorder in the axoplasm. *Cell* 1996;84:663-6.
16. Shaw PJ. Biochemical pathology. In: Brown RH, Meininger V and Swash M, eds. *Amyotrophic Lateral Sclerosis*. London, UK: Martin Dunitz Ltd, 2000:113-141.
17. Berthod F, Gros-Louis F. In Vivo and In Vitro Models to Study Amyotrophic Lateral Sclerosis.
18. Saxena S, Caroni P. Selective neuronal vulnerability in neurodegenerative diseases: from stressor thresholds to degeneration. *Neuron* 2011;71:35-48.
19. Frey D, Schneider C, Xu L, Borg J, Spooren W, Caroni P. Early and selective loss of neuromuscular synapse subtypes with low sprouting competence in motoneuron diseases. *J Neurosci* 2000;20:2534-42.
20. Fischer LR, Culver DG, Tennant P, Davis AA, Wang M, Castellano-Sanchez A, Khan J, Polak MA, Glass JD. Amyotrophic lateral sclerosis is a distal axonopathy: evidence in mice and man. *Exp Neurol* 2004;185:232-40.
21. SUNDERLAND S, RAY LJ. Denervation changes in mammalian striated muscle. *J Neurol Neurosurg Psychiatry* 1950;13:159-77.
22. Midrio M. The denervated muscle: facts and hypotheses. A historical review. *Eur J Appl Physiol* 2006;98:1-21.
23. Ravits J, Paul P, Jorg C. Focality of upper and lower motor neuron degeneration at the clinical onset of ALS. *Neurology* 2007;68:1571-5.
24. Ravits J, Laurie P, Fan Y, Moore DH. Implications of ALS focality: rostral-caudal distribution of lower motor neuron loss postmortem. *Neurology* 2007;68:1576-82.
25. Jennum P, Ibsen R, Pedersen SW, Kjellberg J. Mortality, health, social and economic consequences of amyotrophic lateral sclerosis: a controlled national study. *J Neurol* 2013;260:785-93.
26. Tripodoro VA, De Vito EL. Management of dyspnea in advanced motor neuron diseases. *Curr Opin Support Palliat Care* 2008;2:173-9.
27. Lechtzin N. Respiratory effects of amyotrophic lateral sclerosis: problems and solutions. *Respir Care* 2006;51:871,81; discussion 881-4.
28. Talbot K. Motor neuron disease: the bare essentials. *Pract Neurol* 2009;9:303-9.

29. Regal L, Vanopdenbosch L, Tilkin P, Van den Bosch L, Thijs V, Sciot R, Robberecht W. The G93C mutation in superoxide dismutase 1: clinicopathologic phenotype and prognosis. *Arch Neurol* 2006;63:262-7.
30. Yu Y, Su FC, Callaghan BC, Goutman SA, Batterman SA, Feldman EL. Environmental Risk Factors and Amyotrophic Lateral Sclerosis (ALS): A Case-Control Study of ALS in Michigan. *PLoS One* 2014;9:e101186.
31. Armon C. Smoking may be considered an established risk factor for sporadic ALS. *Neurology* 2009;73:1693-8.
32. Weisskopf MG, Morozova N, O'Reilly EJ, McCullough ML, Calle EE, Thun MJ, Ascherio A. Prospective study of chemical exposures and amyotrophic lateral sclerosis. *J Neurol Neurosurg Psychiatry* 2009;80:558-61.
33. Harwood CA, McDermott CJ, Shaw PJ. Physical activity as an exogenous risk factor in motor neuron disease (MND): a review of the evidence. *Amyotroph Lateral Scler* 2009;10:191-204.
34. Longstreth WT, Nelson LM, Koepsell TD, van Belle G. Hypotheses to explain the association between vigorous physical activity and amyotrophic lateral sclerosis. *Med Hypotheses* 1991;34:144-8.
35. Weisskopf MG, O'Reilly EJ, McCullough ML, Calle EE, Thun MJ, Cudkowicz M, Ascherio A. Prospective study of military service and mortality from ALS. *Neurology* 2005;64:32-7.
36. Chio A, Benzi G, Dossena M, Mutani R, Mora G. Severely increased risk of amyotrophic lateral sclerosis among Italian professional football players. *Brain* 2005;128:472-6.
37. Wicks P, Ganesalingham J, Collin C, Prevett M, Leigh NP, Al-Chalabi A. Three soccer playing friends with simultaneous amyotrophic lateral sclerosis. *Amyotroph Lateral Scler* 2007;8:177-9.
38. Worrall BB, Rowland LP, Chin SS, Mastrianni JA. Amyotrophy in prion diseases. *Arch Neurol* 2000;57:33-8.
39. Cox PA, Sacks OW. Cycad neurotoxins, consumption of flying foxes, and ALS-PDC disease in Guam. *Neurology* 2002;58:956-9.
40. Murch SJ, Cox PA, Banack SA. A mechanism for slow release of biomagnified cyanobacterial neurotoxins and neurodegenerative disease in Guam. *Proc Natl Acad Sci U S A* 2004;101:12228-31.

41. Dunlop RA, Cox PA, Banack SA, Rodgers KJ. The non-protein amino acid BMAA is misincorporated into human proteins in place of L-serine causing protein misfolding and aggregation. *PLoS One* 2013;8:e75376.
42. Vinceti M, Guidetti D, Pinotti M, Rovesti S, Merlin M, Vescovi L, Bergomi M, Vivoli G. Amyotrophic Lateral Sclerosis after Long-Term Exposure to Drinking Water with High Selenium Content. *Epidemiology* 1996;7:529-32.
43. Miyata S, Nakamura S, Nagata H, Kameyama M. Increased manganese level in spinal cords of amyotrophic lateral sclerosis determined by radiochemical neutron activation analysis. *J Neurol Sci* 1983;61:283-93.
44. Kirpekar SM, Dixon W, Prat JC. Inhibitory effect of manganese on norepinephrine release from the splenic nerves of cats. *J Pharmacol Exp Ther* 1970;174:72-6.
45. Yase Y. The pathogenesis of amyotrophic lateral sclerosis. *Lancet* 1972;2:292-6.
46. Morahan JM, Pamphlett R. Amyotrophic lateral sclerosis and exposure to environmental toxins: an Australian case-control study. *Neuroepidemiology* 2006;27:130-5.
47. Malek AM, Barchowsky A, Bowser R, Heiman-Patterson T, Lacomis D, Rana S, Youk A, Stickler D, Lackland DT, Talbott EO. Environmental and occupational risk factors for amyotrophic lateral sclerosis: a case-control study. *Neurodegener Dis* 2014;14:31-8.
48. Sutedja NA, Veldink JH, Fischer K, Kromhout H, Heederik D, Huisman MH, Wokke JH, van den Berg LH. Exposure to chemicals and metals and risk of amyotrophic lateral sclerosis: a systematic review. *Amyotroph Lateral Scler* 2009;10:302-9.
49. Wills AM, Cronin S, Slowik A, Kasperaviciute D, Van Es MA, Morahan JM, Valdmanis PN, Meininger V, Melki J, Shaw CE, et al. A large-scale international meta-analysis of paraoxonase gene polymorphisms in sporadic ALS. *Neurology* 2009;73:16-24.
50. Al-Chalabi A, Jones A, Troakes C, King A, Al-Sarraj S, van den Berg LH. The genetics and neuropathology of amyotrophic lateral sclerosis. *Acta Neuropathol* 2012;124:339-52.
51. Boillee S, Vande Velde C, Cleveland DW. ALS: a disease of motor neurons and their nonneuronal neighbors. *Neuron* 2006;52:39-59.
52. Boillee S, Yamanaka K, Lobsiger CS, Copeland NG, Jenkins NA, Kassiotis G, Kollias G, Cleveland DW. Onset and progression in inherited ALS determined by motor neurons and microglia. *Science* 2006;312:1389-92.

53. Brooks BR. El Escorial World Federation of Neurology criteria for the diagnosis of amyotrophic lateral sclerosis. Subcommittee on Motor Neuron Diseases/Amyotrophic Lateral Sclerosis of the World Federation of Neurology Research Group on Neuromuscular Diseases and the El Escorial "Clinical limits of amyotrophic lateral sclerosis" workshop contributors. *J Neurol Sci* 1994;124 Suppl:96-107.
54. Brooks BR, Miller RG, Swash M, Munsat TL, World Federation of Neurology Research Group on Motor Neuron Diseases. El Escorial revisited: revised criteria for the diagnosis of amyotrophic lateral sclerosis. *Amyotroph Lateral Scler Other Motor Neuron Disord* 2000;1:293-9.
55. Kiernan MC, Vucic S, Cheah BC, Turner MR, Eisen A, Hardiman O, Burrell JR, Zoing MC. Amyotrophic lateral sclerosis. *Lancet* 2011;377:942-55.
56. Anonymous The Amyotrophic Lateral Sclerosis Functional Rating Scale. Assessment of activities of daily living in patients with amyotrophic lateral sclerosis. The ALS CNTF treatment study (ACTS) phase I-II Study Group. *Arch Neurol* 1996;53:141-7.
57. Rosen DR, Siddique T, Patterson D, Figlewicz DA, Sapp P, Hentati A, Donaldson D, Goto J, O'Regan JP, Deng HX. Mutations in Cu/Zn superoxide dismutase gene are associated with familial amyotrophic lateral sclerosis. *Nature* 1993;362:59-62.
58. Mitchell JD. Amyotrophic lateral sclerosis: toxins and environment. *Amyotroph Lateral Scler Other Motor Neuron Disord* 2000;1:235-50.
59. Renton AE, Chio A, Traynor BJ. State of play in amyotrophic lateral sclerosis genetics. *Nat Neurosci* 2014;17:17-23.
60. Gianforcaro A, Hamadeh MJ. Vitamin D as a potential therapy in amyotrophic lateral sclerosis. *CNS Neurosci Ther* 2014;20:101-11.
61. Wang, , Ming-Dong AND Gomes, , James AND Cashman, , Neil R. AND Little, , Julian AND Krewski,,Daniel. Intermediate CAG Repeat Expansion in the *ATXN2* Gene Is a Unique Genetic Risk Factor for ALS^A Systematic Review and Meta-Analysis of Observational Studies. *PLoS ONE* 2014;9:e105534.
62. Gros-Louis F, Gaspar C, Rouleau GA. Genetics of familial and sporadic amyotrophic lateral sclerosis. *Biochim Biophys Acta* 2006;1762:956-72.
63. McCord JM, Fridovich I. Superoxide dismutase. An enzymic function for erythrocuprein (hemocuprein). *J Biol Chem* 1969;244:6049-55.
64. Valdmanis PN, Rouleau GA. Genetics of familial amyotrophic lateral sclerosis. *Neurology* 2008;70:144-52.

65. Nagai M, Re DB, Nagata T, Chalazonitis A, Jessell TM, Wichterle H, Przedborski S. Astrocytes expressing ALS-linked mutated SOD1 release factors selectively toxic to motor neurons. *Nat Neurosci* 2007;10:615-22.
66. Pasinelli P, Brown RH. Molecular biology of amyotrophic lateral sclerosis: insights from genetics. *Nat Rev Neurosci* 2006;7:710-23.
67. Levanon D, Lieman-Hurwitz J, Dafni N, Wigderson M, Sherman L, Bernstein Y, Laver-Rudich Z, Danciger E, Stein O, Groner Y. Architecture and anatomy of the chromosomal locus in human chromosome 21 encoding the Cu/Zn superoxide dismutase. *EMBO J* 1985;4:77-84.
68. Okado-Matsumoto A, Fridovich I. Subcellular distribution of superoxide dismutases (SOD) in rat liver: Cu,Zn-SOD in mitochondria. *J Biol Chem* 2001;276:38388-93.
69. Delisle MB, Carpenter S. Neurofibrillary axonal swellings and amyotrophic lateral sclerosis. *J Neurol Sci* 1984;63:241-50.
70. Kaal EC, Veldman H, Sondaar P, Joosten EA, Dop Bar PR. Oxidant treatment causes a dose-dependent phenotype of apoptosis in cultured motoneurons. *J Neurosci Res* 1998;54:778-86.
71. Said Ahmed M, Hung WY, Zu JS, Hockberger P, Siddique T. Increased reactive oxygen species in familial amyotrophic lateral sclerosis with mutations in SOD1. *J Neurol Sci* 2000;176:88-94.
72. Fridovich I. Biological effects of the superoxide radical. *Arch Biochem Biophys* 1986;247:1-11.
73. Cadenas E, Boveris A. Enhancement of hydrogen peroxide formation by protophores and ionophores in antimycin-supplemented mitochondria. *Biochem J* 1980;188:31-7.
74. Boveris A, Cadenas E, Stoppani AO. Role of ubiquinone in the mitochondrial generation of hydrogen peroxide. *Biochem J* 1976;156:435-44.
75. Forman HJ, Fridovich I. On the stability of bovine superoxide dismutase. The effects of metals. *J Biol Chem* 1973;248:2645-9.
76. Bosco DA, Morfini G, Karabacak NM, Song Y, Gros-Louis F, Pasinelli P, Goolsby H, Fontaine BA, Lemay N, McKenna-Yasek D, et al. Wild-type and mutant SOD1 share an aberrant conformation and a common pathogenic pathway in ALS. *Nat Neurosci* 2010;13:1396-403.
77. Yim MB, Kang JH, Yim HS, Kwak HS, Chock PB, Stadtman ER. A gain-of-function of an amyotrophic lateral sclerosis-associated Cu,Zn-superoxide dismutase mutant: An

enhancement of free radical formation due to a decrease in Km for hydrogen peroxide. *Proc Natl Acad Sci U S A* 1996;93:5709-14.

78. Drechsel DA, Estevez AG, Barbeito L, Beckman JS. Nitric oxide-mediated oxidative damage and the progressive demise of motor neurons in ALS. *Neurotox Res* 2012;22:251-64.

79. Andersen PM, Nilsson P, Keranen ML, Forsgren L, Hagglund J, Karlsborg M, Ronnevi LO, Gredal O, Marklund SL. Phenotypic heterogeneity in motor neuron disease patients with CuZn-superoxide dismutase mutations in Scandinavia. *Brain* 1997;120 ( Pt 10):1723-37.

80. Al-Chalabi A, Andersen PM, Chioza B, Shaw C, Sham PC, Robberecht W, Matthijs G, Camu W, Marklund SL, Forsgren L, et al. Recessive amyotrophic lateral sclerosis families with the D90A SOD1 mutation share a common founder: evidence for a linked protective factor. *Hum Mol Genet* 1998;7:2045-50.

81. Broom WJ, Johnson DV, Auwarter KE, Iafrate AJ, Russ C, Al-Chalabi A, Sapp PC, McKenna-Yasek D, Andersen PM, Brown RH, Jr. SOD1A4V-mediated ALS: absence of a closely linked modifier gene and origination in Asia. *Neurosci Lett* 2008;430:241-5.

82. Yim MB, Chock PB, Stadtman ER. Copper, zinc superoxide dismutase catalyzes hydroxyl radical production from hydrogen peroxide. *Proc Natl Acad Sci U S A* 1990;87:5006-10.

83. Hamadeh MJ, Rodriguez MC, Kaczor JJ, Tarnopolsky MA. Caloric restriction transiently improves motor performance but hastens clinical onset of disease in the Cu/Zn-superoxide dismutase mutant G93A mouse. *Muscle Nerve* 2005;31:214-20.

84. Bruijn LI, Houseweart MK, Kato S, Anderson KL, Anderson SD, Ohama E, Reaume AG, Scott RW, Cleveland DW. Aggregation and motor neuron toxicity of an ALS-linked SOD1 mutant independent from wild-type SOD1. *Science* 1998;281:1851-4.

85. Jaarsma D, Teuling E, Haasdijk ED, De Zeeuw CI, Hoogenraad CC. Neuron-specific expression of mutant superoxide dismutase is sufficient to induce amyotrophic lateral sclerosis in transgenic mice. *J Neurosci* 2008;28:2075-88.

86. Pramatarova A, Laganriere J, Roussel J, Brisebois K, Rouleau GA. Neuron-specific expression of mutant superoxide dismutase 1 in transgenic mice does not lead to motor impairment. *J Neurosci* 2001;21:3369-74.

87. Evans MC, Couch Y, Sibson N, Turner MR. Inflammation and neurovascular changes in amyotrophic lateral sclerosis. *Molecular and Cellular Neuroscience* 2013;53:34-41.

88. Venerosi A, Martire A, Rungi A, Pieri M, Ferrante A, Zona C, Popoli P, Calamandrei G. Complex behavioral and synaptic effects of dietary branched chain amino acids in a mouse model of amyotrophic lateral sclerosis. *Mol Nutr Food Res* 2011;55:541-52.
89. Trumbull KA, Beckman JS. A role for copper in the toxicity of zinc-deficient superoxide dismutase to motor neurons in amyotrophic lateral sclerosis. *Antioxid Redox Signal* 2009;11:1627-39.
90. Crow JP, Sampson JB, Zhuang Y, Thompson JA, Beckman JS. Decreased zinc affinity of amyotrophic lateral sclerosis-associated superoxide dismutase mutants leads to enhanced catalysis of tyrosine nitration by peroxynitrite. *J Neurochem* 1997;69:1936-44.
91. Estevez AG, Crow JP, Sampson JB, Reiter C, Zhuang Y, Richardson GJ, Tarpey MM, Barbeito L, Beckman JS. Induction of nitric oxide-dependent apoptosis in motor neurons by zinc-deficient superoxide dismutase. *Science* 1999;286:2498-500.
92. Gong YH, Parsadanian AS, Andreeva A, Snider WD, Elliott JL. Restricted expression of G86R Cu/Zn superoxide dismutase in astrocytes results in astrocytosis but does not cause motoneuron degeneration. *J Neurosci* 2000;20:660-5.
93. Gurney ME, Pu H, Chiu AY, Dal Canto MC, Polchow CY, Alexander DD, Caliando J, Hentati A, Kwon YW, Deng HX. Motor neuron degeneration in mice that express a human Cu,Zn superoxide dismutase mutation. *Science* 1994;264:1772-5.
94. Hamadeh MJ, Tarnopolsky MA. Transient caloric restriction in early adulthood hastens disease endpoint in male, but not female, Cu/Zn-SOD mutant G93A mice. *Muscle Nerve* 2006;34:709-19.
95. Solomon JA, Tarnopolsky MA, Hamadeh MJ. One universal common endpoint in mouse models of amyotrophic lateral sclerosis. *PLoS One* 2011;6:e20582.
96. Stieber A, Gonatas JO, Collard J, Meier J, Julien J, Schweitzer P, Gonatas NK. The neuronal Golgi apparatus is fragmented in transgenic mice expressing a mutant human SOD1, but not in mice expressing the human NF-H gene. *J Neurol Sci* 2000;173:63-72.
97. Jaarsma D, Rognoni F, van Duijn W, Verspaget HW, Haasdijk ED, Holstege JC. CuZn superoxide dismutase (SOD1) accumulates in vacuolated mitochondria in transgenic mice expressing amyotrophic lateral sclerosis-linked SOD1 mutations. *Acta Neuropathol* 2001;102:293-305.
98. Teuling E, van Dis V, Wulf PS, Haasdijk ED, Akhmanova A, Hoogenraad CC, Jaarsma D. A novel mouse model with impaired dynein/dynactin function develops amyotrophic lateral sclerosis (ALS)-like features in motor neurons and improves lifespan in SOD1-ALS mice. *Hum Mol Genet* 2008;17:2849-62.

99. Vlug AS, Teuling E, Haasdijk ED, French P, Hoogenraad CC, Jaarsma D. ATF3 expression precedes death of spinal motoneurons in amyotrophic lateral sclerosis-SOD1 transgenic mice and correlates with c-Jun phosphorylation, CHOP expression, somato-dendritic ubiquitination and Golgi fragmentation. *Eur J Neurosci* 2005;22:1881-94.
100. Sasaki S, Iwata M. Impairment of fast axonal transport in the proximal axons of anterior horn neurons in amyotrophic lateral sclerosis. *Neurology* 1996;47:535-40.
101. Zhang B, Tu P, Abtahian F, Trojanowski JQ, Lee VM. Neurofilaments and orthograde transport are reduced in ventral root axons of transgenic mice that express human SOD1 with a G93A mutation. *J Cell Biol* 1997;139:1307-15.
102. Puttaparthi K, Van Kaer L, Elliott JL. Assessing the role of immuno-proteasomes in a mouse model of familial ALS. *Exp Neurol* 2007;206:53-8.
103. Heiman-Patterson TD, Deitch JS, Blankenhorn EP, Erwin KL, Perreault MJ, Alexander BK, Byers N, Toman I, Alexander GM. Background and gender effects on survival in the TgN(SOD1-G93A)1Gur mouse model of ALS. *J Neurol Sci* 2005;236:1-7.
104. Shibata N. Transgenic mouse model for familial amyotrophic lateral sclerosis with superoxide dismutase-1 mutation. *Neuropathology* 2001;21:82-92.
105. Acevedo-Arozena A, Kalmar B, Essa S, Ricketts T, Joyce P, Kent R, Rowe C, Parker A, Gray A, Hafezparast M, et al. A comprehensive assessment of the SOD1G93A low-copy transgenic mouse, which models human amyotrophic lateral sclerosis. *Dis Model Mech* 2011;4:686-700.
106. Alexander GM, Erwin KL, Byers N, Deitch JS, Augelli BJ, Blankenhorn EP, Heiman-Patterson TD. Effect of transgene copy number on survival in the G93A SOD1 transgenic mouse model of ALS. *Brain Res Mol Brain Res* 2004;130:7-15.
107. Bhasin J, Latt R, Macallum E, McCutcheon K, Olfert E, Rainnie D, Schunk M. Canadian Council on Animal Care Guidelines: Choosing an Appropriate Endpoint in Experiments Using Animals for Research, Teaching, and Testing. Ottawa Ontario: CCAC.p 1998;15-6.
108. Chance B, Sies H, Boveris A. Hydroperoxide metabolism in mammalian organs. *Physiol Rev* 1979;59:527-605.
109. Barnham KJ, Masters CL, Bush AI. Neurodegenerative diseases and oxidative stress. *Nat Rev Drug Discov* 2004;3:205-14.
110. Huang TT, Naemuddin M, Elchuri S, Yamaguchi M, Kozy HM, Carlson EJ, Epstein CJ. Genetic modifiers of the phenotype of mice deficient in mitochondrial superoxide dismutase. *Hum Mol Genet* 2006;15:1187-94.

111. Halliwell B. Free Radicals and Other Reactive Species in Disease. 2001;
112. Ignarro LJ. Biosynthesis and metabolism of endothelium-derived nitric oxide. *Annu Rev Pharmacol Toxicol* 1990;30:535-60.
113. Beckman JS, Beckman TW, Chen J, Marshall PA, Freeman BA. Apparent hydroxyl radical production by peroxynitrite: implications for endothelial injury from nitric oxide and superoxide. *Proc Natl Acad Sci U S A* 1990;87:1620-4.
114. Beckman JS, Koppenol WH. Nitric oxide, superoxide, and peroxynitrite: the good, the bad, and ugly. *Am J Physiol* 1996;271:C1424-37.
115. Radi R. Nitric oxide, oxidants, and protein tyrosine nitration. *Proc Natl Acad Sci U S A* 2004;101:4003-8.
116. Beckman JS. Peroxynitrite versus hydroxyl radical: the role of nitric oxide in superoxide-dependent cerebral injury. *Ann N Y Acad Sci* 1994;738:69-75.
117. Denicola A, Souza JM, Radi R, Lissi E. Nitric oxide diffusion in membranes determined by fluorescence quenching. *Arch Biochem Biophys* 1996;328:208-12.
118. Radi R, Cassina A, Hodara R. Nitric oxide and peroxynitrite interactions with mitochondria. *Biol Chem* 2002;383:401-9.
119. Butcher SP, Hamberger A. In vivo studies on the extracellular, and veratrine-releasable, pools of endogenous amino acids in the rat striatum: effects of corticostriatal deafferentation and kainic acid lesion. *J Neurochem* 1987;48:713-21.
120. Foran E, Trotti D. Glutamate transporters and the excitotoxic path to motor neuron degeneration in amyotrophic lateral sclerosis. *Antioxid Redox Signal* 2009;11:1587-602.
121. Kvamme E, Roberg B, Torgner IA. Phosphate-activated glutaminase and mitochondrial glutamine transport in the brain. *Neurochem Res* 2000;25:1407-19.
122. Kim CH, Lee J, Lee JY, Roche KW. Metabotropic glutamate receptors: phosphorylation and receptor signaling. *J Neurosci Res* 2008;86:1-10.
123. Newpher TM, Ehlers MD. Glutamate receptor dynamics in dendritic microdomains. *Neuron* 2008;58:472-97.
124. Hollmann M, Heinemann S. Cloned glutamate receptors. *Annu Rev Neurosci* 1994;17:31-108.
125. Le Verche V, Ikiz B, Jacquier A. Glutamate pathway implication in amyotrophic lateral sclerosis: what is the signal in the noise? *Journal of Receptor, Ligand and Channel Research* 2011;4:1-22.

126. Isaac JT, Ashby MC, McBain CJ. The role of the GluR2 subunit in AMPA receptor function and synaptic plasticity. *Neuron* 2007;54:859-71.
127. Corona JC, Tapia R. Ca<sup>2+</sup>-permeable AMPA receptors and intracellular Ca<sup>2+</sup> determine motoneuron vulnerability in rat spinal cord in vivo. *Neuropharmacology* 2007;52:1219-28.
128. Moussawi K, Riegel A, Nair S, Kalivas PW. Extracellular glutamate: functional compartments operate in different concentration ranges. *Front Syst Neurosci* 2011;5:94.
129. Attwell D. Brain uptake of glutamate: food for thought. *J Nutr* 2000;130:1023S-5S.
130. Long K, Nguyen LT. Roles of vitamin D in amyotrophic lateral sclerosis: possible genetic and cellular signaling mechanisms. *Mol Brain* 2013;6:16,6606-6-16.
131. Spreux-Varoquaux O, Bensimon G, Lacomblez L, Salachas F, Pradat PF, Le Forestier N, Marouan A, Dib M, Meininger V. Glutamate levels in cerebrospinal fluid in amyotrophic lateral sclerosis: a reappraisal using a new HPLC method with coulometric detection in a large cohort of patients. *J Neurol Sci* 2002;193:73-8.
132. Rothstein JD, Tsai G, Kuncl RW, Clawson L, Cornblath DR, Drachman DB, Pestronk A, Stauch BL, Coyle JT. Abnormal excitatory amino acid metabolism in amyotrophic lateral sclerosis. *Ann Neurol* 1990;28:18-25.
133. Danbolt NC. Glutamate uptake. *Prog Neurobiol* 2001;65:1-105.
134. Haugeto O, Ullensvang K, Levy LM, Chaudhry FA, Honore T, Nielsen M, Lehre KP, Danbolt NC. Brain glutamate transporter proteins form homomultimers. *J Biol Chem* 1996;271:27715-22.
135. Tanaka K, Watase K, Manabe T, Yamada K, Watanabe M, Takahashi K, Iwama H, Nishikawa T, Ichihara N, Kikuchi T, et al. Epilepsy and exacerbation of brain injury in mice lacking the glutamate transporter GLT-1. *Science* 1997;276:1699-702.
136. Howland DS, Liu J, She Y, Goad B, Maragakis NJ, Kim B, Erickson J, Kulik J, DeVito L, Psaltis G, et al. Focal loss of the glutamate transporter EAAT2 in a transgenic rat model of SOD1 mutant-mediated amyotrophic lateral sclerosis (ALS). *Proc Natl Acad Sci U S A* 2002;99:1604-9.
137. Mark LP, Prost RW, Ulmer JL, Smith MM, Daniels DL, Strottmann JM, Brown WD, Hancein-Bey L. Pictorial review of glutamate excitotoxicity: fundamental concepts for neuroimaging. *AJNR Am J Neuroradiol* 2001;22:1813-24.
138. Choi DW. Excitotoxic cell death. *J Neurobiol* 1992;23:1261-76.

139. Del Rio P, Montiel T, Chagoya V, Massieu L. Exacerbation of excitotoxic neuronal death induced during mitochondrial inhibition in vivo: relation to energy imbalance or ATP depletion? *Neuroscience* 2007;146:1561-70.
140. Ikonomidou C, Turski L. Excitotoxicity and neurodegenerative diseases. *Curr Opin Neurol* 1995;8:487-97.
141. Plaitakis A, Carosco JT. Abnormal glutamate metabolism in amyotrophic lateral sclerosis. *Ann Neurol* 1987;22:575-9.
142. Rothstein JD, Martin LJ, Kuncl RW. Decreased glutamate transport by the brain and spinal cord in amyotrophic lateral sclerosis. *N Engl J Med* 1992;326:1464-8.
143. Ischiropoulos H, Zhu L, Chen J, Tsai M, Martin JC, Smith CD, Beckman JS. Peroxynitrite-mediated tyrosine nitration catalyzed by superoxide dismutase. *Arch Biochem Biophys* 1992;298:431-7.
144. Quijano C, Alvarez B, Gatti RM, Augusto O, Radi R. Pathways of peroxynitrite oxidation of thiol groups. *Biochem J* 1997;322 ( Pt 1):167-73.
145. Radi R, Cassina A, Hodara R, Quijano C, Castro L. Peroxynitrite reactions and formation in mitochondria. *Free Radic Biol Med* 2002;33:1451-64.
146. Pedersen WA, Fu W, Keller JN, Markesbery WR, Appel S, Smith RG, Kasarskis E, Mattson MP. Protein modification by the lipid peroxidation product 4-hydroxynonenal in the spinal cords of amyotrophic lateral sclerosis patients. *Ann Neurol* 1998;44:819-24.
147. Mark RJ, Hensley K, Butterfield DA, Mattson MP. Amyloid beta-peptide impairs ion-motive ATPase activities: evidence for a role in loss of neuronal Ca<sup>2+</sup> homeostasis and cell death. *J Neurosci* 1995;15:6239-49.
148. Kruman I, Bruce-Keller AJ, Bredesen D, Waeg G, Mattson MP. Evidence that 4-hydroxynonenal mediates oxidative stress-induced neuronal apoptosis. *J Neurosci* 1997;17:5089-100.
149. Patel BP, Safdar A, Raha S, Tarnopolsky MA, Hamadeh MJ. Caloric restriction shortens lifespan through an increase in lipid peroxidation, inflammation and apoptosis in the G93A mouse, an animal model of ALS. *PLoS One* 2010;5:e9386.
150. Freeman BA, Crapo JD. Biology of disease: free radicals and tissue injury. *Lab Invest* 1982;47:412-26.
151. Jokic N, Di Scala F, Dupuis L, Rene F, Muller A, Gonzalez De Aguilar JL, Loeffler JP. Early activation of antioxidant mechanisms in muscle of mutant Cu/Zn-superoxide dismutase-linked amyotrophic lateral sclerosis mice. *Ann N Y Acad Sci* 2003;1010:552-6.

152. Lebovitz RM, Zhang H, Vogel H, Cartwright J, Jr, Dionne L, Lu N, Huang S, Matzuk MM. Neurodegeneration, myocardial injury, and perinatal death in mitochondrial superoxide dismutase-deficient mice. *Proc Natl Acad Sci U S A* 1996;93:9782-7.
153. Andreassen OA, Ferrante RJ, Klivenyi P, Klein AM, Shinobu LA, Epstein CJ, Beal MF. Partial deficiency of manganese superoxide dismutase exacerbates a transgenic mouse model of amyotrophic lateral sclerosis. *Ann Neurol* 2000;47:447-55.
154. MacMillan-Crow LA, Crow JP, Kerby JD, Beckman JS, Thompson JA. Nitration and inactivation of manganese superoxide dismutase in chronic rejection of human renal allografts. *Proc Natl Acad Sci U S A* 1996;93:11853-8.
155. Quijano C, Hernandez-Saavedra D, Castro L, McCord JM, Freeman BA, Radi R. Reaction of peroxynitrite with Mn-superoxide dismutase. Role of the metal center in decomposition kinetics and nitration. *J Biol Chem* 2001;276:11631-8.
156. Surmeli NB, Litterman NK, Miller AF, Groves JT. Peroxynitrite mediates active site tyrosine nitration in manganese superoxide dismutase. Evidence of a role for the carbonate radical anion. *J Am Chem Soc* 2010;132:17174-85.
157. Palacios-Callender M, Quintero M, Hollis VS, Springett RJ, Moncada S. Endogenous NO regulates superoxide production at low oxygen concentrations by modifying the redox state of cytochrome c oxidase. *Proc Natl Acad Sci U S A* 2004;101:7630-5.
158. Alfonso-Prieto M, Biarnes X, Vidossich P, Rovira C. The molecular mechanism of the catalase reaction. *J Am Chem Soc* 2009;131:11751-61.
159. Fransen M. Peroxisome Dynamics: Molecular Players, Mechanisms, and (Dys)functions. *ISRN Cell Biology* 2012;2012:24.
160. Wanders RJ. Peroxisomes, lipid metabolism, and peroxisomal disorders. *Mol Genet Metab* 2004;83:16-27.
161. Dixit E, Boulant S, Zhang Y, Lee AS, Odendall C, Shum B, Hacohen N, Chen ZJ, Whelan SP, Fransen M, et al. Peroxisomes are signaling platforms for antiviral innate immunity. *Cell* 2010;141:668-81.
162. Islinger M, Grille S, Fahimi HD, Schrader M. The peroxisome: an update on mysteries. *Histochem Cell Biol* 2012;137:547-74.
163. Wang B, Van Veldhoven PP, Brees C, Rubio N, Nordgren M, Apanasets O, Kunze M, Baes M, Agostinis P, Fransen M. Mitochondria are targets for peroxisome-derived oxidative stress in cultured mammalian cells. *Free Radic Biol Med* 2013;65C:882-94.

164. Ivashchenko O, Van Veldhoven PP, Brees C, Ho YS, Terlecky SR, Fransen M. Intraperoxisomal redox balance in mammalian cells: oxidative stress and interorganellar cross-talk. *Mol Biol Cell* 2011;22:1440-51.
165. Raps SP, Lai JC, Hertz L, Cooper AJ. Glutathione is present in high concentrations in cultured astrocytes but not in cultured neurons. *Brain Res* 1989;493:398-401.
166. Makar TK, Nedergaard M, Preuss A, Gelbard AS, Perumal AS, Cooper AJ. Vitamin E, ascorbate, glutathione, glutathione disulfide, and enzymes of glutathione metabolism in cultures of chick astrocytes and neurons: evidence that astrocytes play an important role in antioxidative processes in the brain. *J Neurochem* 1994;62:45-53.
167. Desagher S, Glowinski J, Premont J. Astrocytes protect neurons from hydrogen peroxide toxicity. *J Neurosci* 1996;16:2553-62.
168. Castro LA, Robalinho RL, Cayota A, Meneghini R, Radi R. Nitric oxide and peroxynitrite-dependent aconitase inactivation and iron-regulatory protein-1 activation in mammalian fibroblasts. *Arch Biochem Biophys* 1998;359:215-24.
169. Lizasoain I, Moro MA, Knowles RG, Darley-Usmar V, Moncada S. Nitric oxide and peroxynitrite exert distinct effects on mitochondrial respiration which are differentially blocked by glutathione or glucose. *Biochem J* 1996;314 ( Pt 3):877-80.
170. Koga M, Serritella AV, Messmer MM, Hayashi-Takagi A, Hester LD, Snyder SH, Sawa A, Sedlak TW. Glutathione is a physiologic reservoir of neuronal glutamate. *Biochem Biophys Res Commun* 2011;409:596-602.
171. Przedborski S, Donaldson D, Jakowec M, Kish SJ, Guttman M, Rosoklija G, Hays AP. Brain superoxide dismutase, catalase, and glutathione peroxidase activities in amyotrophic lateral sclerosis. *Ann Neurol* 1996;39:158-65.
172. McCombe PA, Henderson RD. The Role of immune and inflammatory mechanisms in ALS. *Curr Mol Med* 2011;11:246-54.
173. Mitchell RM, Freeman WM, Randazzo WT, Stephens HE, Beard JL, Simmons Z, Connor JR. A CSF biomarker panel for identification of patients with amyotrophic lateral sclerosis. *Neurology* 2009;72:14-9.
174. Aschner M, Sonnewald U, Tan KH. Astrocyte modulation of neurotoxic injury. *Brain Pathol* 2002;12:475-81.
175. Bezzi P, Volterra A. A neuron-glia signalling network in the active brain. *Curr Opin Neurobiol* 2001;11:387-94.

176. Dawson VL, Brahmabhatt HP, Mong JA, Dawson TM. Expression of inducible nitric oxide synthase causes delayed neurotoxicity in primary mixed neuronal-glia cortical cultures. *Neuropharmacology* 1994;33:1425-30.
177. Cassina P, Peluffo H, Pehar M, Martinez-Palma L, Ressia A, Beckman JS, Estevez AG, Barbeito L. Peroxynitrite triggers a phenotypic transformation in spinal cord astrocytes that induces motor neuron apoptosis. *J Neurosci Res* 2002;67:21-9.
178. Pasinelli P, Houseweart MK, Brown RH, Jr, Cleveland DW. Caspase-1 and -3 are sequentially activated in motor neuron death in Cu,Zn superoxide dismutase-mediated familial amyotrophic lateral sclerosis. *Proc Natl Acad Sci U S A* 2000;97:13901-6.
179. Hughes RA, Sendtner M, Thoenen H. Members of several gene families influence survival of rat motoneurons in vitro and in vivo. *J Neurosci Res* 1993;36:663-71.
180. Oppenheim RW. Neurotrophic survival molecules for motoneurons: an embarrassment of riches. *Neuron* 1996;17:195-7.
181. Zhao P, Ignacio S, Beattie EC, Abood ME. Altered presymptomatic AMPA and cannabinoid receptor trafficking in motor neurons of ALS model mice: implications for excitotoxicity. *Eur J Neurosci* 2008;27:572-9.
182. Estevez AG, Spear N, Thompson JA, Cornwell TL, Radi R, Barbeito L, Beckman JS. Nitric oxide-dependent production of cGMP supports the survival of rat embryonic motor neurons cultured with brain-derived neurotrophic factor. *J Neurosci* 1998;18:3708-14.
183. Estevez AG, Spear N, Manuel SM, Radi R, Henderson CE, Barbeito L, Beckman JS. Nitric oxide and superoxide contribute to motor neuron apoptosis induced by trophic factor deprivation. *J Neurosci* 1998;18:923-31.
184. Estevez AG, Sampson JB, Zhuang YX, Spear N, Richardson GJ, Crow JP, Tarpey MM, Barbeito L, Beckman JS. Liposome-delivered superoxide dismutase prevents nitric oxide-dependent motor neuron death induced by trophic factor withdrawal. *Free Radic Biol Med* 2000;28:437-46.
185. Estevez AG, Kamaid A, Thompson JA, Cornwell TL, Radi R, Barbeito L, Beckman JS. Cyclic guanosine 5' monophosphate (GMP) prevents expression of neuronal nitric oxide synthase and apoptosis in motor neurons deprived of trophic factors in rats. *Neurosci Lett* 2002;326:201-5.
186. Sathasivam S, Ince PG, Shaw PJ. Apoptosis in amyotrophic lateral sclerosis: a review of the evidence. *Neuropathol Appl Neurobiol* 2001;27:257-74.

187. Kostic V, Jackson-Lewis V, de Bilbao F, Dubois-Dauphin M, Przedborski S. Bcl-2: prolonging life in a transgenic mouse model of familial amyotrophic lateral sclerosis. *Science* 1997;277:559-62.
188. Summerday NM, Brown SJ, Allington DR, Rivey MP. Vitamin D and multiple sclerosis: review of a possible association. *J Pharm Pract* 2012;25:75-84.
189. Pierrot-Deseilligny C. Clinical implications of a possible role of vitamin D in multiple sclerosis. *J Neurol* 2009;256:1468-79.
190. Holick MF. Vitamin D deficiency. *N Engl J Med* 2007;357:266-81.
191. Smolders J, Damoiseaux J, Menheere P, Hupperts R. Vitamin D as an immune modulator in multiple sclerosis, a review. *J Neuroimmunol* 2008;194:7-17.
192. Armas LA, Hollis BW, Heaney RP. Vitamin D2 is much less effective than vitamin D3 in humans. *J Clin Endocrinol Metab* 2004;89:5387-91.
193. Smith JE, Goodman DS. The turnover and transport of vitamin D and of a polar metabolite with the properties of 25-hydroxycholecalciferol in human plasma. *J Clin Invest* 1971;50:2159-67.
194. Zehnder D, Bland R, Williams MC, McNinch RW, Howie AJ, Stewart PM, Hewison M. Extrarenal expression of 25-hydroxyvitamin d(3)-1 alpha-hydroxylase. *J Clin Endocrinol Metab* 2001;86:888-94.
195. Knippenberg S, Bol Y, Damoiseaux J, Hupperts R, Smolders J. Vitamin D status in patients with MS is negatively correlated with depression, but not with fatigue. *Acta Neurol Scand* 2011;124:171-5.
196. Dusso AS, Tokumoto M. Defective renal maintenance of the vitamin D endocrine system impairs vitamin D renoprotection: a downward spiral in kidney disease. *Kidney Int* 2011;79:715-29.
197. Ross AC, Taylor CL, Yaktine AL, Del Valle HB. **Dietary Reference Intakes for Calcium and Vitamin D**. Institute of Medicine (US) Committee to Review Dietary Reference Intakes for Vitamin D and Calcium [serial online] 2011;Dec 10 2014. Internet: <http://www.ncbi.nlm.nih.gov/books/NBK56070/>
198. - Tuohimaa P, - Wang J, - Khan S, - Kuuslahti M, - Qian K, - Manninen T, - Auvinen P, - Vihinen M, - Lou Y. - Gene Expression Profiles in Human and Mouse Primary Cells Provide New Insights into the Differential Actions of Vitamin D<sub>3</sub> Metabolites. - *PLoS ONE* - e75338.
199. Holick MF, Binkley NC, Bischoff-Ferrari HA, Gordon CM, Hanley DA, Heaney RP, Murad MH, Weaver CM, Endocrine Society. Evaluation, treatment, and prevention

of vitamin D deficiency: an Endocrine Society clinical practice guideline. *J Clin Endocrinol Metab* 2011;96:1911-30.

200. Hanley DA, Cranney A, Jones G, Whiting SJ, Leslie WD, Cole DE, Atkinson SA, Josse RG, Feldman S, Kline GA, et al. Vitamin D in adult health and disease: a review and guideline statement from Osteoporosis Canada. *CMAJ* 2010;182:E610-8.

201. Saintonge S, Bang H, Gerber LM. Implications of a new definition of vitamin D deficiency in a multiracial us adolescent population: the National Health and Nutrition Examination Survey III. *Pediatrics* 2009;123:797-803.

202. Bischoff-Ferrari HA. Optimal serum 25-hydroxyvitamin D levels for multiple health outcomes. *Adv Exp Med Biol* 2008;624:55-71.

203. Vieth R, Pinto TR, Reen BS, Wong MM. Vitamin D poisoning by table sugar. *Lancet* 2002;359:672.

204. Jones G. Pharmacokinetics of vitamin D toxicity. *Am J Clin Nutr* 2008;88:582S-6S.

205. Masuda S, Byford V, Arabian A, Sakai Y, Demay MB, St-Arnaud R, Jones G. Altered pharmacokinetics of 1alpha,25-dihydroxyvitamin D<sub>3</sub> and 25-hydroxyvitamin D<sub>3</sub> in the blood and tissues of the 25-hydroxyvitamin D-24-hydroxylase (Cyp24a1) null mouse. *Endocrinology* 2005;146:825-34.

206. Shephard RM, Deluca HF. Plasma concentrations of vitamin D<sub>3</sub> and its metabolites in the rat as influenced by vitamin D<sub>3</sub> or 25-hydroxyvitamin D<sub>3</sub> intakes. *Arch Biochem Biophys* 1980;202:43-53.

207. Lim S, Kim MJ, Choi SH, Shin CS, Park KS, Jang HC, Billings LK, Meigs JB. Association of vitamin D deficiency with incidence of type 2 diabetes in high-risk Asian subjects. *Am J Clin Nutr* 2013;97:524-30.

208. Littlejohns TJ, Henley WE, Lang IA, Annweiler C, Beauchet O, Chaves PH, Fried L, Kestenbaum BR, Kuller LH, Langa KM, et al. Vitamin D and the risk of dementia and Alzheimer disease. *Neurology* 2014;83:920-8.

209. Ibi M, Sawada H, Nakanishi M, Kume T, Katsuki H, Kaneko S, Shimohama S, Akaike A. Protective effects of 1 alpha,25-(OH)(2)D(3) against the neurotoxicity of glutamate and reactive oxygen species in mesencephalic culture. *Neuropharmacology* 2001;40:761-71.

210. Kajta M, Makarewicz D, Zieminska E, Jantas D, Domin H, Lason W, Kutner A, Lazarewicz JW. Neuroprotection by co-treatment and post-treating with calcitriol following the ischemic and excitotoxic insult in vivo and in vitro. *Neurochem Int* 2009;55:265-74.

211. Codoner-Franch P, Tavaréz-Alonso S, Simo-Jorda R, Laporta-Martin P, Carratala-Calvo A, Alonso-Iglesias E. Vitamin D status is linked to biomarkers of oxidative stress, inflammation, and endothelial activation in obese children. *J Pediatr* 2012;161:848-54.
212. Halicka HD, Zhao H, Li J, Traganos F, Studzinski GP, Darzynkiewicz Z. Attenuation of constitutive DNA damage signaling by 1,25-dihydroxyvitamin D<sub>3</sub>. *Aging (Albany NY)* 2012;4:270-8.
213. Banakar MC, Paramasivan SK, Chattopadhyay MB, Datta S, Chakraborty P, Chatterjee M, Kannan K, Thygarajan E. 1 $\alpha$ , 25-dihydroxyvitamin D<sub>3</sub> prevents DNA damage and restores antioxidant enzymes in rat hepatocarcinogenesis induced by diethylnitrosamine and promoted by phenobarbital. *World J Gastroenterol* 2004;10:1268-75.
214. Harbuzova VI. Intensity of lipid peroxidation and antioxidant enzyme activity in arterial and venous walls during hypervitaminosis D. *Fiziol Zh* 2002;48:87-90.
215. Gomez JM. The role of insulin-like growth factor I components in the regulation of vitamin D. *Curr Pharm Biotechnol* 2006;7:125-32.
216. Beck KD, Valverde J, Alexi T, Poulsen K, Moffat B, Vandlen RA, Rosenthal A, Hefti F. Mesencephalic dopaminergic neurons protected by GDNF from axotomy-induced degeneration in the adult brain. *Nature* 1995;373:339-41.
217. Tomac A, Lindqvist E, Lin LF, Ogren SO, Young D, Hoffer BJ, Olson L. Protection and repair of the nigrostriatal dopaminergic system by GDNF in vivo. *Nature* 1995;373:335-9.
218. Arenas E, Trupp M, Akerud P, Ibanez CF. GDNF prevents degeneration and promotes the phenotype of brain noradrenergic neurons in vivo. *Neuron* 1995;15:1465-73.
219. Wang Y, Chiang YH, Su TP, Hayashi T, Morales M, Hoffer BJ, Lin SZ. Vitamin D(3) attenuates cortical infarction induced by middle cerebral arterial ligation in rats. *Neuropharmacology* 2000;39:873-80.
220. Smolders J, Moen SM, Damoiseaux J, Huitinga I, Holmoy T. Vitamin D in the healthy and inflamed central nervous system: access and function. *J Neurol Sci* 2011;311:37-43.
221. Spach KM, Hayes CE. Vitamin D<sub>3</sub> confers protection from autoimmune encephalomyelitis only in female mice. *J Immunol* 2005;175:4119-26.
222. Barker T, Martins TB, Hill HR, Kjeldsberg CR, Dixon BM, Schneider ED, Henriksen VT, Weaver LK. Circulating pro-inflammatory cytokines are elevated and

peak power output correlates with 25-hydroxyvitamin D in vitamin D insufficient adults. *Eur J Appl Physiol* 2013;113:1523-34.

223. Schleithoff SS, Zittermann A, Tenderich G, Berthold HK, Stehle P, Koerfer R. Vitamin D supplementation improves cytokine profiles in patients with congestive heart failure: a double-blind, randomized, placebo-controlled trial. *Am J Clin Nutr* 2006;83:754-9.

224. Karam C, Scelsa SN. Can vitamin D delay the progression of ALS? *Med Hypotheses* 2011;76:643-5.

225. Camu W, Tremblier B, Plassot C, Alphantery S, Salsac C, Pageot N, Juntas-Morales R, Scamps F, Daures JP, Raoul C. Vitamin D confers protection to motoneurons and is a prognostic factor of amyotrophic lateral sclerosis. *Neurobiol Aging* 2014;35:1198-205.

226. Solomon JA, Gianforcaro A, Hamadeh MJ. Vitamin D3 deficiency differentially affects functional and disease outcomes in the G93A mouse model of amyotrophic lateral sclerosis. *PLoS One* 2011;6:e29354.

227. Gianforcaro A, Hamadeh MJ. Dietary vitamin D3 supplementation at 10x the adequate intake improves functional capacity in the G93A transgenic mouse model of ALS, a pilot study. *CNS Neurosci Ther* 2012;18:547-57.

228. Gianforcaro A, Solomon JA, Hamadeh MJ. Vitamin D(3) at 50x AI attenuates the decline in paw grip endurance, but not disease outcomes, in the G93A mouse model of ALS, and is toxic in females. *PLoS One* 2013;8:e30243.

229. Parkhomenko E, Millionis A, Gianforcaro A, Solomon JA, Hamadeh MJ. Dietary vitamin D3 at 50x the adequate intake increases apoptosis in the quadriceps of the female G93A mouse model of amyotrophic lateral sclerosis: a pilot study. *The FASEB Journal* 2012;26:255.7.

230. Gupta R, Dixon KM, Deo SS, Holliday CJ, Slater M, Halliday GM, Reeve VE, Mason RS. Photoprotection by 1,25 dihydroxyvitamin D3 is associated with an increase in p53 and a decrease in nitric oxide products. *J Invest Dermatol* 2007;127:707-15.

231. Chakrabarti S, Cheung CC, Davidge ST. Estradiol attenuates high glucose-induced endothelial nitrotyrosine: role for neuronal nitric oxide synthase. *Am J Physiol Cell Physiol* 2012;302:C666-75.

232. Halhali A, Figueras AG, Diaz L, Avila E, Barrera D, Hernandez G, Larrea F. Effects of calcitriol on calbindins gene expression and lipid peroxidation in human placenta. *J Steroid Biochem Mol Biol* 2010;121:448-51.

233. Siddiqui MA, Kashyap MP, Al-Khedhairi AA, Musarrat J, Khanna VK, Yadav S, Pant AB. Protective potential of 17beta-estradiol against co-exposure of 4-hydroxynonenal and 6-hydroxydopamine in PC12 cells. *Hum Exp Toxicol* 2011;30:860-9.
234. Beier K, Volkl A, Fahimi HD. Suppression of peroxisomal lipid beta-oxidation enzymes of TNF-alpha. *FEBS Lett* 1992;310:273-6.
235. Saedisomeolia A, Taheri E, Djalali M, Djazayeri A, Qorbani M, Rajab A, Larijani B. Vitamin D status and its association with antioxidant profiles in diabetic patients: A cross-sectional study in Iran. *Indian J Med Sci* 2013;67:29-37.
236. Jin X, Zhang Z, Beer-Stolz D, Zimmers TA, Koniaris LG. Interleukin-6 inhibits oxidative injury and necrosis after extreme liver resection. *Hepatology* 2007;46:802-12.
237. Frakes AE, Ferraiuolo L, Haidet-Phillips AM, Schmelzer L, Braun L, Miranda CJ, Ladner KJ, Bevan AK, Foust KD, Godbout JP, et al. Microglia induce motor neuron death via the classical NF-kappaB pathway in amyotrophic lateral sclerosis. *Neuron* 2014;81:1009-23.
238. Keeney JT, Forster S, Sultana R, Brewer LD, Latimer CS, Cai J, Klein JB, Porter NM, Butterfield DA. Dietary vitamin D deficiency in rats from middle to old age leads to elevated tyrosine nitration and proteomics changes in levels of key proteins in brain: implications for low vitamin D-dependent age-related cognitive decline. *Free Radic Biol Med* 2013;65:324-34.
239. Tangpong J, Cole MP, Sultana R, Estus S, Vore M, St Clair W, Ratanachaiyavong S, St Clair DK, Butterfield DA. Adriamycin-mediated nitration of manganese superoxide dismutase in the central nervous system: insight into the mechanism of chemobrain. *J Neurochem* 2007;100:191-201.
240. Beckman JS, Carson M, Smith CD, Koppenol WH. ALS, SOD and peroxynitrite. *Nature* 1993;364:584.
241. Bishop A, Gooch R, Eguchi A, Jeffrey S, Smallwood L, Anderson J, Estevez AG. Mitigation of peroxynitrite-mediated nitric oxide (NO) toxicity as a mechanism of induced adaptive NO resistance in the CNS. *J Neurochem* 2009;109:74-84.
242. Garcion E, Sindji L, Montero-Menei C, Andre C, Brachet P, Darcy F. Expression of inducible nitric oxide synthase during rat brain inflammation: regulation by 1,25-dihydroxyvitamin D3. *Glia* 1998;22:282-94.
243. Singh P, Castillo A, Majid DS. Decrease in IL-10 and increase in TNF-alpha levels in renal tissues during systemic inhibition of nitric oxide in anesthetized mice. *Physiol Rep* 2014;2:e00228.

244. Hopkins MH, Owen J, Ahearn T, Fedirko V, Flanders WD, Jones DP, Bostick RM. Effects of supplemental vitamin D and calcium on biomarkers of inflammation in colorectal adenoma patients: a randomized, controlled clinical trial. *Cancer Prev Res (Phila)* 2011;4:1645-54.
245. Maggio M, Basaria S, Ble A, Lauretani F, Bandinelli S, Ceda GP, Valenti G, Ling SM, Ferrucci L. Correlation between testosterone and the inflammatory marker soluble interleukin-6 receptor in older men. *J Clin Endocrinol Metab* 2006;91:345-7.
246. Coletta RD, Reynolds MA, Martelli-Junior H, Graner E, Almeida OP, Sauk JJ. Testosterone stimulates proliferation and inhibits interleukin-6 production of normal and hereditary gingival fibromatosis fibroblasts. *Oral Microbiol Immunol* 2002;17:186-92.
247. Bobjer J, Katrinaki M, Tsatsanis C, Lundberg Giwercman Y, Giwercman A. Negative association between testosterone concentration and inflammatory markers in young men: a nested cross-sectional study. *PLoS One* 2013;8:e61466.
248. Li ZG, Danis VA, Brooks PM. Effect of gonadal steroids on the production of IL-1 and IL-6 by blood mononuclear cells in vitro. *Clin Exp Rheumatol* 1993;11:157-62.
249. Miller RR, Hicks GE, Shardell MD, Cappola AR, Hawkes WG, Yu-Yahiro JA, Keegan A, Magaziner J. Association of serum vitamin D levels with inflammatory response following hip fracture: the Baltimore Hip Studies. *J Gerontol A Biol Sci Med Sci* 2007;62:1402-6.
250. Wootz H, Hansson I, Korhonen L, Napankangas U, Lindholm D. Caspase-12 cleavage and increased oxidative stress during motoneuron degeneration in transgenic mouse model of ALS. *Biochem Biophys Res Commun* 2004;322:281-6.
251. Zhu Y, Qin Z, Gao J, Yang M, Qin Y, Shen T, Liu S. Vitamin D Therapy in Experimental Allergic Encephalomyelitis Could be Limited by Opposing Effects of Sphingosine 1-Phosphate and Gelsolin Dysregulation. *Mol Neurobiol* 2014;50:733-43.
252. Taheri-Shalmani S, Shahsavar S, Gianforcaro A, Solomon JA, Hamadeh MJ. Dietary vitamin D3 supplementation at 50x the adequate intake decreases calbindin d28k and endoplasmic reticulum stress and increases apoptosis, suggesting toxicity, in the female transgenic G93A mouse model of amyotrophic lateral sclerosis. *The FASEB Journal* 2013;27:644.1.
253. Guermonprez L, Ducrocq C, Gaudry-Talarmain YM. Inhibition of acetylcholine synthesis and tyrosine nitration induced by peroxynitrite are differentially prevented by antioxidants. *Mol Pharmacol* 2001;60:838-46.
254. Cervetto C, Frattaroli D, Maura G, Marcoli M. Motor neuron dysfunction in a mouse model of ALS: gender-dependent effect of P2X7 antagonism. *Toxicology* 2013;311:69-77.

255. Suzuki M, Tork C, Shelley B, McHugh J, Wallace K, Klein SM, Lindstrom MJ, Svendsen CN. Sexual dimorphism in disease onset and progression of a rat model of ALS. *Amyotroph Lateral Scler* 2007;8:20-5.
256. Lariviere RC, Julien JP. Functions of intermediate filaments in neuronal development and disease. *J Neurobiol* 2004;58:131-48.
257. Shahsavari S, Taheri-Shalmani S, Solomon JA, Gianforcaro A, Hamadeh MJ. Sexual dichotomy in calcium buffering capacity may be dependent on the severity of endoplasmic reticulum stress in the skeletal muscle of the vitamin D3 deficient transgenic G93A mouse model of amyotrophic lateral sclerosis. *The FASEB Journal* 2013;27:644.2.
258. Vijayalakshmi K, Alladi PA, Ghosh S, Prasanna VK, Sagar BC, Nalini A, Sathyaprabha TN, Raju TR. Evidence of endoplasmic reticular stress in the spinal motor neurons exposed to CSF from sporadic amyotrophic lateral sclerosis patients. *Neurobiol Dis* 2011;41:695-705.

**APPENDIX A**

**A PRIORI HYPOTHESES AND REPRESENTATIVE WESTERN BLOT BANDS  
FOR MANUSCRIPT # 1:**

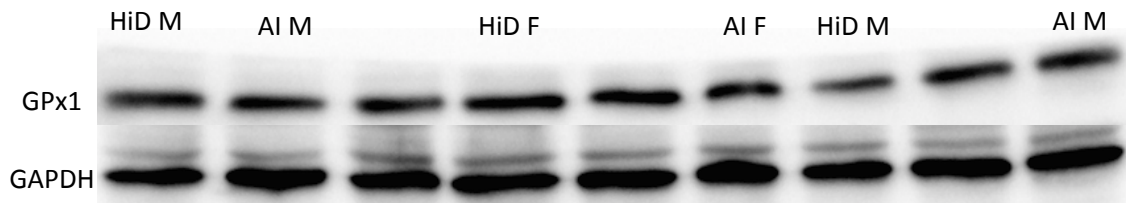
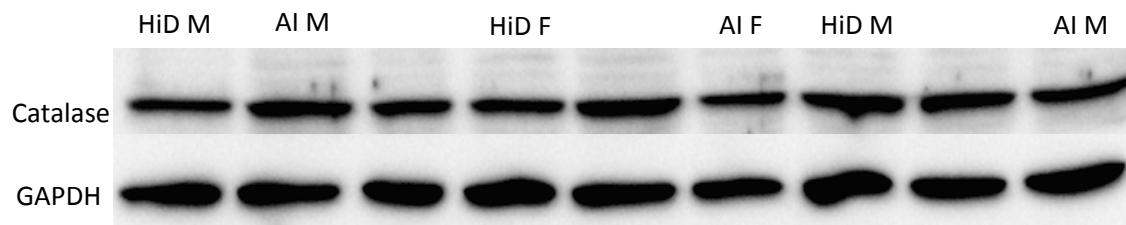
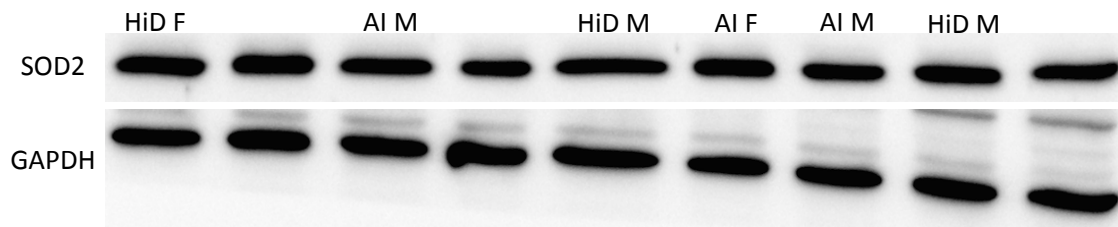
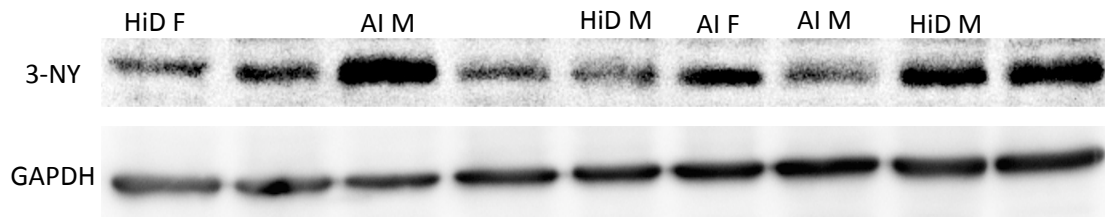
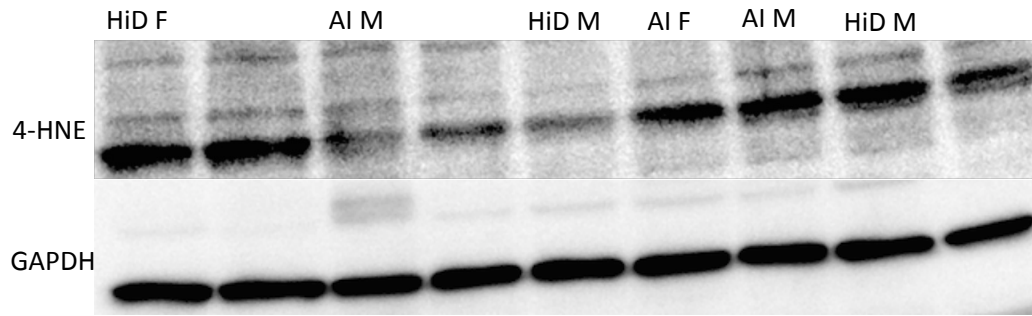
*Vitamin D<sub>3</sub> at 50X the adequate intake attenuates disease pathophysiology in the spinal cord of the male, but is toxic in female, G93A mouse model of amyotrophic lateral sclerosis*

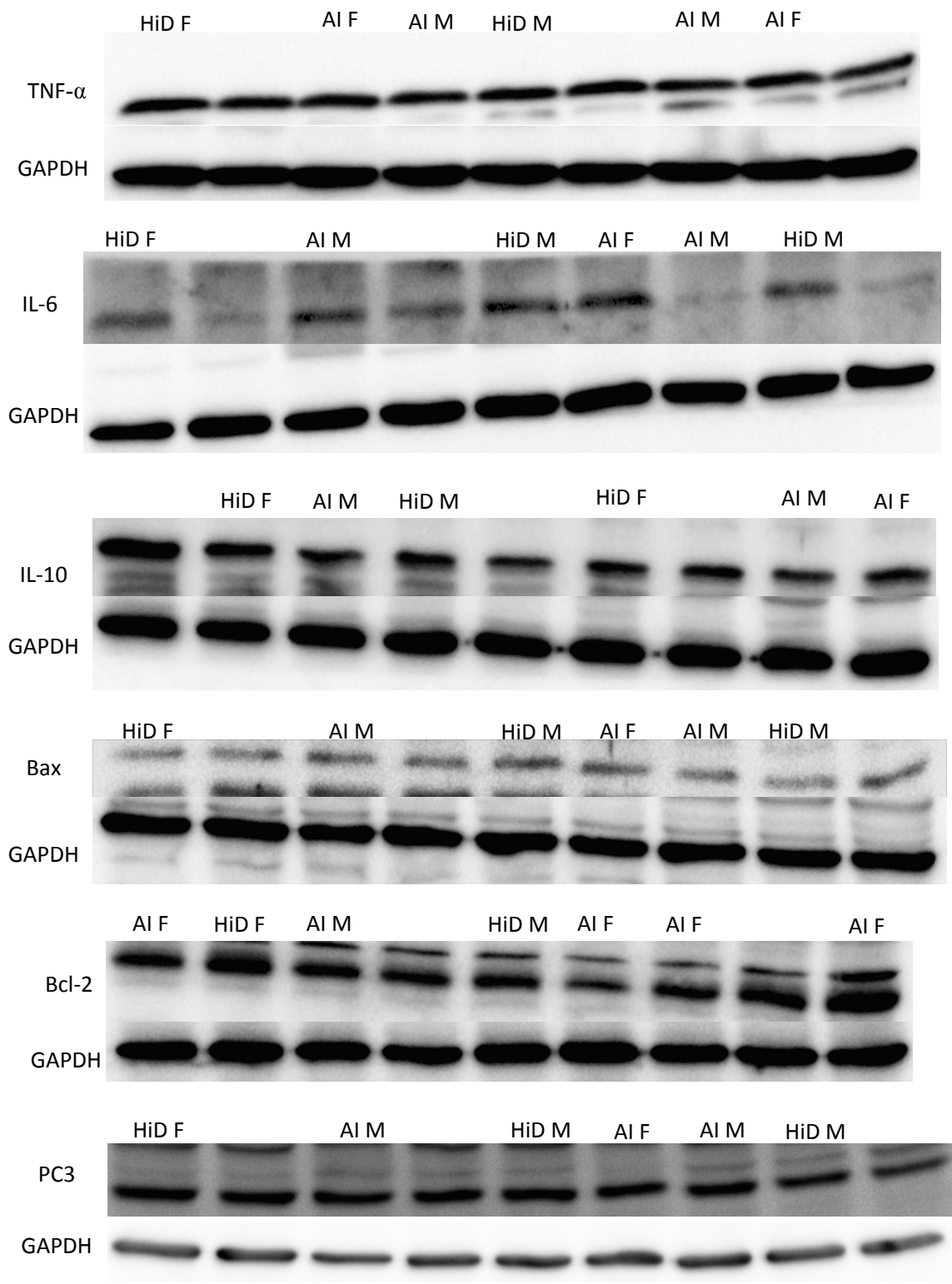
**Table S1.1** Rationale for establishing *a priori* hypotheses

Outcome	Biomarker	Model Used	Rationale for establishing <i>a priori</i> hypotheses	
			Male	Female
Oxidative Damage	3-nitrotyrosine (3-NY)	Mice and Human	<i>Quadriceps</i> of 50x AI (HiD) G93A mice did not show significant difference vs. AI (239)	
	4-Hydroxynonenal (4-HNE)	Mice	<i>Quadriceps</i> of 50x AI (HiD) G93A mice did not show significant difference vs. AI (239)	
Antioxidant Enzymes	Superoxide Dismutase 2 (SOD2)	Mice and Rats	- <i>Quadriceps</i> of 50x AI (HiD) G93A mice showed 13% increase vs. AI (P = 0.15) (239) -Adult male diabetic Wistar rats supplemented with 5000 IU/kg body weight of 1 $\alpha$ ,25(OH) <sub>2</sub> D <sub>3</sub> showed 207% increase vs. control (236)	- <i>Quadriceps</i> of 50x AI (HiD) female G93A mice showed 27% increase vs. AI (P = 0.10) (239)
	Catalase	Mice and Rats	- <i>Quadriceps</i> of 50x AI (HiD) G93A mice showed 13% increase vs. AI (P = 0.07) (239) -Adult male diabetic Wistar rats supplemented with 5000 IU/kg body weight of 1 $\alpha$ ,25(OH) <sub>2</sub> D <sub>3</sub> showed 52% increase vs. control (236)	<i>Quadriceps</i> of 50x AI (HiD) female G93A mice showed 15% increase vs. AI (P = 0.11) (239)
	Glutathione Peroxidase (GPx1)	Rats	Adult male diabetic Wistar rats supplemented with 5000 IU/kg body weight of 1 $\alpha$ ,25(OH) <sub>2</sub> D <sub>3</sub> showed 72% increase vs. control (236)	
Inflammation	Tumour Necrosis Factor Alpha (TNF- $\alpha$ )	Mice and Human	- <i>Quadriceps</i> of 50x AI (HiD) G93A mice did not show significant difference vs. AI (239) -Serum levels of patients with congestive heart failure (CHF) supplemented with 50 $\mu$ g vitamin D(3)/d plus 500 mg Ca/d inhibited rise (223)	
	Interleukin-6 (IL-6)	Mice	<i>Quadriceps</i> of 50x AI (HiD) G93A mice did not show significant difference vs. AI (229)	
	Interleukin-10 (IL-10)	Human	Serum levels of patients with congestive heart failure (CHF) supplemented with 50 $\mu$ g vitamin D(3)/d plus 500 mg Ca/d showed 43% increase vs. placebo (223)	
Apoptosis	Bax/Bcl-2 ratio	Mice		<i>Quadriceps</i> of 50x AI (HiD) female G93A mice showed 242% increase vs. AI (P = 0.080) (238)
	Pro/cleaved Caspase 3 (CASP3) ratio	Mice		<i>Quadriceps</i> of 50x AI (HiD) female G93A mice showed 87% increase vs. AI (P = 0.084) (229)
Neurotrophic Factor	Glial cell-derived Neurotrophic factor (GDNF)	Rats	Adult male Sprague–Dawley rats injected with 8 day pretreatment of 1 mg/kg/day 1,25(OH) <sub>2</sub> had 2 fold increase vs. control (163)	

**Table S1.2** Summary of *a priori* hypotheses and corresponding supporting studies

Outcome	Biomarkers	HiD vs. AI		Source
		Male	Female	
Oxidative Damage	3-nitrotyrosine (3-NY)	↓	↓	(211, 229, 239)
	4-hydroxynonenal (4-HNE)	↓	↓	(239, 243, 244)
Antioxidant Enzymes	SOD2	↑	↓	(236, 239, 244)
	Catalase	↑	↓	(236, 239, 244)
	Glutathione Peroxidase (GPx)	↑	↑	(236, 239, 244)
Inflammation	Tumour Necrosis Factor Alpha (TNF- $\alpha$ )	↓	↑	(223)
	Interleukin-6 (IL-6)	↓	↑	(229)
	Interleukin-10 (IL-10)	↑	↓	(223)
Neurotrophic Factor	Glial cell-derived neurotrophic factor (GDNF)	↑	↑	(163)
	Brain derived neurotrophic factor (BDNF)	↑	↑	(163)
Apoptosis	Bax/Bcl-2 ratio	↓	↑	(229, 245)
	Pro/cleaved Caspase 3 (CASP3) ratio	↓	↑	(229)
Neuron Count	SMI-36/SMI-32 ratio	↓	↑	(229, 238, 245)
	Choline Acetyltransferase (ChAT)	↑	↓	(229, 238, 245)





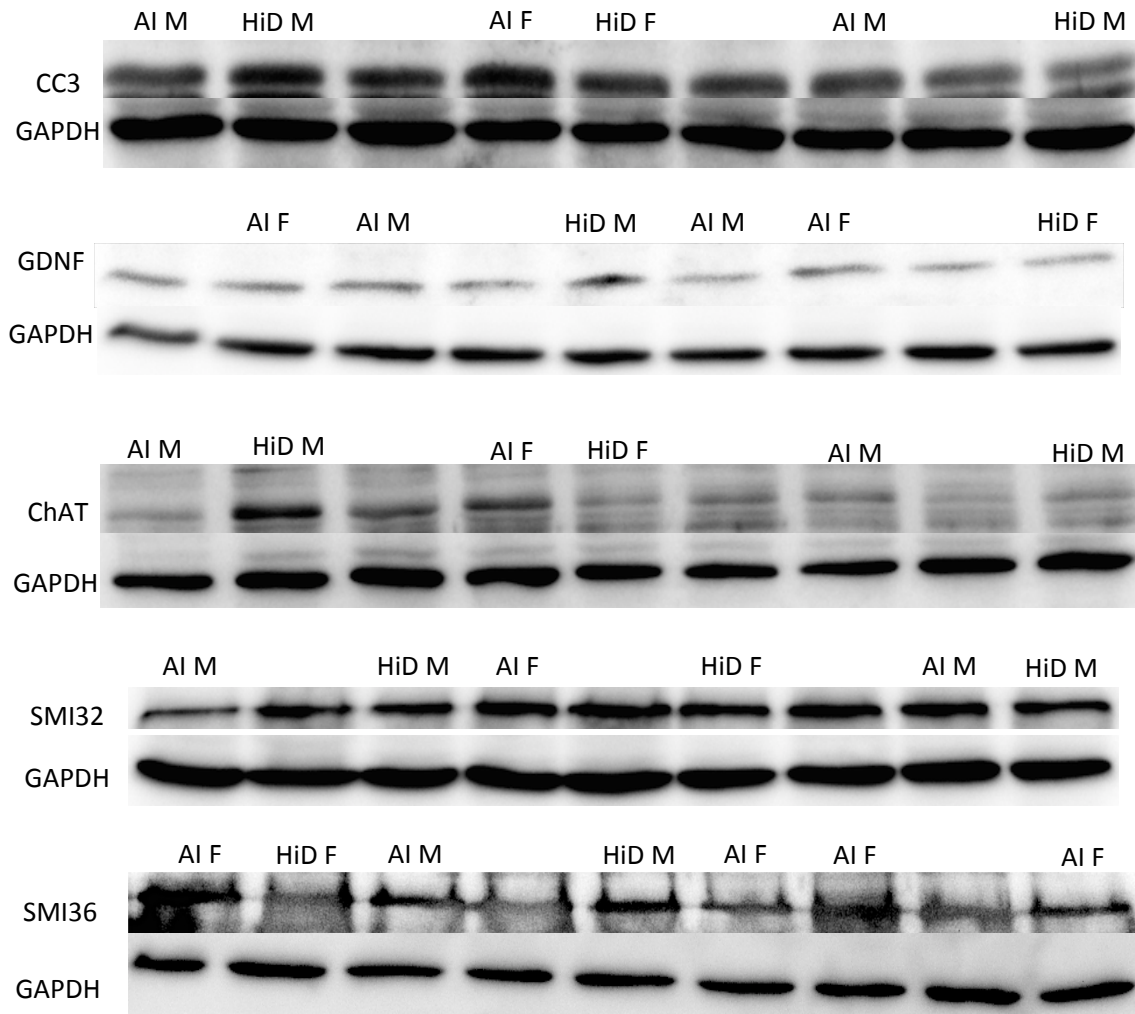


**Figure S1.1 Figure S1. Western blot representative bands for markers of oxidative damage, antioxidant enzymes, inflammation, apoptosis, neurotrophic factor and neuron damage.** Representative immunoblots of 4-HNE, 3-NY, SOD2, catalase, GPx1, TNF- $\alpha$ , IL-6, IL-10, Bax, Bcl-2, pro-caspase 3, cleaved caspase 3, GDNF, ChAT, SMI-32 and SMI-36 protein expression in the spinal cord of 41 G93A mice: 23 adequate vitamin D<sub>3</sub> intake (AI; 1 IU D<sub>3</sub>/g feed; 12 M, 11 F) and 18 high vitamin D<sub>3</sub> intake (HiD; 50 IU D<sub>3</sub>/g feed; 10 M, 8 F). Protein intensity was standardized to GAPDH.

**APPENDIX B**

**A PRIORI HYPOTHESES AND WESTERN BLOT REPRESENTATIVE BANDS  
FOR MANUSCRIPT # 2:**

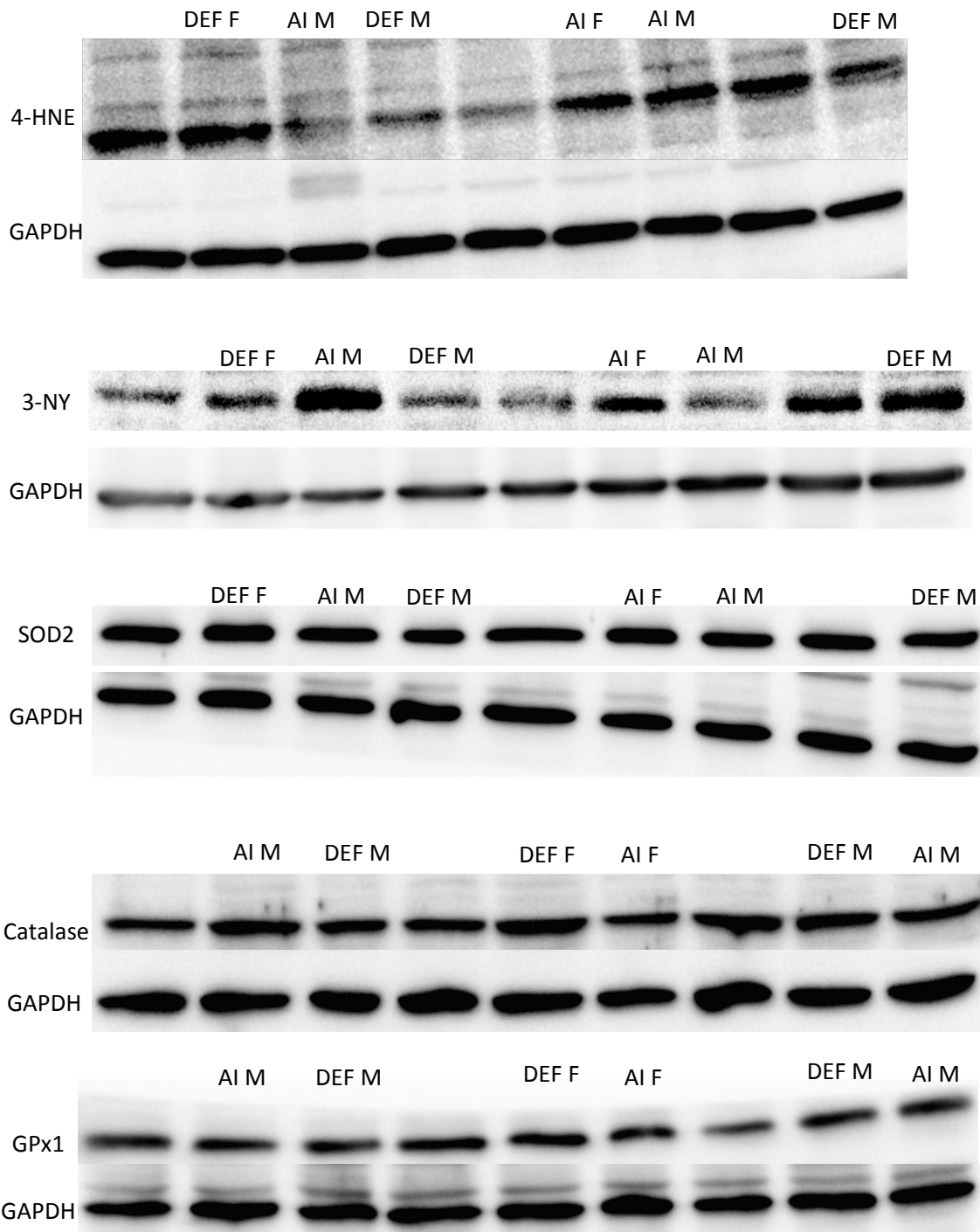
*Dietary D<sub>3</sub> restriction exacerbates disease pathophysiology in the spinal cord of the  
G93A mouse model of amyotrophic lateral sclerosis*

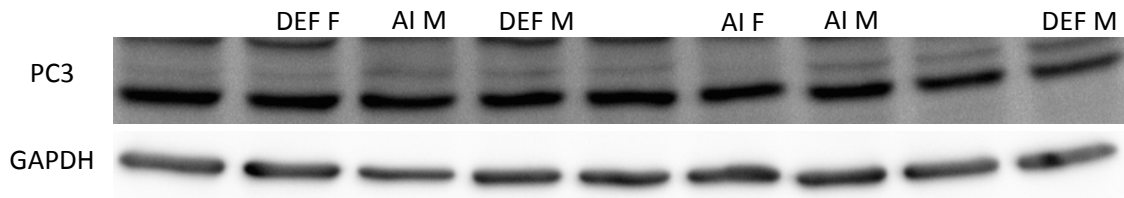
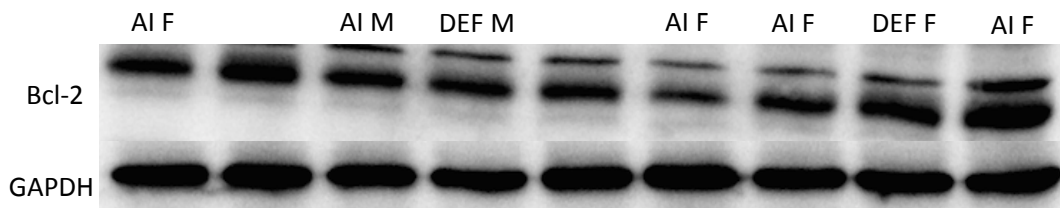
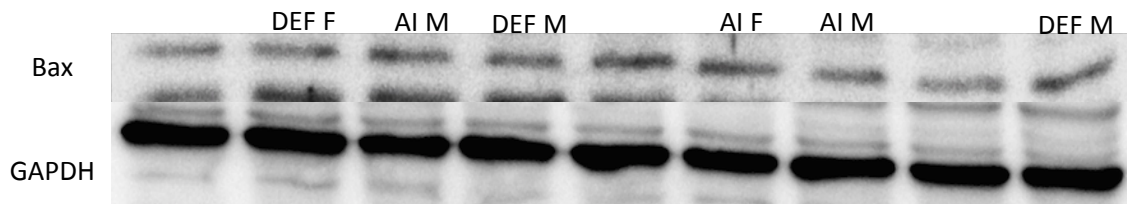
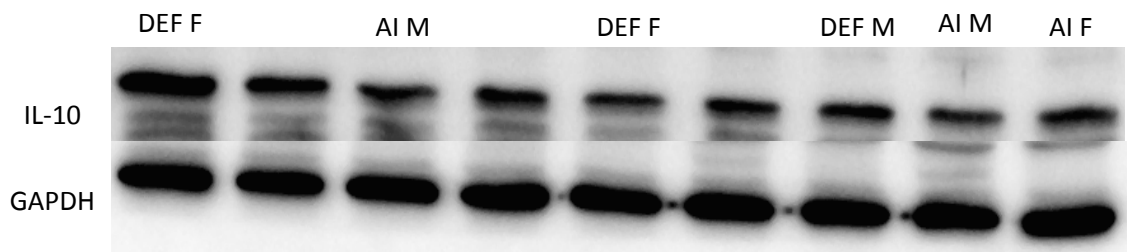
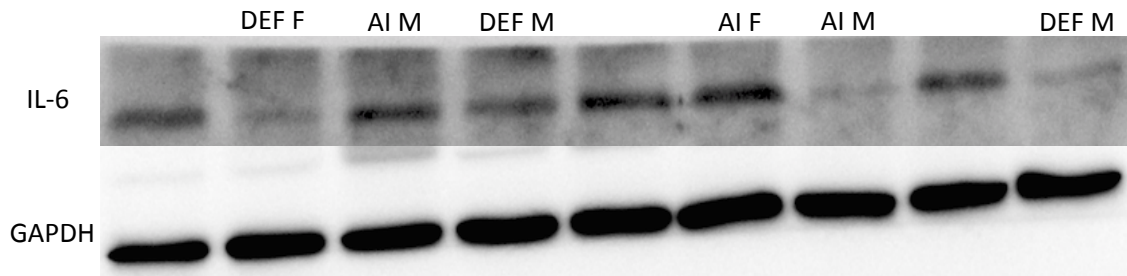
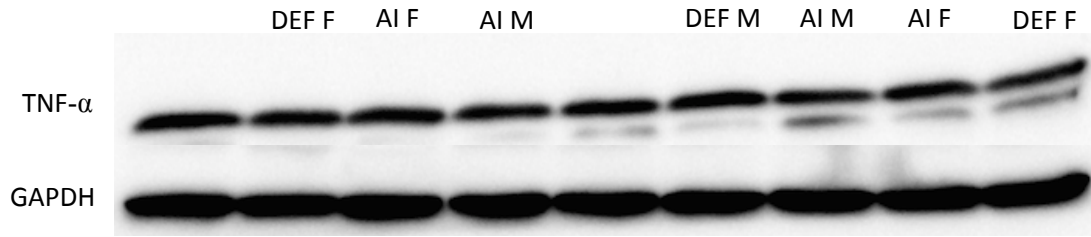
**Table S2.1** Rationale for establishing *a priori* hypotheses

Outcome	Biomarkers	Model Used	Rationale for establishing <i>a priori</i> hypotheses	
			Male	Female
Oxidative Damage	3-nitrotyrosine (3-NY)	Mice and Human	<p>-<i>Quadriceps</i> of 2.5% AI (DEF) G93A mice did not show significant difference vs. AI (244)</p> <p>-Obese children who had serum 25(OH)D levels &lt;20 ng/mL (DEF) had a 55% increase vs. obese children with serum levels <math>\geq</math>20 ng/mL (211)</p>	
	4-Hydroxynonenal (4-HNE)	Mice	<p>-<i>Quadriceps</i> of 2.5% AI (DEF) G93A mice did not show significant difference vs. AI (244)</p>	
Antioxidant Enzymes	SOD2	Mice and Rats	<p>-<i>Quadriceps</i> of 2.5% AI (DEF) G93A mice did not show significant difference vs. AI (244)</p>	
	Catalase	Mice and Rats	<p><i>Quadriceps</i> of 2.5% AI (DEF) male G93A mice showed 32% increase vs. AI (P = 0.009) (244)</p>	
	Glutathione Peroxidase (GPx1)	Rats	<p>-<i>Quadriceps</i> of 2.5% AI (DEF) G93A mice did not show significant difference vs. AI (244)</p>	
Inflammation	Tumour Necrosis Factor Alpha (TNF- $\alpha$ )	Mice and Human	<p>-<i>Quadriceps</i> of 2.5% AI (DEF) G93A mice did not show significant difference vs. AI (244)</p>	
	Interleukin-6 (IL-6)	Mice	<p>-<i>Quadriceps</i> of 2.5% AI (DEF) G93A mice did not show significant difference vs. AI (243)</p>	
	Interleukin-10 (IL-10)	Human	<p>-IL-10 were significantly higher in individuals with deficient (&lt;25 nmol/L) serum 25(OH)D compared with those with sufficient (&gt;75 nmol/L) status after adjustment for age, sex, and body mass index (P &lt; 0.05) (243)</p>	
Neurotrophic Factor	Glial cell-derived Neurotrophic factor (GDNF)	Rats		<p>Offspring of Female Sprague-Dawley rats that were fed D<sub>3</sub>-free diet had decreased serum D<sub>3</sub> levels (&lt;35 nmol/L) and lower free NGF and GDNF levels by 17 and 25% respectively, compared to controls (P &lt; 0.05) (357)</p>
Apoptosis	Bax/Bcl-2 ratio	Mice		<p><i>Quadriceps</i> of 2.5% AI (DEF) female G93A mice showed 103% increase vs. AI (P = 0.057) (245)</p>
	Pro/cleaved Caspase 3 (CASP3) ratio	Mice	<p>-<i>Quadriceps</i> of 2.5% AI (DEF) G93A mice did not show significant difference vs. AI (244)</p>	

**Table S2.2** Summary of *a priori* hypotheses and corresponding supporting studies

Outcome	Biomarkers	DEF vs. AI		Source
		Male	Female	
Oxidative Damage	3-nitrotyrosine (3-NY)	↑	↑	(211, 229, 239, 244)
	4-hydroxynonenal (4-HNE)	↑	↑	(239, 243, 244)
Antioxidant Enzymes	SOD2	↑	↑	(236, 239, 244)
	Catalase	↑	↑	(236, 239, 244)
	Glutathione Peroxidase (GPx)	↑	↑	(236, 239, 244)
Inflammation	Tumour Necrosis Factor Alpha (TNF- $\alpha$ )	↑	↑	(223)
	Interleukin-6 (IL-6)	↑	↑	(229)
	Interleukin-10 (IL-10)	↓	↓	(223)
Neurotrophic Factor	Glial cell-derived neurotrophic factor (GDNF)	↓	↓	(163)
	Brain derived neurotrophic factor (BDNF)	↓	↓	(163)
Apoptosis	Bax/Bcl-2 ratio	↑	↑	(229, 245)
	Pro/cleaved Caspase 3 (CASP3) ratio	↑	↑	(229)
Neuron Count	SMI-36/SMI-32 ratio	↑	↑	(229, 238, 245)
	Choline Acetyltransferase (ChAT)	↓	↓	(229, 238, 245)





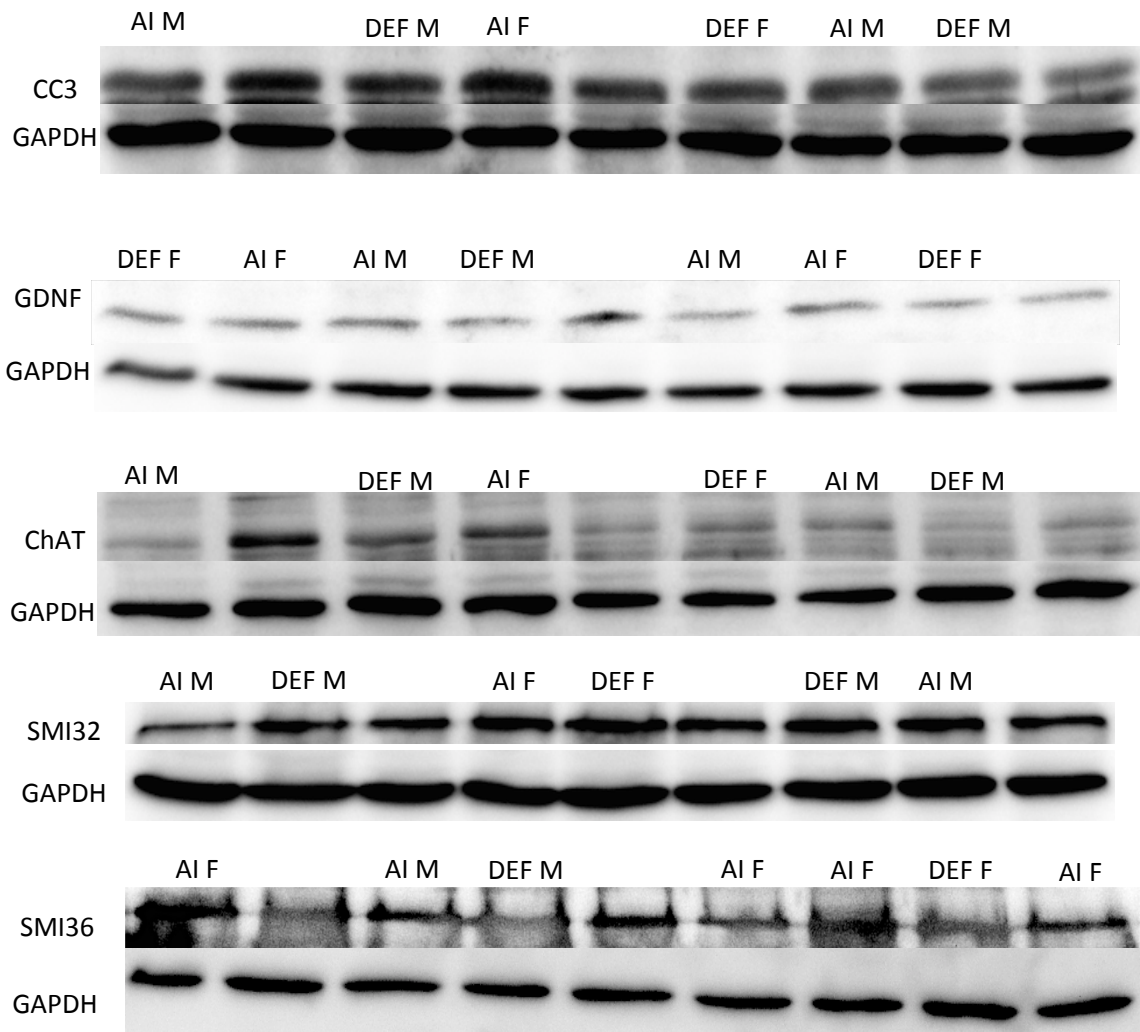


**Figure S2.1 Western blot representative bands for markers of oxidative damage, antioxidant enzymes, inflammation, apoptosis, neurotrophic factor and neuron damage.** Representative immunoblots of 4-HNE, 3-NY, SOD2, catalase, GPx1, TNF- $\alpha$ , IL-6, IL-10, Bax, Bcl-2, pro-caspase 3, cleaved caspase 3, GDNF, ChAT, SMI-32 and SMI-36 protein expression in the spinal cord of 42 G93A mice: 23 adequate vitamin D<sub>3</sub> intake (AI; 1 IU D<sub>3</sub>/g feed; 12 M, 11 F) and 19 deficient vitamin D<sub>3</sub> intake (DEF; 0.025 IU D<sub>3</sub>/g feed; 10 M, 9 F). Protein intensity was standardized to GAPDH.

**APPENDIX C**

**EXTENDED WESTERN BLOT METHODOLOGY FOR MANUSCRIPT #1 AND  
#2**

## Western Blot

### Oxidative damage

#### 4-Hydroxynonenal (4-HNE)

Spinal cord samples were prepared by loading 30 µg of protein to sample buffer and de-ionized water. Samples were heated for 5 min on a heating block and then size-separated along with a protein ladder (GE Healthcare, RPN 800E) by a 12.5% sodium dodecyl sulfate-polyacrylamide gel electrophoresis (SDS-PAGE) set at 120 v (Bio-Rad, 164-5052, Mississauga, Ontario) for ~1.5 h. Gels were then transferred to nitrocellulose membranes (#165-3322, Bio-Rad Mini-PROTEAN 2 electrophoresis system, Mississauga, ON, Canada) at 100 V for 2 h. Membranes were visualized with ponceau stain (Biobasic, 6226795, Mississauga, Ontario) to ensure proper transfer. Membranes were then blocked with 5% bovine serum albumin (BSA) (Bioshop, ALB001.500, Burlington, Ontario) diluted in TBST for 2 h at room temperature (RT) while shaking. After the block, membranes were washed 4 times for 5 min each with TBST at RT while shaking. Membranes were incubated with rabbit polyclonal primary antibody against 4-hydroxynonenal (4-HNE; Abcam, ab46545) at a dilution of 1/800 in 5% BSA diluted in TBST overnight (18 h) at 4°C while shaking. Membranes were washed 4 times for 5 min each and the antigen-antibody complexes were detected by incubating the membrane with goat anti-mouse HRP conjugated secondary antibody at a dilution of 1/5000 (Novus Biologicals, NB7539) in 5% fat free milk diluted in TBST for 2 h at RT. Immunoreactive proteins were visualized with enhanced chemiluminescence (ECL) (Santa Cruz Biotechnology, SC-2048) and exposed to Kodak autoradiographic film. Films were

scanned and the protein intensity was standardized to GAPDH using Carestream MI (v 5.0.2.30, NY, USA).

### 3-Nitrotyrosine

Protein damage was analyzed by measuring 3-NY protein content using the same protocol as 4-HNE but with the following modifications: 30 µg of protein was used; membranes were blocked in 5% BSA diluted in TBST for 1 h at RT while shaking; membranes were washed (4 x 5 min) using TBST; membranes were incubated with mouse monoclonal primary antibody against 3-nitrotyrosine (3-NY; Abcam, ab110282) at a dilution of 1/1000 in 5% BSA diluted in TBST overnight (18 h) at 4°C while shaking; membranes were washed (4 x 5 min) using TBST and then incubated with goat anti-mouse HRP conjugated secondary antibody (Novus Biologicals, NB7539) at a dilution of 1/5000 in 5% BSA diluted in TBST for 2 h at RT. The protein adducts form on several proteins of different molecular weights. Thus, protein intensity of the entire column was determined by summing the area under the curve for all peaks within the column (12-225 kDa). Films were scanned and the protein intensity was standardized to GAPDH using Carestream MI (v 5.0.2.30, NY, USA).

### **Antioxidant Enzymes**

#### Superoxide Dismutase 2 (SOD2)

SOD2 protein content was measured via WB using the same protocol as 4-HNE but with the following modifications: 5 µg of protein was used; membranes were visualized with ponceau stain and were cut at 31 kDa to identify SOD2 (25 kDa); membranes were blocked in 5% fat free milk diluted in TBST for 2 h at RT while shaking; membranes were washed (4 x 5 min) using TBST; membranes were incubated

with rabbit polyclonal primary antibody against superoxide dismutase 2 (SOD2; Abcam, ab13533) at a dilution of 1/2000 in 1% BSA diluted in TBST overnight (18 h) at 4°C while shaking; membranes were washed (4 x 5 min) using TBST and then incubated with goat anti-rabbit HRP conjugated secondary antibody (Novus Biologicals, NB730-H) at a dilution of 1/5000 in 5% fat free milk diluted in TBST for 2 h at RT. Films were scanned and the protein intensity was standardized to GAPDH using Carestream MI (v 5.0.2.30, NY, USA).

#### Catalase

Catalase protein content was measured via WB using the same protocol as 4-HNE but with the following modifications: 15 µg of protein was used; membranes were visualized with ponceau stain and were cut at 31 kDa to identify catalase (60 kDa); membranes were blocked in 5% fat free milk diluted in TBST for 2 h at RT while shaking; membranes were washed (4 x 5 min) using TBST; membranes were incubated with rabbit polyclonal primary antibody against catalase (Abcam, ab1877-10) at a dilution of 1/3500 in 5% fat free milk diluted in TBST overnight (18 h) at 4°C while shaking; membranes were washed (4 x 5 min) using TBST and then incubated with goat anti-rabbit HRP conjugated secondary antibody (Novus Biologicals, NB730-H) at a dilution of 1/5000 in 5% fat free milk diluted in TBST for 2 h at RT. Films were scanned and the protein intensity was standardized to GAPDH using Carestream MI (v 5.0.2.30, NY, USA).

#### Glutathione Peroxidase 1 (GPx1)

GPx1 protein content was measured via WB using the same protocol as 4-HNE but with the following modifications: 20 µg of protein was used; membranes were

visualized with ponceau stain and were cut at 31 kDa to identify GPx1 (22 kDa); membranes were blocked in 5% BSA diluted in TBST for 2 h at RT while shaking; membranes were washed (4 x 5 min) using TBST; membranes were incubated with rabbit polyclonal primary antibody against glutathione peroxidase 1 (GPx1; Abcam, ab22604) at a dilution of 1/800 in 5% BSA diluted in TBST overnight (18 h) at 4°C while shaking; membranes were washed (4 x 5 min) using TBST and then incubated with goat anti-rabbit HRP conjugated secondary antibody (Novus Biologicals, NB730-H) at a dilution of 1/5000 in 5% fat free milk diluted in TBST for 2 h at RT. Films were scanned and the protein intensity was standardized to GAPDH using Carestream MI (v 5.0.2.30, NY, USA).

## **Inflammation**

### Tumor necrosis factor $\alpha$ (TNF- $\alpha$ )

TNF-  $\alpha$  protein content was measured via WB using the same protocol as 4-HNE but with the following modifications: 35  $\mu$ g of protein was used; membranes were visualized with ponceau stain and were cut at 31 kDa to identify TNF-  $\alpha$  (17 kDa); membranes were blocked in 5% fat free milk diluted in TBST for 2 h at RT while shaking; membranes were washed (4 x 5 min) using TBST; membranes were incubated with rabbit polyclonal primary antibody against tumor necrosis factor  $\alpha$  (TNF-  $\alpha$ ; Abcam, ab9739) at a dilution of 1/2000 in 5% fat free milk diluted in TBST overnight (18 h) at 4°C while shaking; membranes were washed (4 x 5 min) using TBST and then incubated with goat anti-rabbit HRP conjugated secondary antibody (Novus Biologicals, NB730-H) at a dilution of 1/5000 in 5% fat free milk diluted in TBST for 2 h at RT. Films were

scanned and the protein intensity was standardized to GAPDH using Carestream MI (v 5.0.2.30, NY, USA).

#### Interleukin-6 (IL-6)

IL-6 protein content was measured via WB using the same protocol as 4-HNE but with the following modifications: 20 µg of protein was used; membranes were visualized with ponceau stain and were cut at 31 kDa to identify IL-6 (band between 21-28 kDa); membranes were blocked in 5% fat free milk diluted in TBST for 2 h at RT while shaking; membranes were washed (4 x 5 min) using TBST; membranes were incubated with rabbit polyclonal primary antibody against interleukin-6 (IL-6; Abcam, ab6672) at a dilution of 1/1000 in 5% fat free milk diluted in TBST overnight (18 h) at 4°C while shaking; membranes were washed (4 x 5 min) using TBST and then incubated with goat anti-rabbit HRP conjugated secondary antibody (Novus Biologicals, NB730-H) at a dilution of 1/5000 in 5% fat free milk diluted in TBST for 2 h at RT. Films were scanned and the protein intensity was standardized to GAPDH using Carestream MI (v 5.0.2.30, NY, USA)

#### Interleukin-10 (IL-10)

IL-10 protein content was measured via WB using the same protocol as 4-HNE but with the following modifications: 10 µg of protein was used; membranes were visualized with ponceau stain and were cut at 31 kDa to identify IL-10 (20 kDa); membranes were blocked in 5% BSA diluted in TBST for 2 h at RT while shaking; membranes were washed (4 x 5 min) using TBST; membranes were then incubated with rabbit polyclonal primary antibody against interleukin-10 (IL-10; Abcam, ab9969) at a dilution of 1/2000 in 3% BSA overnight (18 h) at 4°C while shaking; membranes were

washed (4 x 5 min) using TBST and then incubated with goat anti-rabbit HRP conjugated secondary antibody (Novus Biologicals, NB730-H) at a dilution of 1/5000 in 3% BSA diluted in TBST for 2 h at RT. Films were scanned and the protein intensity was standardized to GAPDH using Carestream MI (v 5.0.2.30, NY, USA).

## **Apoptosis**

### Bcl-2-associated X protein (Bax)

Bax protein content was measured via WB using the same protocol as 4-HNE but with the following modifications: 25 µg of protein was used; membranes were visualized with ponceau stain and were cut at 31 kDa to identify TNF- α (20 kDa); membranes were blocked in 5% BSA diluted in TBST for 2 h at RT while shaking; membranes were washed (4 x 5 min) using TBST; membranes were incubated with rabbit polyclonal primary antibody against Bax (Cell Signaling Technology, 2772) at a dilution of 1/1000 in 5% BSA diluted in TBST overnight (18 h) at 4°C while shaking; membranes were washed (4 x 5 min) using TBST and then incubated with goat anti-rabbit HRP conjugated secondary antibody (Novus Biologicals, NB730-H) at a dilution of 1/4000 in 5% BSA diluted in TBST for 2 h at RT. Films were scanned and the protein intensity was standardized to GAPDH using Carestream MI (v 5.0.2.30, NY, USA).

### B-cell lymphoma 2 (Bcl-2)

Bcl-2 protein content was measured via WB using the same protocol as 4-HNE but with the following modifications: 25 µg of protein was used; membranes were visualized with ponceau stain and were cut at 31 kDa to identify Bcl-2 (17 kDa); membranes were blocked in 5% BSA diluted in TBST for 2 h at RT while shaking; membranes were washed (4 x 5 min) using TBST; membranes were incubated with rabbit

polyclonal primary antibody against Bcl-2 (Cell Signaling Technology, 2870) at a dilution of 1/1000 in 5% BSA diluted in TBST overnight (18 h) at 4°C while shaking; membranes were washed (4 x 5 min) using TBST and then incubated with goat anti-rabbit HRP conjugated secondary antibody (Novus Biologicals, NB730-H) at a dilution of 1/5000 in 5% BSA diluted in TBST for 2 h at RT. Films were scanned and the protein intensity was standardized to GAPDH using Carestream MI (v 5.0.2.30, NY, USA).

### Pro-caspase 3

Pro-caspase 3 protein content was measured via WB using the same protocol as 4-HNE but with the following modifications: 20 µg of protein was used; membranes were blocked in 5% BSA diluted in TBST for 2 h at RT while shaking; membranes were washed (4 x 5 min) using TBST; membranes were incubated with rabbit polyclonal primary antibody against pro-caspase 3 (Millipore 04-440) at a dilution of 1/1000 in 5% BSA diluted in TBST overnight (18 h) at 4°C while shaking; membranes were washed (4 x 5 min) using TBST and then incubated with goat anti-rabbit HRP conjugated secondary antibody (Novus Biologicals, NB730-H) at a dilution of 1/5000 in 5% BSA diluted in TBST for 2 h at RT. Membranes were scanned and the protein intensity was standardized to GAPDH using Carestream MI (v 5.0.2.30, NY, USA).

### Cleaved caspase 3

Cleaved caspase 3 protein content was measured via WB using the same protocol as 4-HNE but with the following modifications: 25 µg of protein was used; membranes were visualized with ponceau stain and were cut at 31 kDa to identify cleaved caspase 3 (17 kDa); membranes were blocked in 5% BSA diluted in TBST for 2 h at RT while shaking; membranes were washed (4 x 5 min) using TBST; membranes were incubated

with rabbit polyclonal primary antibody against cleaved caspase 3 (Millipore 04-439) at a dilution of 1/1000 in 1% BSA diluted in TBST overnight (18 h) at 4°C while shaking; membranes were washed (4 x 5 min) using TBST and then incubated with goat anti-rabbit HRP conjugated secondary antibody (Novus Biologicals, NB730-H) at a dilution of 1/5000 in 1% BSA diluted in TBST for 2 h at RT. Films were scanned and the protein intensity was standardized to GAPDH using Carestream MI (v 5.0.2.30, NY, USA).

### **Neurotrophic Factor**

#### Glial cell-derived neurotrophic factor (GDNF)

GDNF protein content was measured via western blot using the same protocol as 4-HNE but with the following modifications: 25 µg of protein was used; membranes were visualized with ponceau stain to identify catalase (~24 kDa); membranes were blocked in 5% BSA diluted in TBST for 1 h at RT while shaking; membranes were washed (4 x 5 min) using TBST; membranes were incubated with rabbit polyclonal primary antibody against GDNF (Abcam, ab18956) at a dilution of 1/1000 in 1% BSA diluted in TBST overnight (18 h) at 4°C while shaking; membranes were washed (4 x 5 min) using TBST and then incubated with goat anti-rabbit HRP conjugated secondary antibody (Novus Biologicals, NB730-H) at a dilution of 1/5000 in 1% BSA diluted in TBST for 2 h at RT. Films were scanned and the protein intensity was standardized to GAPDH using Carestream MI (v 5.0.2.30, NY, USA)..

### **Neuronal Damage**

#### Choline acetyltransferase (ChAT)

ChAT protein content was measured via WB using the same protocol as 4-HNE but with the following modifications: 10 µg of protein was used; membranes were

visualized with ponceau stain and were cut at 31 kDa to identify ChAT (75 kDa); membranes were blocked in 5% BSA diluted in TBST for 2 h at RT while shaking; membranes were washed (4 x 5 min) using TBST; membranes were incubated with rabbit polyclonal primary antibody against choline acetyltransferase (ChAT; Abcam, ab85609) at a dilution of 1/1000 in 5% fat free milk diluted in TBST overnight (18 h) at 4°C while shaking; membranes were washed (4 x 5 min) using TBST and then incubated with goat anti-rabbit HRP conjugated secondary antibody (Novus Biologicals, NB730-H) at a dilution of 1/5000 in 5% fat free milk diluted in TBST for 2 h at RT. Films were scanned and the protein intensity was standardized to GAPDH using Carestream MI (v 5.0.2.30, NY, USA).

#### Neurofilament Heavy (unphosphorylated) antibody (SMI-32)

SMI-32 protein content was measured via WB using the same protocol as 4-HNE but with the following modifications: 25 µg of protein was used; membranes were visualized with ponceau stain and were cut at 76 kDa to identify SMI-32 (180-200 kDa); membranes were blocked in 5% BSA diluted in TBST for 2 h at RT while shaking; membranes were washed (4 x 5 min) using TBST; membranes were incubated with mouse monoclonal primary antibody against SMI-32 (Abcam, ab28029) at a dilution of 1/1000 in 3% BSA diluted in TBST overnight (18 h) at 4°C while shaking; membranes were washed (4 x 5 min) using TBST and then incubated with anti-mouse HRP conjugated secondary antibody against SMI-32 (Novus Biologicals, NB7539) at a dilution of 1/5000 in 3% milk diluted in TBST for 2 h at RT. Films were scanned and the protein intensity was standardized to GAPDH using Carestream MI (v 5.0.2.30, NY, USA)

### Neurofilament heavy (phosphorylated) protein (SMI-36)

SMI-36 protein content was measured via WB using the same protocol as 4-HNE but with the following modifications: 25 µg of protein was used; membranes were visualized with ponceau stain and were cut at 76 kDa to identify SMI-36 (200 kDa); membranes were blocked in 3% milk diluted in TBST for 2 h at RT while shaking; membranes were washed (4 x 5 min) using TBST; membranes were incubated with mouse monoclonal primary antibody against SMI-36 (Abcam, ab24572) at a dilution of 1/1000 in 3% milk diluted in TBST overnight (18 h) at 4°C while shaking; membranes were washed (4 x 5 min) using TBST and then incubated with goat anti-rabbit HRP conjugated secondary antibody (Novus Biologicals, NB730-H) at a dilution of 1/5000 in 3% milk diluted in TBST for 2 h at RT. Films were scanned and the protein intensity was standardized to GAPDH using Carestream MI (v 5.0.2.30, NY, USA)

### *Loading Control*

To correct for loading differences, ponceau staining was used as well as probing for glyceraldehyde 3-phosphate dehydrogenase (GAPDH). Membranes were either cut between 31-52 kDa to identify GAPDH protein content (38 kDa) or re-probed using mild stripping buffer

(<http://www.abcam.com/ps/pdf/protocols/Stripping%20for%20reprobing.pdf>). If

membranes were re-probed, the membranes were incubated in stripping buffer twice for 10 minutes at RT while shaking and then washed with tris-buffered saline (TBS) 2 times for 10 min each and subsequently in tris-buffered saline with tween (TBST) 2 times for 5 min each. Membranes were blocked for 2 h at room temperature (RT) while shaking. They were then washed in TBST 4 times for 5 min each. The membranes were then

incubated with mouse monoclonal primary antibody against GAPDH (Millipore, MAB374) at a dilution of 1:100 000 overnight (18 h) at 4°C while shaking. Membranes were then washed with TBST 4 times for 5 min each. The antigen-antibody complexes were detected by incubating the membrane with anti-mouse HRP conjugated secondary antibody at a dilution of 1/5000 (Novus Biologicals, NB7539). Films were scanned and the protein intensity was measured using Carestream MI (v 5.0.2.30, NY, USA).